Supplementary Information

Combining Free Energy Calculations with Tailored Enzyme Activity Assays to Elucidate Substrate Binding of a Phospho-Lysine Phosphatase

Anett Hauser[1,2], Songhwan Hwang[3], Han Sun[3], Christian P.R. Hackenberger[1,2]

[1] Department of Chemical Biology II, Leibniz-Forschungsinstitut für Molekulare Pharmakologie (FMP), Berlin, Germany

[2] Institute for Chemistry, Humboldt-Universität zu Berlin, Berlin, Germany

[3] Group of Structural Chemistry and Computational Biophysics, Leibniz-Forschungsinstitut für Molekulare Pharmakologie (FMP), Berlin, Germany

Table of Content

1 Materials and Methods

General

Reagents and solvents were, unless stated otherwise, commercially available as reagent grade and did not require further purification. Chemicals were purchased either from Sigma-Aldrich Chemie GmbH (Munich, Germany) or TCI (TCI Deutschland GmbH, Eschborn, Germany). Resins, coupling reagents and amino acids suitable for SPPS were purchased either from IRIS Biotech GmbH (Marktrewitz, Germany) or Novabiochem© (Merck KGaA, Darmstadt, Germany). All water- and air-sensitive reactions were performed under Schlenk conditions.

Peptide Synthesis

Peptides were prepared using the Fmoc solid phase strategy unless specifically noted either by manual peptide synthesis in 8 mL Extract Clean^{TM} reservoirs (Grace Davison Discovery Sciences, Deerfield, Illinois, USA) of 40 mL reactors (Activotec, Cambridge, UK) both equipped with fitting teflon frits or by automated synthesis in a Syro parallel synthesizer (MultiSynTech GmbH, Witten, Germany) in 5 mL syringe reactors equipped with a fritted disc (MultiSynTech GmbH).

Coupling of first amino acid on Rink amide resin

Swelling: 3.5 g Rink Amide resin (Novabiochem, 100-200 mesh, Fmoc on, average loading: 0.73 mmol·g^{-1}) were swollen in DMF for 45 min.

Fmoc-deprotection: After 2x 10 min shaking, each with 10 mL of piperidine (Pip):DMF (1:4, v/v) the resin was washed with 5x DMF, 5x DCM, 5x DMF.

Coupling: A 0.1 M solution of 0.4 eq. (1 mmol) Fmoc-protected AA, 0.4 eq (1 mmol) PyBop and 0.8 eq. (2 mmol) DIPEA in DMF was added to the resin. After 2 h of shaking at r.t., the resin was washed (5x DMF, 5x DCM, 5x DMF).

Capping: A solution of Ac_2O:2,6-lutidine:DMF (5:6:89, v/v/v, 10 mL) was added and the mixture shaken for 10 min. The resin was washed (5x DMF, 10x DCM) and dried completely under reduced pressure.

The loading was determined photometrically as described in the UV/Vis spectroscopy section.

Resin	*Sequence*	*Loading* [µmol·mg^{-1}]
14	^{Fmoc}Gly-resin	0.4385

Manual peptide synthesis

Swelling: The corresponding amount of resin for a 100 µmol scale was swollen in DMF (2000 µL) for 30 min.

Fmoc-deprotection: Pip:DMF (1:4, v/v, 1000 µL) was added to the resin. After 5 min, the solution was discarded and another portion of Pip:DMF (1:4, v/v, 1000 µL) was added to the resin. After 5 min, the solution was discarded and the resin washed with DMF, DCM, DMF (3x 1000 µL each).

Coupling: AAs were dissolved together with HCTU (500 µmol, 5 eq.) and Oxyma (500 µmol, 5 eq.) to a 0.2 M solution in DMF. Directly before adding the mixture to the resin, DIPEA (1000 µmol, 10 eq.) was added. The resulting reaction mixture was shaken for 45 min at r.t., the resin then filtered and washed with DMF, DCM, DMF (3x 1000 µL each).

Fmoc-Lys(N_3)-OH, Fmoc-Ser(PO(OBzl)OH)-OH, Fmoc-Thr(PO(OBzl)OH)-OH, Fmoc-Tyr(PO(OBzl)OH)-OH and Fmoc-Arg(PO($OTc)_2$)-OH **11** were incorporated by using 2 eq. AA, 1.95 eq. HATU and 4 eq. DIPEA in DMF and reacting the mixture for 2 h at r.t.

Acetylation: *N*-terminal acetylation was performed by treating the resin with a mixture of Ac_2O:2,6-lutidine:DMF (5:6:89, 1 mL) for 10 min at r.t., after which the resin was washed with DMF, DCM, DMF (3x 1000 µL each).

Final cleavage: The resin was either washed with DCM (10x 1000 µL) or used dry and treated with 4 mL of the cleavage cocktail (TFA:TIS:H_2O – 95:2.5:2.5, v/v/v) for 2 h. Peptides containing Cys in the sequence were cleaved with a mixture of TFA:TIS:H_2O:EDT (94:2.5:2.5:1, v/v/v/v). The resin was filtered off, the TFA filtrate collected in a 10-fold excess of deep-frozen Et_2O and let sit for precipitation in the freezer. After at least 15 min, the mixture was centrifuged, the solution decanted, the precipitate dried under nitrogen and re-dissolved in ACN/H_2O for UPLC analysis and preparative HPLC.

Automated peptide synthesis

Swelling: The corresponding amount of resin for a 50 µmol scale was swollen in DMF (500 µL) for 30 min.

Fmoc-deprotection: Pip:DMF (1:4, v/v, 400 µL) was added to the resin. After 5 min, the solution was discarded and the resin washed with DMF (4x 1000 µL).

Coupling: AAs were coupled by charging the reactor with a solution of the corresponding Fmoc and side chain protected AA (0.67 M in DMF, 4 eq.), PyBOP (0.95 M in DMF, 3.98 eq.), NMM (3.99 M in DMF, 7.94 eq.). The resulting solution was shaken for 30 min at r.t., the resin then filtered and subjected to a second coupling following the same procedure.

Fmoc-Lys(N_3)-OH, Fmoc-Ser(PO(OBzl)OH)-OH, Fmoc-Thr(PO(OBzl)OH)-OH, Fmoc-Tyr(PO(OBzl)OH)-OH and Fmoc-Arg(PO($OTc)_2$)-OH **11** were incorporated by using 2 eq. AA, 1.95 eq. HATU and 4 eq. DIPEA in DMF and reacting the mixture for 2 h at r.t.

Acetylation: *N*-terminal acetylation was performed by treating the resin with a mixture of Ac_2O:2,6-lutidine:DMF (5:6:89, 1 mL) for 10 min, after which the resin was washed 5x with DMF.

Final cleavage: The resin was either washed with DCM (10x 1000 µL) or used dry and treated with 2 mL of the cleavage cocktail (TFA:TIS:H_2O – 95:2.5:2.5, v/v/v) for 2 h at r.t. Peptides containing Cys in the sequence were cleaved with a mixture of TFA:TIS:H_2O:EDT (94:2.5:2.5:1, v/v/v/v). The resin was filtered off, the TFA filtrate collected in a 10-fold excess of deep-frozen Et_2O and let sit for precipitation in the freezer. After at least 15 min, the mixture was centrifuged, the solution decanted, the precipitate dried under nitrogen and re-dissolved in ACN/H_2O for UPLC analysis and preparative HPLC.

Analytical UPLC

UPLC®-UV traces for peptides and small molecules were obtained on an ACQUITY H-class instrument (Waters Corporation, Milford, Massachusetts, USA) equipped with an ACQUITY UPLC®-BEH C18 1.7 µm, 2.1x50 mm column (Waters Corporation), applying a flow rate of 0.6 mL·min^{-1} and using eluents A (99.9% H_2O, 0.1% TFA) and B (99.9% ACN, 0.1% TFA) in the corresponding linear gradient. UPLC-UV chromatograms were recorded at 220 nm.

Gradients	I	5% to 95% B in 13 min
	II	0.5% to 60% B in 13 min

High resolution masses were recorded on an ACQUITY H-class instrument (Waters Corporation) equipped with an ESI-MS Xevo® G2-XS QTof spectrometer (Waters Corporation).

TLC analysis

The thin layer chromatography (TLC) was performed on silica gel plates with fluorescence indicator F254 (Merck KGaA). Detection was performed at 254 or 366 nm. Compounds without any chromophore were stained with any of staining solutions such as Potassium permanganate solution, Ninhydrin or Vanillin reagent.

Purification

Peptidic substrates were purified by preparative, semi-preparative or analytical HPLC, performed either on a Gilson PLC 2020 system (Gilson Inc., Middleton, Wisconsin, USA), a Shimadzu Prominence 20A system or a Shimadzu Prominence 8A system (both Shimadzu Corporation, Kyoto, Japan) equipped with columns as followed: preparative column – Nucleodur C18 HTec, 5 µm, 250x32 mm; semi-preparative column – Nucleodur C18 HTec, 5 µm, 250x21 mm; analytical column – Nucleodur C18 HTec, 5 µm, 250x10 mm (all columns purchased from Macherey-Nagel, GmbH & Co. KG, Düren, Germany). Eluents A (99.9% H_2O, 0.1% TFA) and B (B**I**: 99.9% ACN, 0.1% TFA or B**II**: 9.9% ACN, 20% H_2O, 0.1% TFA) were applied in the corresponding linear gradient. Peak detection was performed at 220 nm.

Small molecules were purified by silica gel column chromatography (VWR Chemicals, Normasil 60 Å, 40–63 µm). The samples were applied pre-absorbed on silica gel or, if liquid, directly diluted with suitable solvents.

Desalting of small molecules or peptides was performed with Sep-Pak® Vac C18 cartridges (Waters Corporation). Samples were loaded with maximum 10% ACN in H_2O, washed 3x with 3 column volumes H_2O and eluted with increasing ACN concentration.

FPLC purification was performed at 4 °C on an NGCTM Quest 10 Chromatography System (Bio-Rad Laboratories GmbH, Feldkirchen, Germany) equipped with a BioFrac fraction collector and a HiPrep Q HP 16/10 strong anion exchange column (GE Healthcare UK Limited, Buckinghamshire, England). Eluents A (0.1 M Tris, pH 8.25, 4 °C) and B (0.1 M Tris, 1 M LiCl, pH 8.25, 4 °C) were applied in the corresponding linear gradient. Peak detection was performed at 255 nm.

NMR

NMR spectra were recorded either with a Bruker Ultrashield 300 MHz spectrometer or a Bruker Ultrashield 600 MHz spectrometer (both Bruker Corporation, Billerica, Massachusetts USA) at ambient temperature if not stated differently. The chemical shifts are reported in ppm relative to the shift of tetramethylsilane.

Photodeprotection

UV-irradiation was carried out with a Hg (Xe) arc lamp (LOT-QuantumDesign GmbH, Darmstadt, Germany) using a 297 nm filter with 15% transmission (Andover Inc., Salem, New Haven, USA). Samples were dissolved in MeOH at a concentration of 7.5 mM, positioned in 20 cm distance to the source and irradiated while stirring. The deprotection progress was followed by UPLC analysis. Upon complete conversion, a 10-fold excess of deep-frozen Et_2O was added and the mixture let sit in the freezer for 10 min. After centrifugation, the liquid phase was discarded and the precipitate re-suspended in the same amount of deep-frozen Et_2O. The mixture was kept in the freezer again for 10 min, centrifuged, decanted and the precipitate dried under reduced pressure for 15 min. Deprotected pLys substrates were stored in the freezer until applied in the assay.

Phosphatase and Phosphoramidate Hydrolase Activity Assay

Phosphoramidate hydrolase as well as phosphatase activities were determined on a SAFIRE^2 microplate reader (Tecan Group Ltd., Männedorf, Switzerland) by photometric detection at 360 nm of released inorganic phosphate with the EnzCheck™ Phosphatase Assay Kit (Thermo Fisher Scientific™, Waltham, Massachusetts, USA) following the protocol for enzymatic kinetics.[5] Briefly, substrates were incubated at a concentration of 100 µM in 50 mM Tris-HCl buffer containing 1 mM $MgCl_2$ at pH 7.8 in the presence or absence of 0.25 µg LHPP ($3.7{\cdot}10^{-4}$ eq., purchased at ProSpec-Tany TechnoGene Ltd. International, Ness-Ziona, Israel) for the overall phosphate release (enzymatic plus background reaction, $[E{+}BG]_{\mathrm{wBL}}$) or the non-enzymatic hydrolysis ($[BG]_{\mathrm{wBL}}$), respectively. The absorbance values of microplate, buffer, EnzCheck™ reagent and LHPP were determined in separated wells without adding substrate to the solution, considered as baseline ($[BL]_{\mathrm{w/LHPP}}$ and $[BL]_{\mathrm{w/oLHPP}}$). Reactions were run for 90 min in total, UV-absorbance was measured every 10 min. The enzymatic hydrolysis yield $[E]$ was determined by substraction of $[BG]_{\mathrm{w/oBL}}$ from $[E{+}BG]_{\mathrm{w/oBL}}$.

$$\begin{aligned}[E] &= [E+BG]_{\mathrm{w/oBL}} - [BG]_{\mathrm{w/oBL}} \\ &= ([E+BG]_{\mathrm{w/BL}} - [BL]_{\mathrm{w/LHPP}}) - ([BG]_{\mathrm{w/BL}} - [BL]_{\mathrm{w/oLHPP}})\end{aligned} \tag{1}$$

UV/Vis Spectroscopy

UV/Vis spectra and absorbance values were determined either on a V-630 spectrophotometer at r.t. or a V-550 UV/Vis spectrophotometer equipped with an ETC-505T temperature controller at 20 °C (both Jasco, Tokyo, Japan).

Determination of resin loading for peptide synthesis

1-2 mg dried resin were weighed into a microcentrifuge tube and covered with 1 mL Fmoc-deprotection solution (Pip:DMF, 1:4, v/v). After 10 min of shaking at r.t., the loading was determined in a 1 mL quartz cuvette. An aliquot of the deprotection solution was diluted to such an extend that the expected resulting absorbance was approx. 0.3. The actually measured absorbance was used top calculate the loading by the help of the following equations:

$$A_\lambda = \epsilon_\lambda \cdot c \cdot d \tag{2}$$

A: Absorbance at given wavelength, ϵ: molar attenuation coefficient at given wavelength in L·mol^{-1}·cm^{-1} (ϵ_{301nm} = 7800 L·mol^{-1}·cm^{-1} for 1-((9H-fluoren-9-yl)methyl)piperidine), c: concentration in mol·L^{-1}, d: cuvette length in cm.

$$L_{resin} = \frac{A \cdot V_{deprotection} \cdot V_{cuvette}}{\epsilon_{301nm} \cdot d \cdot V_{aliquot} \cdot m_{resin}} \tag{3}$$

L_{resin}: loading in µmol·mg^{-1}; A: Absorbance at 301 nm; $V_{deprotection}$: volume of Fmoc deprotection solution in µL (1000 µL); $V_{cuvette}$: total volume in cuvette for measuring in µL; ϵ_{301nm} = 7800 µL·µmol^{-1}·cm^{-1}; d: cuvette length in cm; m_{resin}: weighed amount in mg.

2 Synthetic Procedures

2.1 Synthesis of Phospho-Lysine Substrates

2.1.1 Synthesis overview

Phospho-Lys substrates and their precursors were prepared following the procedures described by Bertran-Vicente *et al.* with some adjustments as outlined below.[17] Phosphite **9** was prepared from 1-(2-nitrophenyl)ethanol **8**[6] *via* a different route than introduced previously.

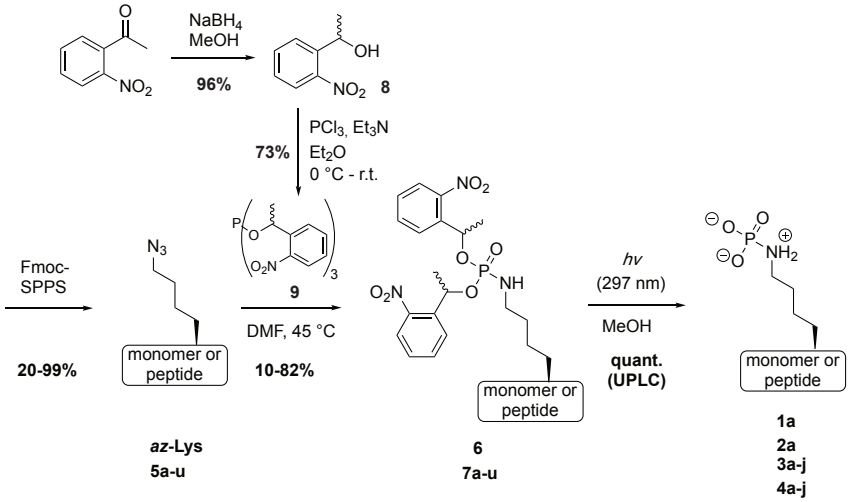

2.1.2 Azido-lysine containing peptides (5a-u)

Peptides containing azido-lysine were obtained as described in the peptide synthesis section on a 100 µmol scale on resin **14**. The crude peptides were used in the next step without further purification.

Table S1: Overview over synthesized azido-lysine peptides including yields (with regard to initial resin loading), high resolution masses and retention times.

#	Sequence	Yield [%] = [µmol]	m/z calc. $[M+H^+]^+$	m/z obs. $[M+H^+]^+$	t_R [min]
5a	$^{Ac}GGK^{N_3}GG^{CONH_2}$	99	442.2152	442.2164	4.066**
5b	$^{Ac}GAK^{N_3}GG^{CONH_2}$	57	456.2314	456.2314	4.450**
5c	$^{Ac}GCK^{N_3}GG^{CONH_2}$	60	488.2034	488.2033	4.727**
5d	$^{Ac}GDK^{N_3}GG^{CONH_2}$	52	500.2212	500.2217	4.053**
5e	$^{Ac}GFK^{N_3}GG^{CONH_2}$	68	532.2627	533.2628	6.446**
5f	$^{Ac}GIK^{N_3}GG^{CONH_2}$	56	498.2783	498.2787	6.034**
5g	$^{Ac}GKK^{N_3}GG^{CONH_2}$	20	513.2892	513.2894	4.017**
5h	$^{Ac}GPK^{N_3}GG^{CONH_2}$	41	482.2470	482.2475	4.910**
5i	$^{Ac}GQK^{N_3}GG^{CONH_2}$	78	513.2528	513.2534	3.937**
5j	$^{Ac}GRK^{N_3}GG^{CONH_2}$	52	541.2954	541.2955	4.149**
5k	$^{Ac}GSK^{N_3}GG^{CONH_2}$	99	472.2263	472.2267	3.854**
5l	$^{Ac}GGK^{N_3}AG^{CONH_2}$	62	456.2314	456.2316	4.333**
5m	$^{Ac}GGK^{N_3}CG^{CONH_2}$	55	488.2034	488.2040	4.870**
5n	$^{Ac}GGK^{N_3}DG^{CONH_2}$	28	500.2212	500.2214	3.949**
5o	$^{Ac}GGK^{N_3}FG^{CONH_2}$	60	532.2627	532.2631	6.693**
5p	$^{Ac}GGK^{N_3}IG^{CONH_2}$	56	498.2783	498.2788	5.945**
5q	$^{Ac}GGK^{N_3}KG^{CONH_2}$	23	513.2892	513.2893	3.754**
5r	$^{Ac}GGK^{N_3}PG^{CONH_2}$	66	482.2470	482.2473	4.812**
5s	$^{Ac}GGK^{N_3}QG^{CONH_2}$	51	513.2528	513.2527	3.716**
5t	$^{Ac}GGK^{N_3}RG^{CONH_2}$	44	541.2954	541.2965	3.784**
5u	$^{Ac}GGK^{N_3}SG^{CONH_2}$	68	472.2263	472.2267	3.643**

* gradient **I** ** gradient **II**

2.1.3 1-(2-Nitrophenyl)ethanol (8)

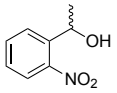

1-(2-nitrophenyl)ethanol was synthesized as previously described.[6] Briefly, in a 500 mL round-bottom flask 10 g (60.6 mmol) 2'-nitroacteophenone were dissolved in 100 mL MeOH:di- oxane (3:2, v/v) and cooled with an ice bath. Under vigorous stirring, 2.5 eq. sodium borohydride (151.4 mmol, 5.7 g) were added portionwise over 90 min. The resulting mixture was equipped a with septum and balloon and left to warm to r.t. 17 h while stirring. After 16 h residual $NaBH_4$ was quenched by the addition of 50 mL of acetone and the solvents evaporated under reduced pressure. The residual oil was diluted with H_2O and EE and the layers separated. The organic layer was washed twice with water, the combined aqueous layers were washed once with EE, eventually, the combined organic layers were washed with brine, dried over $MgSO_4$ and the filtered solution concentrated under reduced pressure. The residual solvent was evaporated under high vacuum for 20 h. The product (9.7 g, 58.2 mmol, 96%)

was obtained as a yellow oil. ^{1}H-NMR (600 MHz, CD_3CN) δ 7.86 (dd, J = 8.1, 1.4 Hz, 2H), 7.71 (td, J = 7.6, 1.3 Hz, 1H), 7.47 (ddd, J = 8.7, 7.4, 1.5 Hz, 1H), 5.30 (qd, J = 6.4, 4.1 Hz, 1H), 3.55 (dd, J = 4.2, 1.3 Hz, 1H), 1.48 (d, J = 6.4 Hz, 3H). ^{13}C-NMR (151 MHz, CD_3CN) δ 147.84, 141.58, 133.31, 127.91, 127.62, 123.75, 64.64, 24.19. HR-MS for $C_8H_9NO_3$: m/z calc. $[M+H^+]^+$ = 166.0499, m/z obs. $[M+H^+]^+$ = 166.0505.

2.1.4 Tris(1-(2-nitrophenyl)ethyl) phosphite (9)

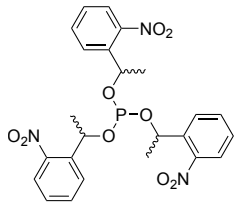

Phosphite **9** was synthesized by the condensation of trichlorophosphane and alcohol **8** under inert conditions. A Schlenk flask was equipped with 1.7 g 1-(2-nitrophenyl)ethanol **8** (10.2 mmol, 3.4 eq.) and magnetic stir bar and set under high vacuum for 10 min. After balancing the pressure with argon, 10 mL dry THF were added and the solution cooled in an ice bath for 5 min. 1.33 mL Et_3N (9.6 mmol, 3.2 eq.) were added, the mixture left for another 2 min, while preparing a 0.6 M solution of 0.27 mL trichlorophosphane (3 mmol, 1.0 eq.) in dry THF (5 mL). The PCl_3 solution was added dropwise to the Schlenk flask, whereby a white precipitate was formed. After complete addition the mixture was kept in the ice bath for another 15 min, then stirred at r.t. under exclusion of light over night. After 18 h the precipitate was filtered, washed with EE and the filtrate concentrated under reduced pressure. 1.03 g (2.19 mmol, 73%) product were obtained after column chromatography (hex/EE 9/1+1% Et_3N → hex/EE 7/3+1% Et_3N, the product eluting at 25% EE) as yellow oil and kept under argon, protected from light in the freezer until further usage. ^{1}H-NMR (300 MHz, CD_3CN) δ 7.92 – 7.74 (m, 3H), 7.70 – 7.34 (m, 9H), 5.84 – 5.57 (m, 3H), 1.52 – 1.37 (m, 6H), 1.29 – 1.19 (m, 3H). ^{31}P-NMR (122 MHz, CD_3CN) δ 137.82, 135.97. ^{13}C-NMR (75 MHz, CD_3CN) δ 146.95, 146.86, 146.71, 146.44, 139.09, 139.04, 138.92, 138.89, 133.75, 133.73, 128.51, 128.42, 128.29, 128.02, 127.98, 127.90, 127.68, 124.10, 124.07, 124.06, 67.01, 66.83, 66.76, 66.64, 66.61, 66.50, 24.33, 24.28, 24.24, 24.20, 24.18, 24.13, 24.03, 23.98. R_f (hex/EE 3/1+1% Et_3N) = 0.57.

2.1.5 N^6-(bis(1-(2-nitrophenyl)ethoxy)phosphoryl)-*L*-lysine, Lys(NPO(ONPE)$_2$) (6)

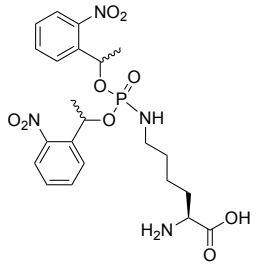

20.8 mg N^6-diazo-*L*-lysine hydrochloride (100 µmol) and 79.4 mg phosphite **9** (150 µmol, 1.5 eq.) were dissolved to a 50 mM solution in dry DMF (with regard to AA) in a round-bottom flask and Ar

was bubbled through the solution for 5 min. After that, the flask was closed with a septum equipped with an Ar filled balloon and the mixture was stirred at 45 °C, while subsequently more phosphite (1.5 eq. each time) was added after 6 and 24 h until UPLC showed full consumption of the AA (48 h). DMF was evaporated under reduced pressure, residual solvent was removed *via* lyophilization and the crude product purified *via* preparative HPLC. The product was obtained as yellow sticky oil (41.4 mg, 79 µmol, 79%). ^{1}H NMR (300 MHz, CD_3CN) δ 8.02 – 7.42 (m, 8H), 5.94 – 5.68 (m, 2H), 3.91 (ddd, J = 18.4, 14.2, 6.1 Hz, 2H), 2.66 (d, J = 7.7 Hz, 2H), 1.95 – 1.15 (m, 12H). ^{31}P NMR (122 MHz, CD_3CN) δ 8.13, 7.79, 7.43. ^{13}C NMR (151 MHz, CD_3CN) δ 171.24, 160.23, 159.99, 146.96, 146.79, 137.49, 134.03, 133.95, 129.01, 128.91, 128.83, 127.93, 127.81, 127.64, 124.32, 124.29, 124.26, 70.98, 70.81, 70.71, 53.16, 39.85, 39.65, 39.56, 30.14, 30.02, 29.16, 28.99, 23.58, 21.07, 20.96, 20.85. HR-MS for$C_{22}H_{29}N_4O_9P$: m/z calc. $[M+H^+]^+$ = 525.1745, m/z obs. $[M+H^+]^+$ = 525.1756. t_R (gradient **I**) = 5.605 min.

2.1.6 NPE-caged phospho-lysine (cpK-) peptides (7a-u)

Caged phosphoramidates peptide were synthesized as described above with the following changes. 10 µmol azido-peptide and 30 µmol phosphite **9** (3 eq., 15.9 mg) were dissolved to 25 mM in dry DMF (400 µL) and shaken at 950 rpm at 45 °C. After 6 h and 24 h, 3 eq. phosphite were added again. The solvent was evaporated under reduced pressure after 48 h and residuals removed during lyophilisation. The final product was obtained as white powder after purification *via* semi-preparative HPLC.

Table S2: Overview over synthesized NPE-caged phospho-lysine peptides including yields, high resolution masses and retention times.

#	Sequence	Yield [%] = 10x [µmol]	m/z calc. $[M+H^+]^+$	m/z obs. $[M+H^+]^+$	t_R [min]
7a	^{Ac}GGcpKGG^{CONH_2}	82	794.2864	794.2885	5.621*
7b	^{Ac}GAcpKGG^{CONH_2}	16	808.3022	808.3034	5.696*
7c	^{Ac}GCcpKGG^{CONH_2}	20	840.2742	840.2742	5.819*
7d	^{Ac}GDcpKGG^{CONH_2}	42	852.2920	852.2918	5.662*
7e	^{Ac}GFcpKGG^{CONH_2}	62	884.3335	884.3325	6.379*
7f	^{Ac}GIcpKGG^{CONH_2}	79	850.3491	850.3493	6.212*
7g	^{Ac}GKcpKGG^{CONH_2}	59	865.3600	865.3610	5.460*
7h	^{Ac}GPcpKGG^{CONH_2}	58	834.3178	831.3177	5.844*
7i	^{Ac}GQcpKGG^{CONH_2}	62	865.3236	865.3236	5.523*
7j	^{Ac}GRcpKGG^{CONH_2}	48	893.3662	893.3664	5.508*
7k	^{Ac}GScpKGG^{CONH_2}	26	824.2971	824.2971	5.579*
7l	^{Ac}GGcpKAG^{CONH_2}	12	808.3022	808.3022	5.684*
7m	^{Ac}GGcpKCG^{CONH_2}	10	840.2742	840.2740	5.867*
7n	^{Ac}GGcpKDG^{CONH_2}	57	852.2920	852.2920	5.625*
7o	^{Ac}GGcpKFG^{CONH_2}	53	884.3335	884.3325	6.464*
7p	^{Ac}GGcpKIG^{CONH_2}	59	850.3491	850.3491	6.190*
7q	^{Ac}GGcpKKG^{CONH_2}	49	865.3600	865.3596	5.410*
7r	^{Ac}GGcpKPG^{CONH_2}	37	834.3178	834.3177	5.739*

7s	^{Ac}GGcpKQG^{CONH_2}	73	865.3236	865.3237	5.486*
7t	^{Ac}GGcpKRG^{CONH_2}	60	893.3662	893.3663	5.430*
7u	^{Ac}GGcpKSG^{CONH_2}	42	824.2971	824.2971	5.556*

* gradient **I** ** gradient **II**

2.1.7 N^6-phosphono-*L*-lysine, pLys (1a)

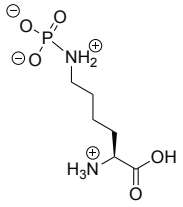

1 µmol caged-pLys **30** (0.52 mg) was deprotected and worked up as described in the photodeprotection section under 1. ^{1}H NMR (300 MHz, H_2O) δ 3.43 (t, J = 6.5 Hz, 1H), 2.73 (td, J = 8.2, 4.4 Hz, 2H), 1.48 (ddt, J = 113.3, 16.2, 9.1 Hz, 4H), 1.13 (dddt, J = 31.0, 21.7, 15.9, 8.7 Hz, 2H). ^{31}P NMR (122 MHz, H_2O) δ −1.06. ^{13}C NMR (151 MHz, H_2O) δ 157.86, 54.35, 42.69, 29.74, 26.30, 21.10. HR-MS for $C_6H_{15}N_2O_5P$: m/z calc. $[M+H^+]^+$ = 227.0792, m/z obs. $[M+H^+]^+$ = 227.0794. t_R (gradient **II**) = 0.545 min.

2.1.8 Phospho-lysine (pLys-) peptides (2a, 3a-j, 4a-j)

pLys-peptides were obtained as described in the photodeprotection section (1) on a 1 µmol scale.

Table S3: Overview over synthesized phospho-lysine peptides including high resolution masses and retention times.

#	Sequence	m/z calc. $[M+H^+]^+$	m/z obs. $[M+H^+]^+$	t_R [min]
2a	^{Ac}GGpKGG^{CONH_2}	496.1911	496.1956	0.481**
3a	^{Ac}GApKGG^{CONH_2}	510.2068	510.2074	0.450**
3b	^{Ac}GCpKGG^{CONH_2}	542.1788	542.1791	0.347**
3c	^{Ac}GDpKGG^{CONH_2}	554.1966	554.1981	0.349**
3d	^{Ac}GFpKGG^{CONH_2}	586.2381	586.2385	0.373**
3e	^{Ac}GIpKGG^{CONH_2}	552.2537	552.2545	0.374**
3f	^{Ac}GKpKGG^{CONH_2}	567.2646	567.2653	0.355**
3g	^{Ac}GPpKGG^{CONH_2}	536.2224	536.2245	0.675**
3h	^{Ac}GQpKGG^{CONH_2}	567.2282	567.2299	0.347**
3i	^{Ac}GRpKGG^{CONH_2}	595.2708	595.2714	0.509**
3j	^{Ac}GSpKGG^{CONH_2}	526.2017	526.2018	0.345**
4a	^{Ac}GGpKAG^{CONH_2}	510.2068	510.2070	0.574**
4b	^{Ac}GGpKCG^{CONH_2}	542.1788	542.1789	0.374**
4c	^{Ac}GGpKDG^{CONH_2}	554.1966	554.1985	0.347**
4d	^{Ac}GGpKFG^{CONH_2}	586.2381	586.2388	0.373**

4e	^{Ac}GGpKIG^{CONH_2}	552.2537	552.2542	0.458**
4f	^{Ac}GGpKKG^{CONH_2}	567.2646	567.2652	0.494**
4g	^{Ac}GGpKPG^{CONH_2}	536.2224	536.2228	0.683**
4h	^{Ac}GGpKQG^{CONH_2}	567.2282	567.2286	0.347**
4i	^{Ac}GGpKRG^{CONH_2}	595.2708	595.2719	0.436**
4j	^{Ac}GGpKSG^{CONH_2}	526.2017	526.2018	0.433**

* gradient **I** ** gradient **II**

2.2 Synthesis of Phospho-Serine, -Threonine and -Tyrosine Substrates

2.2.1 Synthesis overview

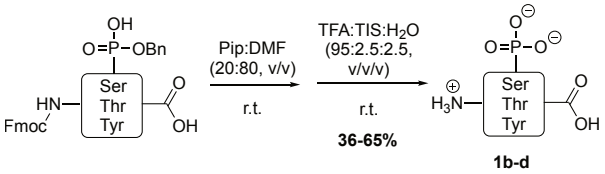

2.2.2 *O*-phosphorylated monomers (1b-d)

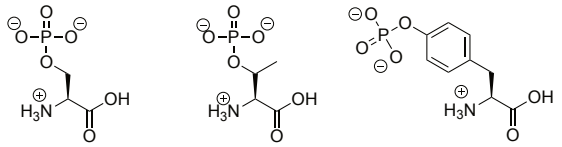

Phosphate amino acids **1b**, **1c** and **1d** were obtained by subsequent global deprotection of commercially available the SPPS-building blocks Fmoc-Ser(PO(OBzl)OH)-OH, Fmoc-Thr(PO(OBzl)OH)-OH, and Fmoc-Tyr(PO(OBzl)OH)-OH. Briefly, 100 µmol AA were dissolved to a 50 mM solution in Pip:DMF (20:80, v/v) and shaken at r.t. for 10 min. The solvent was evaporated under reduced pressure and residuals removed *via* lyophilization. The product was purified from the fluoren adduct *via* flash prep HPLC, concentrated under reduced pressure and directly treated with 1 mL TFA:TIS:H_2O (95:2.5:2.5, v/v/v)) for 90 min. The crude product was precipitated in a 10-fold excess of cold Et_2O, kept in the freezer for 10 min, separated from the ether by centrifugation and purified by semi-preparative HPLC.

pSer **1b**: white powder, 11.6 mg (65 µmol, 65%). ^{1}H NMR (600 MHz, D_2O) δ 4.28 (dt, J = 11.6, 5.7 Hz, 1H), 4.25 – 4.19 (m, 2H). ^{31}P NMR (243 MHz, D_2O) δ -0.28. ^{13}C NMR (151 MHz, D_2O) δ 169.83, 62.96, 62.93, 53.87, 53.81. HR-MS for $C_3H_8NO_6P$: m/z calc. $[M+H^+]^+$ = 186.0162, m/z obs. $[M+H^+]^+$ = 186.0171. t_R (gradient **II**) = 0.359 min.

pThr **1c**: white powder, 7.2 mg (36 µmol, 36%). ^{1}H NMR (600 MHz, D_2O) δ 4.70 (s, 1H), 3.95 (ddd, J = 4.0, 2.6, 1.3 Hz, 1H), 1.41 (d, J = 6.6 Hz, 3H). ^{31}P NMR (243 MHz, D_2O) δ -1.29. ^{13}C NMR (151 MHz, D_2O) δ 170.46, 70.31, 58.58, 18.26. HR-MS for $C_4H_{10}NO_6P$: m/z calc. $[M+H^+]^+$ = 200.0318, m/z obs. $[M+H^+]^+$ = 200.0326. t_R (gradient **II**) = 0.327 min.

pTyr **1d**: white powder, 15.1 mg (58 µmol, 58%). ^{1}H NMR (600 MHz, D_2O) δ 7.32 (d, J = 8.5 Hz, 2H), 7.25 – 7.20 (m, 2H), 4.25 (dd, J = 8.1, 5.2 Hz, 1H), 3.39 – 3.16 (m, 2H). ^{31}P NMR (243 MHz, D_2O) δ -3.95. ^{13}C NMR (151 MHz, D_2O) δ 172.19, 151.60, 151.56, 130.61, 129.95, 121.03, 121.00, 54.70, 35.11. HR-MS for $C_9H_{12}NO_6P$: m/z calc. $[M+H^+]^+$ = 262.0475, m/z obs. $[M+H^+]^+$ = 262.0486. t_R (gradient **II**) = 0.391 min.

2.2.3 *O*-phosphorylated peptides (2b-d)

Peptides **2b**, **2c** and **2d** were obtained as described in the peptide synthesis section on a 50 µmol scale on resin **14** and purified by semi-preparative HPLC.

^{Ac}GGpSGG^{CONH_2} **2b**: 14.5 mg (32 µmol, 64%). HR-MS for $C_{13}H_{23}N_6O_{10}P$: m/z calc. $[M+H^+]^+$ = 455.1282, m/z obs. $[M+H^+]^+$ = 455.1290. t_R (gradient **II**) = 0.341 min.

^{Ac}GGpThrGG^{CONH_2} **2c**: 18.8 mg (40 µmol, 80%). HR-MS for $C_{14}H_{25}N_6O_{10}P$: m/z calc. $[M+H^+]^+$ = 469.1438, m/z obs. $[M+H^+]^+$ = 469.1444. t_R (gradient **II**) = 0.367 min.

^{Ac}GGpTyrGG^{CONH_2} **2d**: 22.6 mg (42.5 µmol, 85%). HR-MS for $C_{19}H_{27}N_6O_{10}P$: m/z calc. $[M+H^+]^+$ = 531.1595, m/z obs. $[M+H^+]^+$ = 531.1602. t_R (gradient **II**) = 0.408 min.

2.3 Synthesis of Phospho-Arginine Substrates

2.3.1 Synthesis overview

The SPPS-compatible building block Fmoc-Arg(PO(OTc)$_2$)-OH **11** was synthesized as previously described [7] with minor adjustments as outlined below.

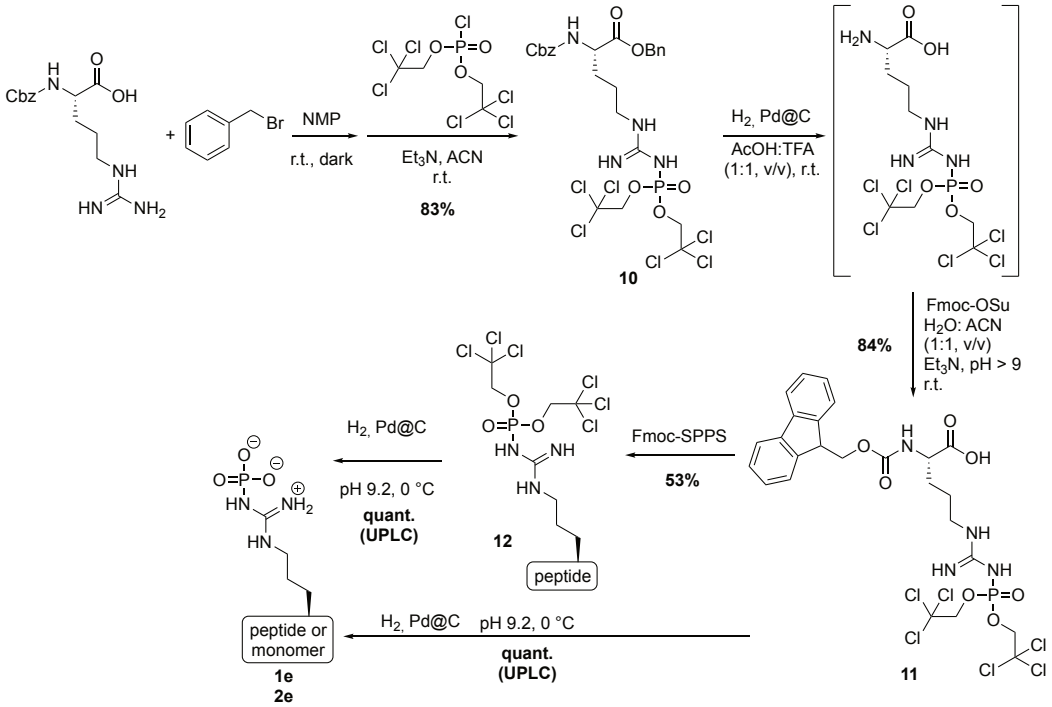

2.3.2 Benzyl N^2-((benzyloxy)carbonyl)-N^ω-(bis(2,2,2-trichloroethoxy)phosphoryl)-*L*-argininate (10)

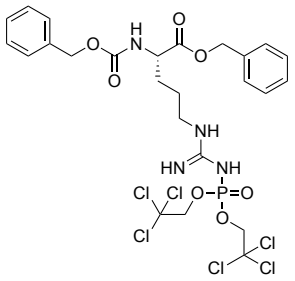

Z-Arg(PO(OTc)$_2$)-OBn **33** was synthesized from Z-Arg-OH. Briefly, 2.5 g Z-Arg-OH (8.1 mmol) were suspended to 0.25 M in NMP and Ar was bubbled through the suspension for 15 min. Equipped with a septum and Ar-balloon, the mixture was heated to 90 °C bath temperature until the AA had dissolved completely. After cooling the mixture to r.t., 1.1 mL benzyl bromide (8.91 mmol, 1.1 eq.) were added dropwise and the mixture left stirring in the dark under Ar overnight. NMP was removed under reduced pressure and the resulting yellow oil dissolved to 67 mM in ACN. Upon addition of 4.52 mL Et_3N (32.4 mmol, 4 eq.), the yellow solution turned colourless. 3.7 g (9.7 mmol, 1.2 eq.) Bis(trichloroethyl)phosphoryloxychloride were added in three equal portions at 0, 60 and 120 min and the reaction stirred at r.t. Since UPLC analysis after 6 h indicated still some intermediate left, 0.1 eq. of the phosphorylation reagent were added and the reaction left for 17.5 h at r.t. The solvents were evaporated under reduced pressure and the crude product adsorbed to silica gel for purification *via* column chromatography (hex/EE 7/3+1% FA → hex/EE 4/6+1% FA, the product eluting at 50% EE). 5.0 g (6.7 mmol, 83%) of a colorless oil were obtained as product. ^{1}H NMR (600 MHz, acetone-d_6) δ 7.43 – 7.27 (m, 10H), 6.75 (d, J = 8.0 Hz, 1H), 6.59 – 6.47 (m, 1H), 6.39 (s, 1H), 5.17 (s, 2H), 5.12 – 5.01 (m, 2H), 4.61 (q, J = 11.2, 8.1 Hz, 4H), 4.31 (td, J = 8.7, 5.0 Hz, 1H), 3.32 (s, 2H), 1.86 (ddtd, J = 88.4, 14.2, 9.7, 9.1, 5.8 Hz, 2H), 1.74 – 1.62 (m, 2H). ^{31}P NMR (243 MHz, acetone-d_6) δ 5.50. ^{13}C NMR (151 MHz, acetone-d_6) δ 172.01, 159.06, 159.00, 156.28, 137.18, 136.19, 128.46, 128.34, 128.19, 128.06, 127.94, 127.80, 127.77, 96.31, 96.23, 76.46, 76.43, 66.29, 66.11, 65.99, 54.09, 40.25, 25.94. HR-MS for $C_{25}H_{29}Cl_6N_4O_7P$: m/z calc. [M+H$^+$]$^+$ = 738.9978, m/z obs. [M+H$^+$]$^+$ = 738.9932. R_f (hex/EE 4/6+1% FA) = 0.33.

2.3.3 N^2-(((9-fluoren-9-yl)methoxy)carbonyl)-N^ω-(bis(2,2,2-trichloroethoxy) phosphoryl)-*L*-arginine, Fmoc-Arg(PO(OTc)$_2$)-OH (11)

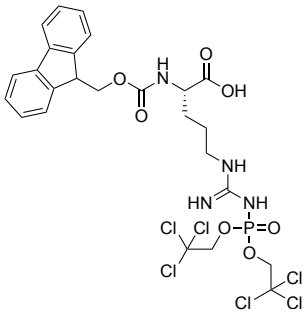

2.5 g Z-Arg(PO(OTc)$_2$)-OBn **11** (3.37 mmol) were dissolved to a 75 mM solution in AcOH:TFA (1:1,

v/v) and set under inert atmosphere. After addition of 375 mg palladium on charcoal (10% wt Pd), Ar was exchanged with hydrogen and the reaction mixture stirred under hydrogen atmosphere at r.t. UPLC analysis after 60 min indicated full Cbz and benzyl deprotection. The catalyst was filtered off, washed with AcOH:TFA (1:1, v/v) and the solvent evaporated under reduced pressure. Residual acid was removed by coevaporation with EtOH and under high vaccum for 14 h. The crude intermediate was suspended in 8.5 mL H_2O and 471 µL Et_3N (3.37 mmol, 1 eq.) were added. Upon adjustment of the pH to 9 by addition of more Et_3N, the solution became clear. A solution of 1.14 g Fmoc-OSu (3.37 mmol, 1 eq.) in 8.5 mL ACN was added dropwise while the pH was maintained above 8.0 by addition of further Et_3N. With stabilized pH of 9.0 after 40 min, UPLC analysis indicated full conversion. The pH was adjusted to 3.5 with AcOH and an equal volume of brine added under vigorous stirring. The mixture was washed 3x with $CHCl_3$, the combined organic layers were dried over Na_2SO_4 and the filtrate concentrated under reduced pressure. The product was obtained after silica column chromatography (hex/EE 5/5+1% FA → EE 100%+1% FA, the product eluting at 85% EE) as white powder (2.01 g, 2.83 mmol, 84%). ^{1}H NMR (600 MHz, CD_3CN+TFA-d_1) δ 8.83 (d, J = 5.6 Hz, 1H), 7.87 (d, J = 7.5 Hz, 2H), 7.70 (t, J = 7.6 Hz, 2H), 7.45 (t, J = 7.5 Hz, 2H), 7.37 (t, J = 7.4 Hz, 2H), 6.18 (d, J = 8.2 Hz, 1H), 4.84 (qd, J = 11.2, 4.5 Hz, 4H), 4.39 (d, J = 7.1 Hz, 2H), 4.28 (t, J = 7.0 Hz, 1H), 4.20 (d, J = 9.9 Hz, 1H), 3.35 – 3.21 (m, 2H), 1.93 (d, J = 10.2 Hz, 1H), 1.74 (dq, J = 14.4, 7.6 Hz, 3H). ^{31}P NMR (243 MHz, CD_3CN+TFA-d_1) δ -3.71. ^{13}C NMR (151 MHz, CD_3CN+TFA-d_1) δ 156.47, 155.02, 144.10, 144.01, 141.17, 127.74, 127.13, 125.20, 120.02, 116.18, 114.28, 112.38, 94.15, 94.08, 76.87, 76.84, 66.51, 53.10, 53.00, 47.04, 41.45, 41.33, 28.40, 28.36, 23.89. HR-MS for $C_{25}H_{27}Cl_6N_4O_7P$: m/z calc. $[M+H^+]^+$ = 736.9822, m/z obs. $[M+H^+]^+$ = 736.9828. R_f (EE: 100%+1% FA) = 0.50.

2.3.4 ^{Ac}Gly-Gly-Arg(NPO(OTc)$_2$)-Gly-Gly^{CONH_2} (12)

2,2,2-Trichloroethyl-protected pArg peptide **12** was obtained as described in the peptide synthesis section on a 50 µmol scale on resin **14**. The crude product was purified by semi-preparative HPLC to give 21 mg (11.5 µmol, 53% with regard to initial resin loading) of a white powder as desired product. HR-MS for $C_{20}H_{32}Cl_6N_9O_9P$: m/z calc. $[M+H^+]^+$ = 784.0261, m/z obs. $[M+H^+]^+$ = 784.0262. t_R (gradient **I**) = 5.291 min.

2.3.5 N^{ω}-phosphono-*L*-arginine, pArg (1e)

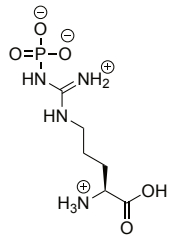

pArg **1e** was obtained by global deprotection of Fmoc-Arg(PO(OTc)$_2$)-OH **11**. Briefly, to 7.4 mg **34** (10 µmol) in 4 mL 25 mM $(NH_4)_2CO_3$ at pH 9.2 18 mg palladium on charcoal (10% wt Pd) were added under Ar. After addition of 1 mL EtOH, the atmosphere was exchanged to hydrogen and the reaction stirred for 60 min in an ice bath until UPLC indicated full conversion. The catalyst was filtered off,

washed with low amount of water and the solvents removed by lyophilization. Deprotected pArg was stored in the freezer until applied in the assay. ^{1}H NMR (600 MHz, D_2O) δ 3.78 (t, J = 6.2 Hz, 1H), 3.29 (t, J = 6.9 Hz, 2H), 1.99 – 1.87 (m, 2H), 1.80 – 1.63 (m, 2H). ^{31}P NMR (243 MHz, D_2O) δ -3.59. ^{13}C NMR (151 MHz, D_2O) δ 174.65, 155.77, 54.36, 40.42, 27.72, 23.99. HR-MS for $C_6H_{15}N_4O_5P$: m/z calc. $[M+H^+]^+$ = 255.0853, m/z obs. $[M+H^+]^+$ = 255.0860. t_R (gradient **II**) = 0.345 min.

2.3.6 ^{Ac}Gly-Gly-Arg(NPO(OH)$_2$)-Gly-Gly^{CONH_2} (2e)

4.3 mg ^{Ac}Gly-Gly-Arg(NPO(OTc)$_2$)-Gly-Gly^{CONH_2} were dissolved in 550 µL 100 mM $(NH_4)_2CO_3$, pH 9.2 under Ar atmosphere. 10 mg palladium on charcoal (10% wt Pd) were added together with 2.2 mL EtOH, the Ar exchanged with hydrogen and the mixture stirred in an ice bath until UPLC indicated full conversion, usually after 1 h. The catalyst was filtered off, washed with little amount of water and the solvents removed by lyophilization. Deprotected pArg peptide was stored in the freezer until applied in the assay. HR-MS for $C_{16}H_{30}N_9O_9P$: m/z calc. $[M+H^+]^+$ = 524.1973, m/z obs. $[M+H^+]^+$ = 524.1976. t_R (gradient **II**) = 0.420 min.

2.4 Synthesis of Phospho-Histidine Substrate

2.4.1 Synthesis overview

Phospho-His **1f** and the required phosphorylation reagent **13** were prepared as previously described [8] with minor adjustments as outlined below.

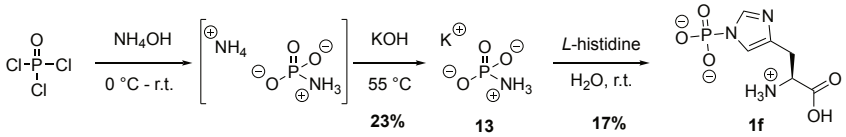

2.4.2 Potassium phosphoramidate, K-PA (13)

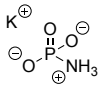

Potassium phosphoramidate (K-PA) was synthesized as previously described. [8] Under vigorous stirring, 4.6 mL phosphorus oxychloride (50 mmol) were added dropwise to 75 mL of pre-cooled 10% ammonium hydroxide in water (396 mmol, 8 eq.) and kept in an ice bath until steam formation ceased. 250 mL acetone were added and the layers separated. The aqueous layer was acidified to pH 6 with AcOH, at which a white precipitate formed. After resting the mixture at r.t. for 60 min, the precipitate was filtered, washed with EtOH and Et_2O, dried under reduced pressure and left under the hood forn 16 h. To the intermediate ammonium salt (1.36 g, 24%) 4 mL 50% KOH in water were added. The bubbling mixture was stirred at 55 °C bath temperature for 15 min to allow ammonia release. After cooling to 5 °C, the mixture was acidified to pH 6 with AcOH and poured into 300 mL EtOH. Gently stirring at r.t. for 60 min led to formation of white precipitate, which was filtered off, washed with

cold EtOH and dried under the hood for 14 h to give the product as white solid (1.55 g, 11.5 mmol, 23%). ^{31}P NMR (122 MHz, D_2O) δ -2.98. HR-MS for H_3NO_3P: m/z calc. $[M+H^+]^+ = 98.0002$, m/z obs. $[M+H^+]^+ = 97.9998$.

2.4.3 N^τ-phosphono-*L*-histidine, pHis (1f)

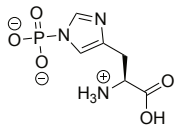

Phosphorylation of histidine was accomplished as described previously.[8] Briefly, 250 mg *L*-histidine (1.6 mmol) and 370 mg K-PA (2.7 mmol, 1.7 eq.) were dissolved in 6.25 mL H_2O and stirred at r.t. for five days. The reaction mixture was purified by SAX on an FPLC system at 4 °C. Fractions giving positive TNBS test result were pooled and diluted with 0.1 M Tris, 0.5 M LiCl (pH 8.25, 4 °C) until addition of three volumes of cold EtOH induced precipitation. The mixture was stirred gently at 4 °C for 5 min and centrifuged 10 min (4,000 × *g*). The precipitate was dried under reduced pressure, while to the supernatant four volumes of cold EtOH were added resulting mixture left at 4 °C for 15 h to induce and evolve precipitation. The product was obtained after filtration and drying of the second precipitate under reduced pressure as white solid (63.9 mg, 272 µmol, 17%). Coupling of phosphorous to both aromatic protons detected by ^{1}H,^{31}P-HMBC indicated the formation of τ-pHis. ^{1}H NMR (600 MHz, D_2O) δ 7.60 (d, J = 1.1 Hz, 1H), 6.92 (d, J = 1.4 Hz, 1H), 3.76 (dd, J = 8.6, 4.6 Hz, 1H), 2.99 (d, J = 4.6 Hz, 1H), 2.85 (dd, J = 15.3, 8.5 Hz, 1H). ^{31}P NMR (243 MHz, D_2O) δ -4.49. ^{13}C NMR (151 MHz, D_2O) δ 174.47, 139.20, 136.27, 134.43, 131.89, 118.43, 118.40, 117.09, 54.68, 28.71. HR-MS for $C_6H_{10}N_3O_5P$: m/z calc. $[M+H^+]^+ = 236.0431$, m/z obs. $[M+H^+]^+ = 236.0428$.

3 Optimization of Assay Conditions

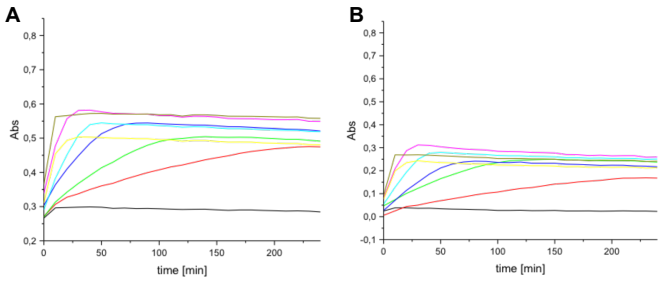

Figure S1: Example of reaction from assay optimization. Absorbance measurements over time of incubation of 100 µM **25a** with varying amounts of LHPP before **A** and after **B** background subtraction. — no enzyme, — 0.03125 µg, — 0.0625 µg, — 0.125 µg, — 0.25 µg, — 0.5 µg, — 0.75 µg, — 1 µg.

In order to gain valuable kinetic data in maximum 120 min assay time, optimal substrate as well as enzyme concentrations needed to be determined. Therefore, varying amounts of pLys **25a** (0 to 250 µmol·L^{-1}) were incubated with varying amounts of LHPP (0 to 1 µg, purchased at ProSpec-Tany TechnoGene Ltd. International, Ness-Ziona, Israel) for 240 min. Absorbance at 360 nm was recorded every ten minutes. Substrate—LHPP combinations were evaluated regarding their kinetic

profile within 90 min reaction time. Hence, 100 µM substrate **25a** with 0.25 µg enzyme ($7.4 \cdot 10^{-3}$ nmol, $3.7 \cdot 10^{-4}$ eq.) were identified as the optimal standard conditions.

4 Computational Methods

4.1 Molecular Docking

First, we used molecular docking (MD) to explore possible binding poses of GGpKGG with the LHPP, where the residues around the catalytic center (Mg^{2+}) of the crystal structure (PDB ID: 2x4d) were defined as the center of the docking pocket. A receptor grid was calculated for LHPP with a box size of 10 Åx 10 Åx 10 Å. We built an atomistic structure of GGpKGG using the software Schrödinger with both *C*- and *N*-termini capped with *N*-methyl (NME) and acetyl (ACE) groups, respectively. The structure was energy-minimized to a convergence threshold of 0.05 $kJ \cdot mol^{-1} \cdot Å^{-1}$ in at most 2500 iterations, where the OPLS3 force field [9] with the implicit GB/SA water solvent model [10] was employed. Docking of the GGpKGG into the pocket was carried out using the Glide module [11–13] implemented in the program Schrödinger. Out of ten docking poses with highest scores, we selected those poses where the phosphate groups of the phosphorylated lysine (pLys) and the one in the crystal structure overlap significantly. From the remaining seven poses, only four of them show significant variation in the binding conformation of GGpKGG with LHPP and they are selected in the subsequent MD simulations.

4.2 Generating AMBER Force Field Parameter for Phosphorylated Lysine

As there are no standard force field parameters available for pLys, we followed the previously described approach for generating AMBER force field parameter of this modified amino acid. [14] Firstly, we build a structural model of the ACE- and NME-capped pLys (Figure S2), where the initial side chain of the pLys adopts the most extended conformation. The structural model was optimized at the HF/6-31G(d) level of theory [15,16] with the P–N bond being restrained. We observed otherwise a break of the N-P bond during the optimization. This observation is not fully unexpected, as previous experiments revealed the intrinsic acid lability of the P–N phosphoramidate bond. [17] Structural optimization was performed using Gaussian16. [18] Restrained electrostatic potential (RESP) charges of the pLys were derived from the calculation of the electrostatic potential of the optimized structure, where the atomic charges of the ACE and NME groups were constrained to their values in the parm99 parameter set. This procedure was performed using the program antechamber. [19,20] The RESP atomic charges of the pLys in fully deprotonated form is shown in Table S4. Following the previous strategy, [14] we only introduced the missing parameters related to atoms p5, O, N4 and H, while all the other parameters were adapted from available AMBER parameters. As in the unrestrained optimization the N-P bond was broken, we could not get information for the bond length. Here the previously reported N–P bond length for the other phosphorylated amino acids was adopted. [14] The other missing parameters were derived from the antechamber software and further converted into the Gromacs topology format using program ACPYPE. [21] All the newly introduced parameters are giving in Table S5.

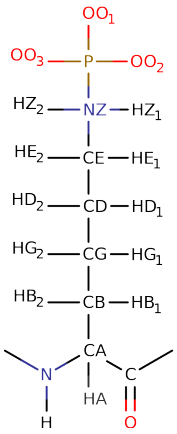

Figure S2: Atom names of the pLys.

Table S4: RESP atomic charges of the pLys in the deprotonated form, where the corresponding atom names are shown in Figure S2.

Atom	RESP atomic charge	Atom	RESP atomic charge
N	-0.4978	**CD**	-0.1166
H	0.2936	**HD**	0.0382
CA	0.1955	**CE**	0.5852
HA	0.0232	**HE**	-0.0805
CB	-0.0152	**NZ**	-0.9358
HB	0.0258	**HZ**	0.4193
CG	0.0358	**P**	1.3509
HG	-0.0100	**OO**	-0.8783

Table S5: New parameters for the pLys.

Atom	ϵ **[kJ·mol^{-1}]**	σ **[nm]**
P	$3.74177 \cdot 10^{-1}$	$8.36800 \cdot 10^{-1}$
OO	$2.9599 \cdot 10^{-1}$	$8.78640 \cdot 10^{-1}$
NZ	$3.25000 \cdot 10^{-1}$	$7.11280 \cdot 10^{-1}$
HZ	$1.06908 \cdot 10^{-1}$	$6.56888 \cdot 10^{-2}$
Bond	$\mathbf{r}_{eq}$ **[nm]**	$\mathbf{k}_r$ **[kJ·mol^{-1}·nm^{-2}]**
CE-N4	$1.4990 \cdot 10^{-1}$	$2.4568 \cdot 10^{5}$
NZ-HZ	$1.0330 \cdot 10^{-1}$	$3.0878 \cdot 10^{5}$
NZ-P	$1.8400 \cdot 10^{-1}$	$1.0460 \cdot 10^{5}$
P-OO	$1.4810 \cdot 10^{-1}$	$4.0811 \cdot 10^{5}$
Angles	θ_{eq} [°]	$\mathbf{K}_{eq}$ **[kJ·mol^{-1}·rad^{-2}]**
CD-CE-NZ	$1.1432 \cdot 10^{2}$	$5.3932 \cdot 10^{2}$
HE-CE-NZ	$1.0791 \cdot 10^{2}$	$4.1020 \cdot 10^{2}$
CE-NZ-HZ	$1.1011 \cdot 10^{2}$	$3.8652 \cdot 10^{2}$
CE-NZ-P	$1.1322 \cdot 10^{2}$	$4.9664 \cdot 10^{2}$
HZ1-NZ-HZ2	$1.0811 \cdot 10^{2}$	$3.3907 \cdot 10^{2}$
NZ-P-OO	$1.0978 \cdot 10^{2}$	$5.4969 \cdot 10^{2}$
P-NZ-HZ	$1.1000 \cdot 10^{2}$	$3.3916 \cdot 10^{2}$
OO1-P-OO2	$1.1580 \cdot 10^{2}$	$6.1530 \cdot 10^{2}$
Dihedrals	**K [kJ·mol^{-1}]**	
CG-CD-CE-NZ	0.65084	
HD-CD-CE-NZ	0.65084	
CD-CE-NZ-P	0.65084	
P-NZ-CE-HE	0.65084	
CD-CE-NZ-HZ	0.65084	
HE-CE-NZ-HZ	0.65084	
CE-NZ-P-OO	0.37191	
OO-P-NZ-HZ	0.37191	

4.3 Equilibrium MD Simulations

For the MD simulations, dimeric structure of LHPP (PDB ID: 2x4d) with one GGpKGG peptide chain bound at chain A of LHPP was used. In the starting structure of the systems listed in Table S3, the peptide was manually mutated in Pymol.[22] The LHPP-peptide complexes were solvated in the SPC/E water.[23] We added 100 mM NaCl together with one Mg^{2+} at its crystallographic position in the catalytic center. Amber99SB*ILDN force field[24] was employed for both LHPP and the peptide. In order to prevent a net charge change during the non-equilibrium transition from non-charged residue to the charged one, we used a double-system/single-box approach for those charged peptides (Table

S6).[25,26] For the equilibration, we performed a 10 ns simulation starting from each docking poses by positionally restraining the heavy atoms with a force constant of 1000 kJ·mol^{-1}·nm^{-2} and further relaxed the system by releasing the position restraints for 20 ns. Starting from the end states of the equilibrium simulations, production runs were performed for each of the four docking poses. For the double-system/double-box setups 4 independent runs of 100 ns were performed for the LHPP-complexes, while for the double-system/single-box setup two runs of 100 ns were carried out for the entire system. Furthermore, for the double-system/double-box setups one production run of 100 ns was performed independently for the solvated peptide itself. In the double-system/single-box setups, we kept the distance to be at least 3 nm between the single peptide chain and the LHPP-peptide complex.[27] To avoid two systems became closer during the simulations, position restraints on a single backbone atom close to the center of mass of the LHPP as well as the peptide were applied. Both in equilibration and production simulations, NPT ensembles were generated using velocity rescaling as temperature coupling thermosta[28] at 300 K with the time constant of 0.1 ps and Parrinello-Rahman as pressure coupling barostat[29] at 1 bar with the time constant of 4 ps. Short-range electrostatic interactions were calculated with a cutoff of 1.0 nm, whereas long-range electrostatic interactions were treated by the particle mesh Ewald method.[30,31] The cutoff for van-der-Waals interactions were set to 1.0 nm. All bonds were constrained with the LINCS algorithm.[32] All the MD simulations were performed with the software package Gromacs version 5.1.2.[33,34]

Table S6: System used in the MD simulations.

System	Method
GApKGG	double-system/double-box
GSpKGG	double-system/double-box
GKpKGG	double-system/single-box
GRpKGG	double-system/single-box
GGpKAG	double-system/double-box
GGpKSG	double-system/double-box
GGpKKG	double-system/single-box
GGpKRG	double-system/single-box

4.4 Non-Equilibrium Transition and Analysis

For each equilibrium simulation of 100 ns the first 10 ns was discarded. From the remaining trajectory one frame was extracted after every 1.8 ns, so that in total 50 frames were obtained. Using the pmx software package,[26,35] hybrid structures and topologies were generated comprising the states before and after the mutation. It is important to note that a single topology approach[36] was applied here. The generated hybrid structures were firstly energy-minimized using steepest descent algorithm to a convergence threshold of 10 kJ·mol^{-1}·nm^{-1} in at most 2000 iterations. Subsequently, 20 ps of equilibrium simulations with NPT were carried out. Starting from the end states of the equilibrium simulations, 100 ps of non-equilibrium transitions were performed from the WT to the mutated state (e.g. GGpKGG->GApKGG) and back (e.g. GApKGG-> GGpKGG). The non-equilibrium work values were recorded for every transition. Expect otherwise stated, in the non-equilibrium simulations all

the parameters kept the same as they were in the equilibrium simulations described above. From the output of the work values obtained from the non-equilibrium simulations, the free energy differences were estimated using Crooks Gaussian Intersection (CGI) and Bennet's Acceptance Ratio (BAR) methods [37] that are implemented in the pmx. [26,35]

4.5 Free Energy Differences Upon Mutation

Table S7: Calculated ΔΔG and errors of eight mutated substrates relative to the wild type model substrate **2a** estimated from the MD simulations starting from four different docking poses. CGI and BAR estimators were employed for the analysis of ΔΔG.

Substrate	Description	Docking pose	$\Delta\Delta G_{CGI}$ [kJ·mol^{-1}]	Error ±	$\Delta\Delta G_{BAR}$ [kJ·mol^{-1}]	Error ±
3a	Ala_N	**1**	1.34	1.07	3.18	0.69
		2	-2.41	1.06	-0.55	0.44
		3	-0.77	1.02	-0.03	1.34
		4	3.00	1.03	4.69	0.51
3f	Lys_N	**1**	24.49	3.45	22.49	0.83
		2	-15.32	2.45	-9.70	0.82
		3	-15.57	2.17	-11.58	0.83
		4	27.26	2.31	21.83	0.98
3i	Arg_N	**1**	-7.89	4.53	-7.89	2.67
		2	-4.99	3.80	-4.38	2.70
		3	-0.9	5.57	-0.5	2.57
		4	22.43	4.46	13.28	2.22
3j	Ser_N	**1**	6.27	0.88	7.79	0.87
		2	-1.04	0.84	1.66	0.83
		3	-1.25	0.83	0.21	0.67
		4	8.27	0.85	7.79	0.63
4a	Ala_C	**1**	2.30	0.69	1.89	0.54
		2	-2.15	0.62	-1.14	0.46
		3	0.36	0.60	0.70	0.47
		4	3.59	0.59	4.80	0.38
4f	Lys_C	**1**	0.75	3.41	-2.78	2.20
		2	-14.58	2.48	-10.92	2.04
		3	-18.96	2.75	-15.38	1.97
		4	-13.84	2.49	-11.95	1.84
4i	Arg_C	**1**	9.88	4.58	9.88	2.65
		2	0.53	3.22	-1.68	1.60
		3	9.16	3.35	2.95	2.46

		4	22.33	4.32	10.61	2.74
4j	Ser_C	**1**	8.73	1.35	6.11	1.24
		2	-0.62	1.17	-2.07	0.64
		3	-4.10	1.20	-4.93	0.82
		4	1.89	1.34	-2.31	0.60

4.6 Protein Data Bank (PDB) Files for 2a

The coordinates in the PDBs of four docking poses for peptide **2a** are referenced to the PDB structure of the LHPP (PDB ID: 2X4D)

Pose 1

ATOM 1 HH31 ACE A 1 27.157 9.422 98.476 0.00 0.00 H
ATOM 2 CH3 ACE A 1 26.844 10.375 98.044 0.00 0.00 C
ATOM 3 HH32 ACE A 1 27.042 11.163 98.772 0.00 0.00 H
ATOM 4 HH33 ACE A 1 27.456 10.566 97.160 0.00 0.00 H
ATOM 5 C ACE A 1 25.359 10.335 97.698 0.00 0.00 C
ATOM 6 O ACE A 1 24.520 10.274 98.598 0.00 0.00 O
ATOM 7 N GLY A 2 25.049 10.374 96.390 0.00 0.00 N
ATOM 8 H GLY A 2 25.797 10.421 95.713 0.00 0.00 H
ATOM 9 CA GLY A 2 23.686 10.368 95.856 0.00 0.00 C
ATOM 10 HA1 GLY A 2 23.085 9.611 96.365 0.00 0.00 H
ATOM 11 HA2 GLY A 2 23.705 10.100 94.799 0.00 0.00 H
ATOM 12 C GLY A 2 23.029 11.748 95.991 0.00 0.00 C
ATOM 13 O GLY A 2 23.697 12.767 96.179 0.00 0.00 O
ATOM 14 N GLY A 3 21.692 11.752 95.877 0.00 0.00 N
ATOM 15 H GLY A 3 21.215 10.877 95.715 0.00 0.00 H
ATOM 16 CA GLY A 3 20.847 12.932 96.028 0.00 0.00 C
ATOM 17 HA1 GLY A 3 19.928 12.757 95.467 0.00 0.00 H
ATOM 18 HA2 GLY A 3 21.311 13.813 95.587 0.00 0.00 H
ATOM 19 C GLY A 3 20.501 13.168 97.508 0.00 0.00 C
ATOM 20 O GLY A 3 21.129 12.629 98.421 0.00 0.00 O
ATOM 21 N LYP A 4 19.439 13.967 97.722 0.00 0.00 N
ATOM 22 H LYP A 4 19.013 14.410 96.921 0.00 0.00 H
ATOM 23 CA LYP A 4 18.640 14.052 98.950 0.00 0.00 C
ATOM 24 HA LYP A 4 19.310 14.153 99.802 0.00 0.00 H
ATOM 25 CB LYP A 4 17.741 15.335 98.880 0.00 0.00 C
ATOM 26 HB1 LYP A 4 17.081 15.255 98.016 0.00 0.00 H
ATOM 27 HB2 LYP A 4 17.090 15.355 99.752 0.00 0.00 H
ATOM 28 CG LYP A 4 18.473 16.717 98.819 0.00 0.00 C
ATOM 29 HG1 LYP A 4 19.076 16.838 99.720 0.00 0.00 H
ATOM 30 HG2 LYP A 4 19.177 16.725 97.988 0.00 0.00 H

ATOM 31 CD LYP A 4 17.524 17.948 98.672 0.00 0.00 C
ATOM 32 HD1 LYP A 4 16.899 17.800 97.790 0.00 0.00 H
ATOM 33 HD2 LYP A 4 16.848 17.963 99.528 0.00 0.00 H
ATOM 34 CE LYP A 4 18.223 19.340 98.563 0.00 0.00 C
ATOM 35 HE1 LYP A 4 18.822 19.514 99.458 0.00 0.00 H
ATOM 36 HE2 LYP A 4 18.904 19.337 97.712 0.00 0.00 H
ATOM 37 NZ LYP A 4 17.260 20.443 98.388 0.00 0.00 N
ATOM 38 HZ1 LYP A 4 16.758 20.212 97.542 0.00 0.00 H
ATOM 39 HZ2 LYP A 4 16.571 20.290 99.110 0.00 0.00 H
ATOM 40 P LYP A 4 17.828 22.073 98.384 0.00 0.00 P
ATOM 41 O1 LYP A 4 17.281 22.697 97.156 0.00 0.00 O
ATOM 42 O2 LYP A 4 17.307 22.767 99.588 0.00 0.00 O
ATOM 43 O3 LYP A 4 19.305 21.967 98.387 0.00 0.00 O
ATOM 44 C LYP A 4 17.849 12.715 99.132 0.00 0.00 C
ATOM 45 O LYP A 4 18.106 11.747 98.404 0.00 0.00 O
ATOM 46 N GLY A 5 16.905 12.646 100.091 0.00 0.00 N
ATOM 47 H GLY A 5 16.740 13.447 100.684 0.00 0.00 H
ATOM 48 CA GLY A 5 15.978 11.506 100.239 0.00 0.00 C
ATOM 49 HA1 GLY A 5 15.433 11.376 99.304 0.00 0.00 H
ATOM 50 HA2 GLY A 5 15.233 11.690 101.010 0.00 0.00 H
ATOM 51 C GLY A 5 16.686 10.192 100.608 0.00 0.00 C
ATOM 52 O GLY A 5 16.329 9.142 100.070 0.00 0.00 O
ATOM 53 N GLY A 6 17.713 10.272 101.471 0.00 0.00 N
ATOM 54 H GLY A 6 17.949 11.174 101.862 0.00 0.00 H
ATOM 55 CA GLY A 6 18.653 9.187 101.742 0.00 0.00 C
ATOM 56 HA1 GLY A 6 18.169 8.210 101.693 0.00 0.00 H
ATOM 57 HA2 GLY A 6 19.033 9.308 102.756 0.00 0.00 H
ATOM 58 C GLY A 6 19.821 9.281 100.744 0.00 0.00 C
ATOM 59 O GLY A 6 20.214 10.373 100.336 0.00 0.00 O
ATOM 60 N NME A 7 20.398 8.122 100.387 0.00 0.00 N
ATOM 61 H NME A 7 20.060 7.252 100.772 0.00 0.00 H
ATOM 62 CH3 NME A 7 21.530 8.044 99.472 0.00 0.00 C
ATOM 63 HH31 NME A 7 21.653 7.020 99.118 0.00 0.00 H
ATOM 64 HH32 NME A 7 22.449 8.347 99.976 0.00 0.00 H
ATOM 65 HH33 NME A 7 21.387 8.686 98.602 0.00 0.00 H

Pose 2

ATOM 1 HH31 ACE B 1 16.264 4.475 96.002 0.00 0.00 H
ATOM 2 CH3 ACE B 1 15.971 5.525 96.043 0.00 0.00 C
ATOM 3 HH32 ACE B 1 16.384 6.027 95.168 0.00 0.00 H
ATOM 4 HH33 ACE B 1 14.882 5.573 95.986 0.00 0.00 H
ATOM 5 C ACE B 1 16.497 6.172 97.322 0.00 0.00 C

ATOM 6 O ACE B 1 17.710 6.222 97.525 0.00 0.00 O
ATOM 7 N GLY B 2 15.578 6.662 98.173 0.00 0.00 N
ATOM 8 H GLY B 2 14.601 6.587 97.931 0.00 0.00 H
ATOM 9 CA GLY B 2 15.883 7.297 99.458 0.00 0.00 C
ATOM 10 HA1 GLY B 2 16.663 6.745 99.983 0.00 0.00 H
ATOM 11 HA2 GLY B 2 14.989 7.254 100.080 0.00 0.00 H
ATOM 12 C GLY B 2 16.308 8.765 99.288 0.00 0.00 C
ATOM 13 O GLY B 2 16.506 9.246 98.170 0.00 0.00 O
ATOM 14 N GLY B 3 16.451 9.461 100.434 0.00 0.00 N
ATOM 15 H GLY B 3 16.280 8.972 101.302 0.00 0.00 H
ATOM 16 CA GLY B 3 16.782 10.886 100.575 0.00 0.00 C
ATOM 17 HA1 GLY B 3 16.931 11.108 101.632 0.00 0.00 H
ATOM 18 HA2 GLY B 3 15.927 11.477 100.242 0.00 0.00 H
ATOM 19 C GLY B 3 18.041 11.312 99.802 0.00 0.00 C
ATOM 20 O GLY B 3 18.900 10.481 99.505 0.00 0.00 O
ATOM 21 N LYP B 4 18.106 12.621 99.493 0.00 0.00 N
ATOM 22 H LYP B 4 17.360 13.210 99.833 0.00 0.00 H
ATOM 23 CA LYP B 4 19.009 13.304 98.553 0.00 0.00 C
ATOM 24 HA LYP B 4 18.510 13.252 97.587 0.00 0.00 H
ATOM 25 CB LYP B 4 19.128 14.792 98.930 0.00 0.00 C
ATOM 26 HB1 LYP B 4 19.362 14.908 99.987 0.00 0.00 H
ATOM 27 HB2 LYP B 4 19.987 15.189 98.393 0.00 0.00 H
ATOM 28 CG LYP B 4 17.906 15.661 98.576 0.00 0.00 C
ATOM 29 HG1 LYP B 4 17.538 15.381 97.588 0.00 0.00 H
ATOM 30 HG2 LYP B 4 17.087 15.460 99.267 0.00 0.00 H
ATOM 31 CD LYP B 4 18.273 17.157 98.603 0.00 0.00 C
ATOM 32 HD1 LYP B 4 18.251 17.508 99.633 0.00 0.00 H
ATOM 33 HD2 LYP B 4 19.305 17.267 98.281 0.00 0.00 H
ATOM 34 CE LYP B 4 17.420 18.051 97.682 0.00 0.00 C
ATOM 35 HE1 LYP B 4 17.303 17.567 96.713 0.00 0.00 H
ATOM 36 HE2 LYP B 4 16.411 18.198 98.069 0.00 0.00 H
ATOM 37 NZ LYP B 4 18.106 19.313 97.411 0.00 0.00 N
ATOM 38 HZ1 LYP B 4 19.084 19.084 97.314 0.00 0.00 H
ATOM 39 HZ2 LYP B 4 17.828 19.550 96.470 0.00 0.00 H
ATOM 40 P LYP B 4 17.781 20.584 98.487 0.00 0.00 P
ATOM 41 O1 LYP B 4 17.706 19.962 99.833 0.00 0.00 O
ATOM 42 O2 LYP B 4 18.905 21.549 98.387 0.00 0.00 O
ATOM 43 O3 LYP B 4 16.499 21.150 97.988 0.00 0.00 O
ATOM 44 C LYP B 4 20.419 12.709 98.362 0.00 0.00 C
ATOM 45 O LYP B 4 21.155 12.544 99.336 0.00 0.00 O
ATOM 46 N GLY B 5 20.758 12.423 97.092 0.00 0.00 N
ATOM 47 H GLY B 5 20.091 12.602 96.355 0.00 0.00 H
ATOM 48 CA GLY B 5 22.033 11.837 96.683 0.00 0.00 C

ATOM 49 HA1 GLY B 5 22.861 12.390 97.132 0.00 0.00 H
ATOM 50 HA2 GLY B 5 22.132 11.929 95.601 0.00 0.00 H
ATOM 51 C GLY B 5 22.101 10.352 97.068 0.00 0.00 C
ATOM 52 O GLY B 5 21.073 9.681 97.188 0.00 0.00 O
ATOM 53 N GLY B 6 23.333 9.847 97.247 0.00 0.00 N
ATOM 54 H GLY B 6 24.133 10.451 97.121 0.00 0.00 H
ATOM 55 CA GLY B 6 23.618 8.466 97.641 0.00 0.00 C
ATOM 56 HA1 GLY B 6 24.681 8.274 97.494 0.00 0.00 H
ATOM 57 HA2 GLY B 6 23.076 7.773 96.993 0.00 0.00 H
ATOM 58 C GLY B 6 23.264 8.202 99.115 0.00 0.00 C
ATOM 59 O GLY B 6 23.121 9.129 99.916 0.00 0.00 O
ATOM 60 N NME B 7 23.152 6.911 99.458 0.00 0.00 N
ATOM 61 H NME B 7 23.294 6.196 98.759 0.00 0.00 H
ATOM 62 CH3 NME B 7 22.833 6.461 100.804 0.00 0.00 C
ATOM 63 HH31 NME B 7 22.672 5.383 100.804 0.00 0.00 H
ATOM 64 HH32 NME B 7 21.927 6.940 101.178 0.00 0.00 H
ATOM 65 HH33 NME B 7 23.655 6.681 101.487 0.00 0.00 H
ATOM 1 HH31 ACE C 1 27.277 9.840 99.438 0.00 0.00 H

Pose 3

ATOM 2 CH3 ACE C 1 26.900 10.768 99.008 0.00 0.00 C
ATOM 3 HH32 ACE C 1 26.766 11.490 99.813 0.00 0.00 H
ATOM 4 HH33 ACE C 1 27.654 11.157 98.323 0.00 0.00 H
ATOM 5 C ACE C 1 25.572 10.520 98.299 0.00 0.00 C
ATOM 6 O ACE C 1 24.622 10.053 98.927 0.00 0.00 O
ATOM 7 N GLY C 2 25.518 10.837 96.993 0.00 0.00 N
ATOM 8 H GLY C 2 26.343 11.215 96.549 0.00 0.00 H
ATOM 9 CA GLY C 2 24.341 10.670 96.139 0.00 0.00 C
ATOM 10 HA1 GLY C 2 23.933 9.665 96.256 0.00 0.00 H
ATOM 11 HA2 GLY C 2 24.651 10.770 95.100 0.00 0.00 H
ATOM 12 C GLY C 2 23.261 11.722 96.438 0.00 0.00 C
ATOM 13 O GLY C 2 23.532 12.767 97.033 0.00 0.00 O
ATOM 14 N GLY C 3 22.029 11.425 95.993 0.00 0.00 N
ATOM 15 H GLY C 3 21.887 10.554 95.502 0.00 0.00 H
ATOM 16 CA GLY C 3 20.841 12.255 96.191 0.00 0.00 C
ATOM 17 HA1 GLY C 3 20.096 11.970 95.449 0.00 0.00 H
ATOM 18 HA2 GLY C 3 21.073 13.306 96.015 0.00 0.00 H
ATOM 19 C GLY C 3 20.246 12.062 97.597 0.00 0.00 C
ATOM 20 O GLY C 3 20.602 11.134 98.326 0.00 0.00 O
ATOM 21 N LYP C 4 19.308 12.958 97.947 0.00 0.00 N
ATOM 22 H LYP C 4 19.075 13.689 97.291 0.00 0.00 H
ATOM 23 CA LYP C 4 18.531 12.976 99.188 0.00 0.00 C

ATOM 24 HA LYP C 4 19.261 12.988 99.990 0.00 0.00 H
ATOM 25 CB LYP C 4 17.702 14.275 99.210 0.00 0.00 C
ATOM 26 HB1 LYP C 4 17.215 14.395 98.243 0.00 0.00 H
ATOM 27 HB2 LYP C 4 16.906 14.205 99.953 0.00 0.00 H
ATOM 28 CG LYP C 4 18.507 15.547 99.494 0.00 0.00 C
ATOM 29 HG1 LYP C 4 18.907 15.498 100.506 0.00 0.00 H
ATOM 30 HG2 LYP C 4 19.362 15.605 98.820 0.00 0.00 H
ATOM 31 CD LYP C 4 17.661 16.822 99.346 0.00 0.00 C
ATOM 32 HD1 LYP C 4 17.291 16.899 98.323 0.00 0.00 H
ATOM 33 HD2 LYP C 4 16.784 16.765 99.988 0.00 0.00 H
ATOM 34 CE LYP C 4 18.477 18.065 99.711 0.00 0.00 C
ATOM 35 HE1 LYP C 4 18.835 17.982 100.738 0.00 0.00 H
ATOM 36 HE2 LYP C 4 19.347 18.107 99.073 0.00 0.00 H
ATOM 37 NZ LYP C 4 17.705 19.294 99.604 0.00 0.00 N
ATOM 38 HZ1 LYP C 4 16.763 19.052 99.876 0.00 0.00 H
ATOM 39 HZ2 LYP C 4 18.031 19.851 100.381 0.00 0.00 H
ATOM 40 P1 LYP C 4 17.812 20.161 98.153 0.00 0.00 P
ATOM 41 O1 LYP C 4 18.906 21.138 98.387 0.00 0.00 O
ATOM 42 O2 LYP C 4 18.105 19.167 97.085 0.00 0.00 O
ATOM 43 O3 LYP C 4 16.492 20.820 97.987 0.00 0.00 O
ATOM 44 C LYP C 4 17.611 11.749 99.375 0.00 0.00 C
ATOM 45 O LYP C 4 17.171 11.167 98.387 0.00 0.00 O
ATOM 46 N GLY C 5 17.306 11.390 100.637 0.00 0.00 N
ATOM 47 H GLY C 5 17.698 11.924 101.400 0.00 0.00 H
ATOM 48 CA GLY C 5 16.423 10.277 101.013 0.00 0.00 C
ATOM 49 HA1 GLY C 5 15.397 10.525 100.732 0.00 0.00 H
ATOM 50 HA2 GLY C 5 16.440 10.168 102.098 0.00 0.00 H
ATOM 51 C GLY C 5 16.859 8.950 100.368 0.00 0.00 C
ATOM 52 O GLY C 5 18.029 8.573 100.449 0.00 0.00 O
ATOM 53 N GLY C 6 15.902 8.269 99.715 0.00 0.00 N
ATOM 54 H GLY C 6 14.961 8.636 99.713 0.00 0.00 H
ATOM 55 CA GLY C 6 16.135 7.083 98.887 0.00 0.00 C
ATOM 56 HA1 GLY C 6 15.224 6.485 98.878 0.00 0.00 H
ATOM 57 HA2 GLY C 6 16.924 6.458 99.306 0.00 0.00 H
ATOM 58 C GLY C 6 16.487 7.476 97.440 0.00 0.00 C
ATOM 59 O GLY C 6 16.505 8.653 97.076 0.00 0.00 O
ATOM 60 N NME C 7 16.763 6.459 96.610 0.00 0.00 N
ATOM 61 H NME C 7 16.744 5.512 96.961 0.00 0.00 H
ATOM 62 CH3 NME C 7 17.101 6.631 95.202 0.00 0.00 C
ATOM 63 1HH3 NME C 7 16.830 5.734 94.646 0.00 0.00 H
ATOM 64 2HH3 NME C 7 18.173 6.790 95.088 0.00 0.00 H
ATOM 66 3HH3 NME C 7 16.574 7.473 94.752 0.00 0.00 H

Pose 4

ATOM 1 1HH3 ACE D 1 28.267 12.981 95.983 1.00 0.00 H
ATOM 2 CH3 ACE D 1 27.944 11.968 95.755 1.00 0.00 C
ATOM 3 2HH3 ACE D 1 28.576 11.579 94.956 1.00 0.00 H
ATOM 4 3HH3 ACE D 1 28.104 11.353 96.641 1.00 0.00 H
ATOM 5 C ACE D 1 26.481 11.948 95.320 1.00 0.00 C
ATOM 6 O ACE D 1 26.107 12.658 94.387 1.00 0.00 O
ATOM 7 N GLY D 2 25.676 11.105 95.988 1.00 0.00 N
ATOM 8 H GLY D 2 26.062 10.570 96.752 1.00 0.00 H
ATOM 9 CA GLY D 2 24.289 10.809 95.629 1.00 0.00 C
ATOM 10 HA1 GLY D 2 24.034 9.823 96.016 1.00 0.00 H
ATOM 11 HA2 GLY D 2 24.173 10.767 94.545 1.00 0.00 H
ATOM 12 C GLY D 2 23.305 11.841 96.186 1.00 0.00 C
ATOM 13 O GLY D 2 23.675 12.768 96.909 1.00 0.00 O
ATOM 14 N GLY D 3 22.028 11.645 95.818 1.00 0.00 N
ATOM 15 H GLY D 3 21.811 10.851 95.233 1.00 0.00 H
ATOM 16 CA GLY D 3 20.911 12.527 96.139 1.00 0.00 C
ATOM 17 HA1 GLY D 3 20.102 12.312 95.441 1.00 0.00 H
ATOM 18 HA2 GLY D 3 21.190 13.567 95.978 1.00 0.00 H
ATOM 19 C GLY D 3 20.397 12.324 97.572 1.00 0.00 C
ATOM 20 O GLY D 3 20.865 11.466 98.322 1.00 0.00 O
ATOM 21 N LYP D 4 19.385 13.135 97.914 1.00 0.00 N
ATOM 22 H LYP D 4 19.078 13.818 97.236 1.00 0.00 H
ATOM 23 CA LYP D 4 18.575 13.090 99.132 1.00 0.00 C
ATOM 24 HA LYP D 4 19.250 13.105 99.987 1.00 0.00 H
ATOM 25 CB LYP D 4 17.706 14.365 99.148 1.00 0.00 C
ATOM 26 HB1 LYP D 4 17.233 14.484 98.174 1.00 0.00 H
ATOM 27 HB2 LYP D 4 16.906 14.283 99.882 1.00 0.00 H
ATOM 28 CG LYP D 4 18.485 15.643 99.465 1.00 0.00 C
ATOM 29 HG1 LYP D 4 18.906 15.567 100.468 1.00 0.00 H
ATOM 30 HG2 LYP D 4 19.328 15.741 98.782 1.00 0.00 H
ATOM 31 CD LYP D 4 17.609 16.900 99.366 1.00 0.00 C
ATOM 32 HD1 LYP D 4 17.258 17.012 98.340 1.00 0.00 H
ATOM 33 HD2 LYP D 4 16.721 16.797 99.988 1.00 0.00 H
ATOM 34 CE LYP D 4 18.401 18.133 99.808 1.00 0.00 C
ATOM 35 HE1 LYP D 4 18.646 18.053 100.865 1.00 0.00 H
ATOM 36 HE2 LYP D 4 19.343 18.148 99.285 1.00 0.00 H
ATOM 37 NZ LYP D 4 17.706 19.392 99.588 1.00 0.00 N
ATOM 38 HZ1 LYP D 4 16.802 19.278 100.024 1.00 0.00 H
ATOM 39 HZ2 LYP D 4 18.175 20.042 100.202 1.00 0.00 H
ATOM 40 P LYP D 4 17.622 19.995 98.006 1.00 0.00 P
ATOM 41 O1 LYP D 4 16.197 19.906 97.587 1.00 0.00 O

ATOM 42 O2 LYP D 4 18.105 21.395 98.141 1.00 0.00 O
ATOM 43 O3 LYP D 4 18.506 19.128 97.187 1.00 0.00 O
ATOM 44 C LYP D 4 17.706 11.818 99.264 1.00 0.00 C
ATOM 45 O LYP D 4 17.709 10.951 98.388 1.00 0.00 O
ATOM 46 N GLY D 5 16.976 11.740 100.387 1.00 0.00 N
ATOM 47 H GLY D 5 17.031 12.495 101.056 1.00 0.00 H
ATOM 48 CA GLY D 5 16.096 10.630 100.741 1.00 0.00 C
ATOM 49 HA1 GLY D 5 15.683 10.149 99.853 1.00 0.00 H
ATOM 50 HA2 GLY D 5 15.255 11.024 101.311 1.00 0.00 H
ATOM 51 C GLY D 5 16.845 9.599 101.598 1.00 0.00 C
ATOM 52 O GLY D 5 18.035 9.739 101.887 1.00 0.00 O
ATOM 53 N GLY D 6 16.104 8.559 102.015 1.00 0.00 N
ATOM 54 H GLY D 6 15.134 8.512 101.738 1.00 0.00 H
ATOM 55 CA GLY D 6 16.584 7.480 102.878 1.00 0.00 C
ATOM 56 HA1 GLY D 6 17.609 7.202 102.626 1.00 0.00 H
ATOM 57 HA2 GLY D 6 15.963 6.601 102.703 1.00 0.00 H
ATOM 58 C GLY D 6 16.506 7.880 104.360 1.00 0.00 C
ATOM 59 O GLY D 6 16.506 9.064 104.703 1.00 0.00 O
ATOM 60 N NME D 7 16.456 6.859 105.230 0.00 0.00 N
ATOM 61 H NME D 7 16.481 5.914 104.875 0.00 0.00 H
ATOM 62 CH3 NME D 7 16.350 7.008 106.676 0.00 0.00 C
ATOM 63 HH31 NME D 7 15.603 6.312 107.059 0.00 0.00 H
ATOM 64 HH32 NME D 7 16.058 8.013 106.985 0.00 0.00 H
ATOM 65 HH33 NME D 7 17.304 6.768 107.146 0.00 0.00 H
END

5 Chromatograms of Synthesized Peptides

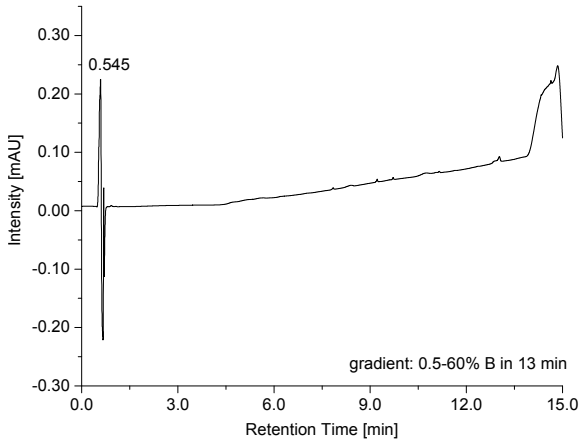

(**A**) pLys **1a**

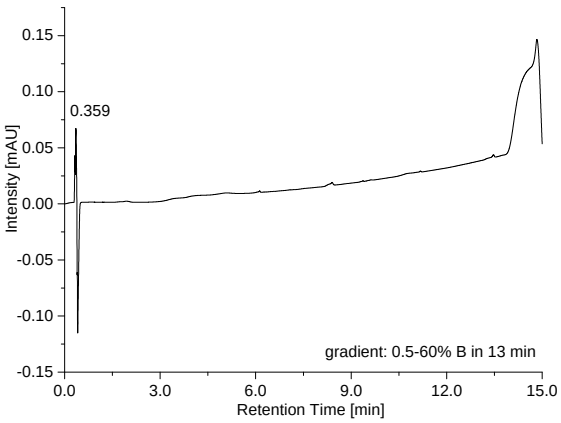

(**B**) pSer **1b**

Figure S3: UPLC-traces (220 nm) of **1a** and **1b**.

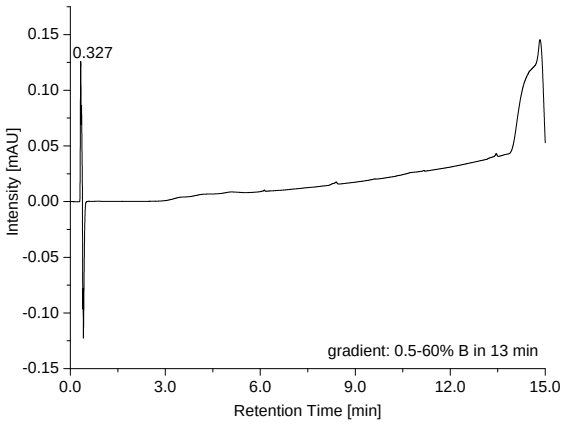

(**A**) pThr **1c**

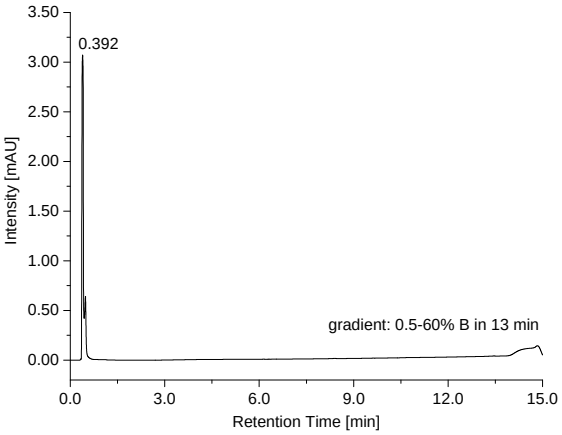

(**B**) pTyr **1d**

Figure S4: UPLC-traces (220 nm) of **1c** and **1d**.

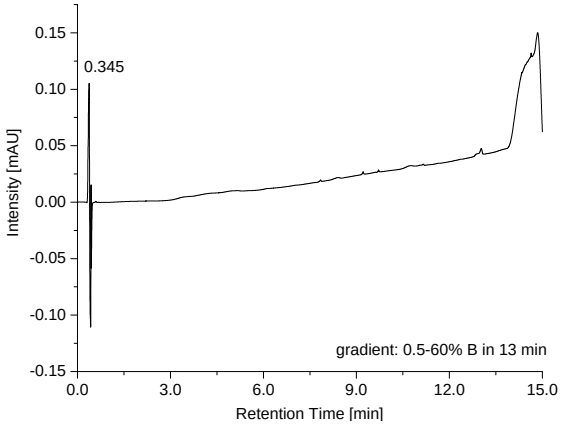

(**A**) pArg **1e**

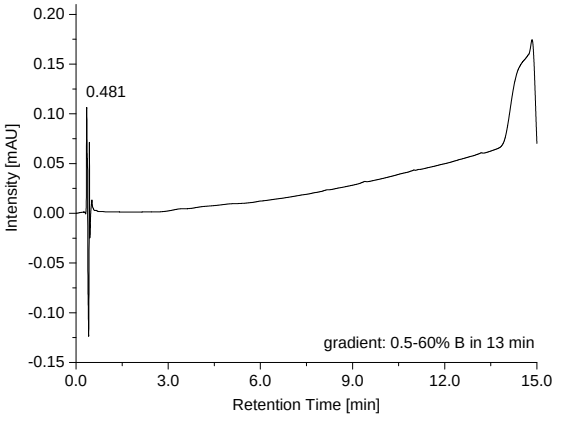

(**B**) ^{Ac}GGpKGG^{CONH_2} **2a**

Figure S5: UPLC-traces (220 nm) of **1e** and **2a**.

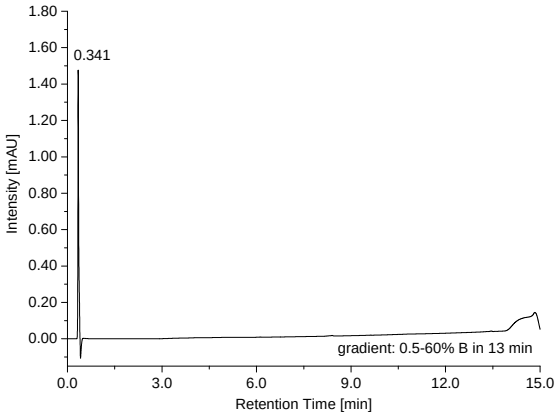

(**A**) ^{Ac}GGpSGG^{CONH_2} **2b**

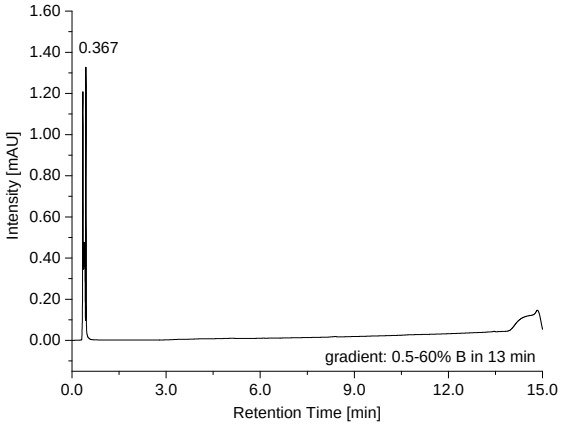

(**B**) ^{Ac}GGpTGG^{CONH_2} **2c**

Figure S6: UPLC-traces (220 nm) of **2b** and **2c**.

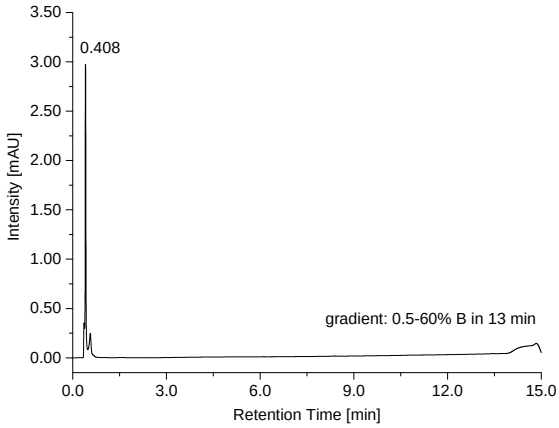

(**A**) ^{Ac}GGpYGG^{CONH_2} **2d**

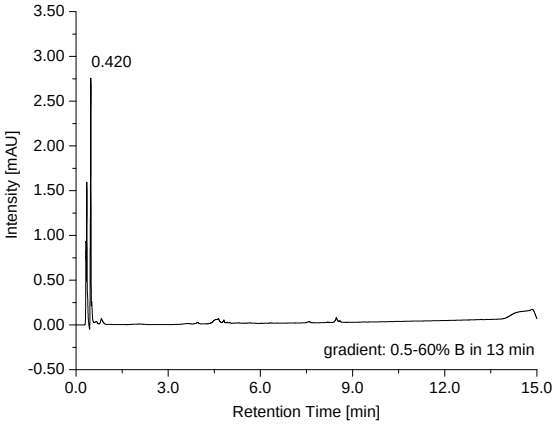

(**B**) ^{Ac}GGpRGG^{CONH_2} **2e**

Figure S7: UPLC-traces (220 nm) of **2d** and **2e**.

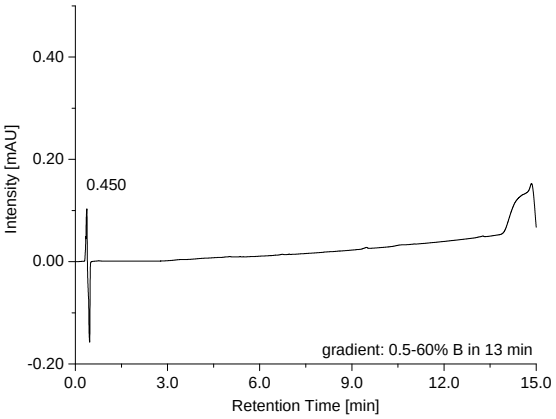

(**A**) ^{Ac}GApKGG^{CONH_2} **3a**

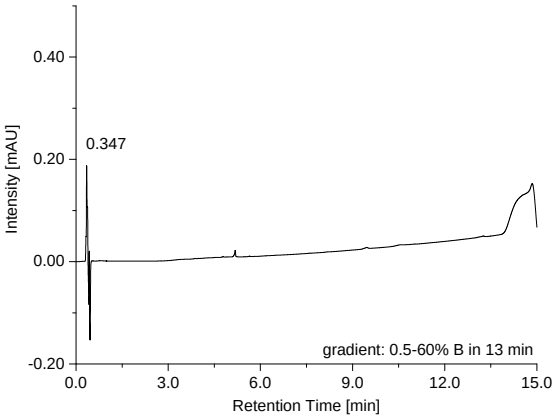

(**B**) ^{Ac}GCpKGG^{CONH_2} **3b**

Figure S8: UPLC-traces (220 nm) of **3a** and **3b**.

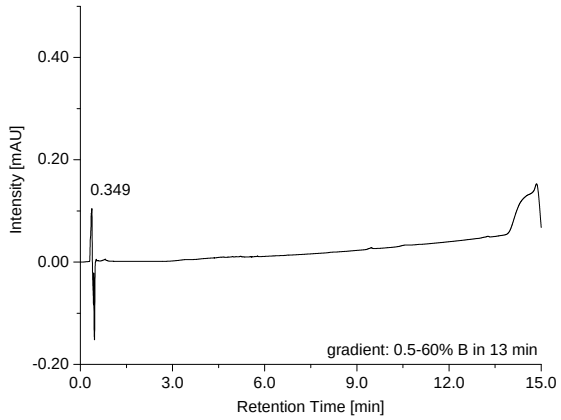

(**A**) ^{Ac}GDpKGG^{CONH_2} **3c**

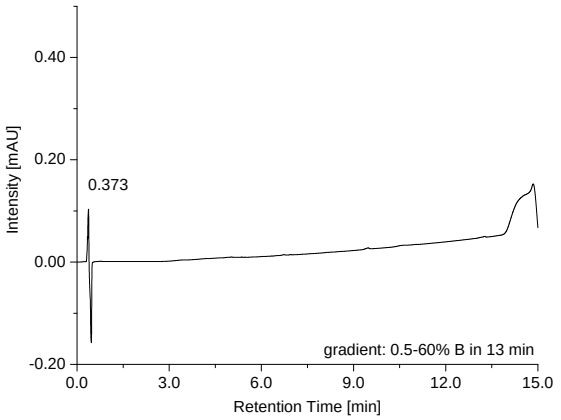

(**B**) ^{Ac}GFpKGG^{CONH_2} **3d**

Figure S9: UPLC-traces (220 nm) of **3c** and **3d**.

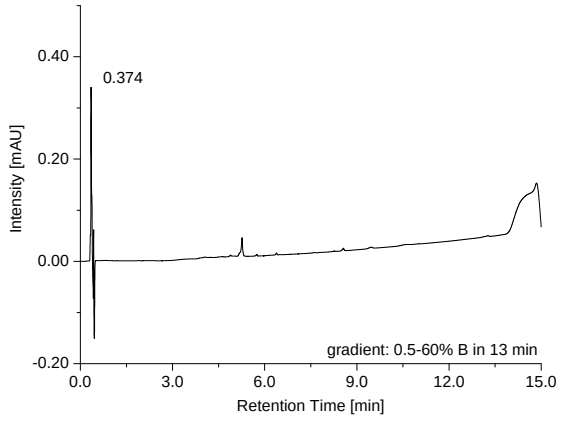

(**A**) ^{Ac}GIpKGG^{CONH_2} **3e**

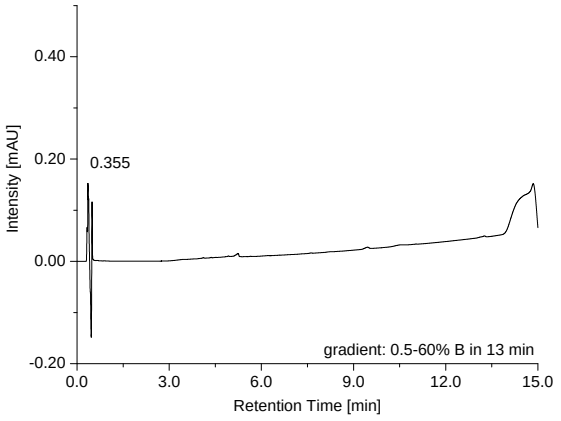

(**B**) ^{Ac}GKpKGG^{CONH_2} **3f**

Figure S10: UPLC-traces (220 nm) of **3e** and **3f**.

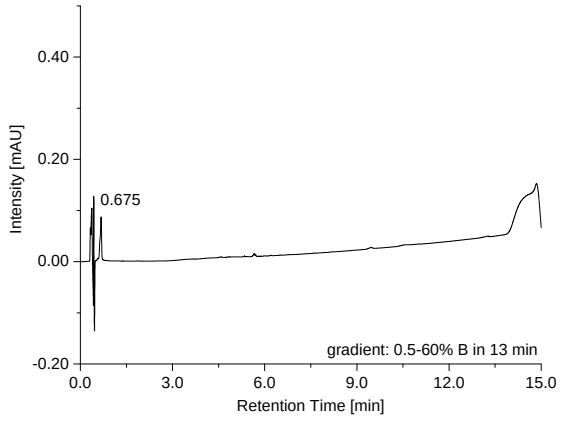

(**A**) ^{Ac}GPpKGG^{CONH_2} **3g**

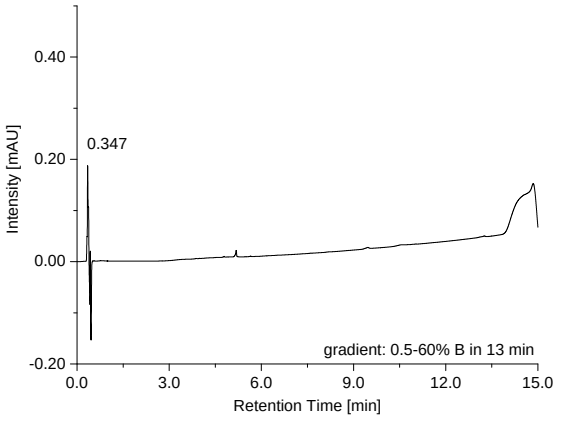

(**B**) ^{Ac}GQpKGG^{CONH_2} **3h**

Figure S11: UPLC-traces (220 nm) of **3g** and **3h**.

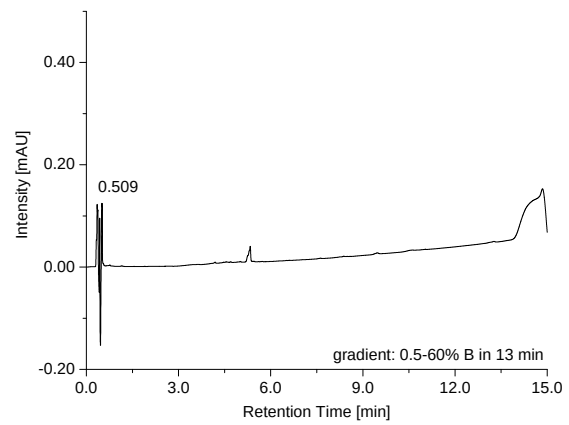

(**A**) ^{Ac}GRpKGG^{CONH_2} **3i**

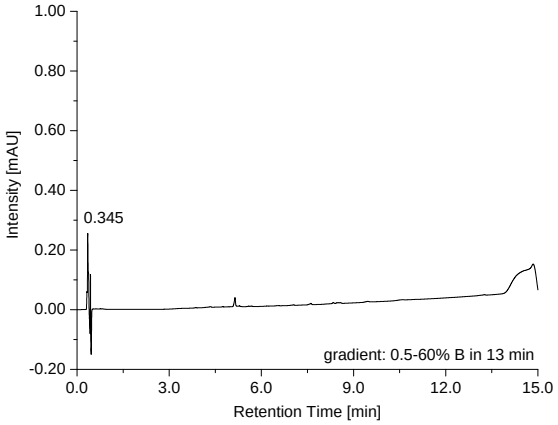

(**B**) ^{Ac}GSpKGG^{CONH_2} **3j**

Figure S12: UPLC-traces (220 nm) of **3i** and **3j**.

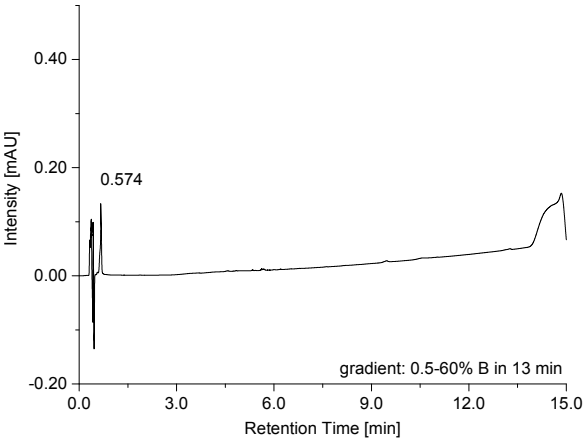

(**A**) ^{Ac}GGpKAG^{CONH_2} **4a**

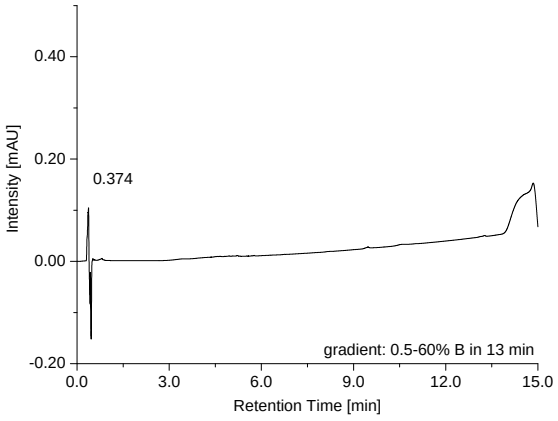

(**B**) ^{Ac}GGpKCG^{CONH_2} **4b**

Figure S13: UPLC-traces (220 nm) of **4a** and **4b**.

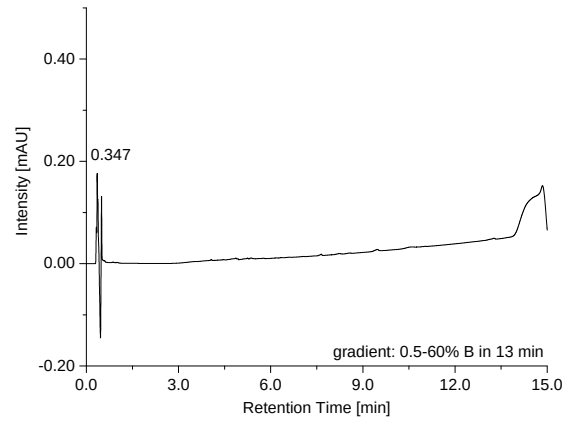

(**A**) ^{Ac}GGpKDG^{CONH_2} **4c**

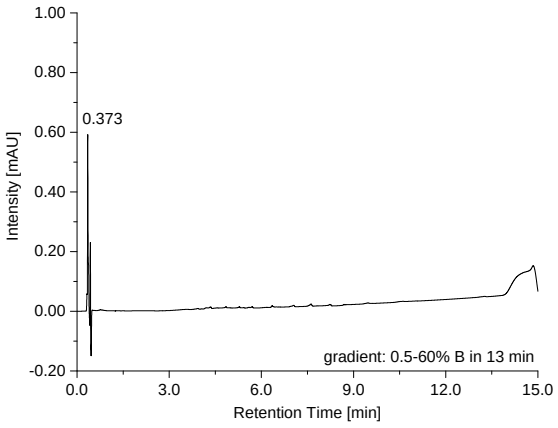

(**B**) ^{Ac}GGpKFG^{CONH_2} **4d**

Figure S14: UPLC-traces (220 nm) of **4c** and **4d**.

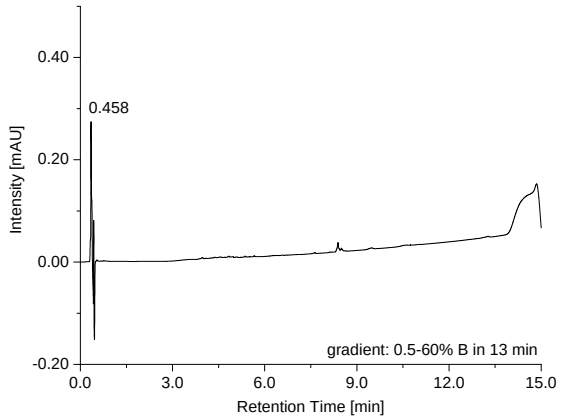

(**A**) ^{Ac}GGpKIG^{CONH_2} **4e**

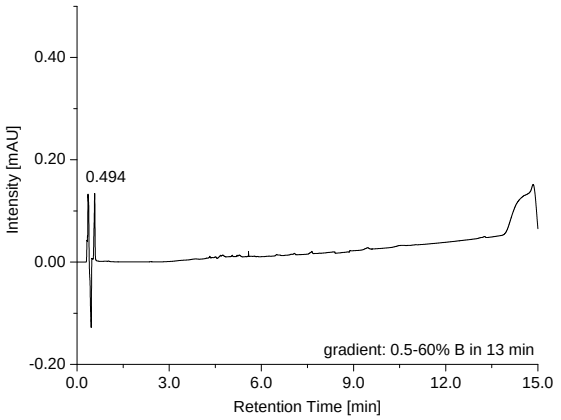

(**B**) ^{Ac}GGpKKG^{CONH_2} **4f**

Figure S15: UPLC-traces (220 nm) of **4e** and **4f**.

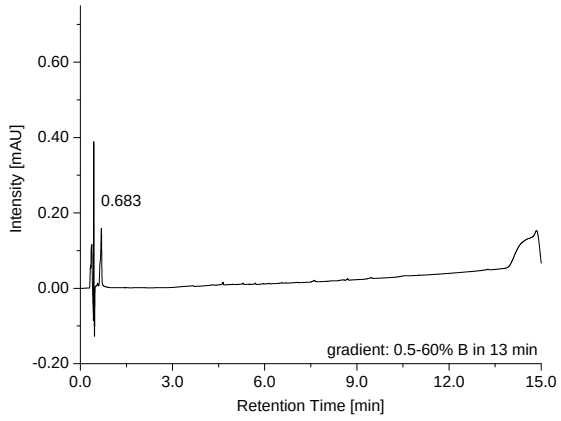

(**A**) ^{Ac}GGpKPG^{CONH_2} **4g**

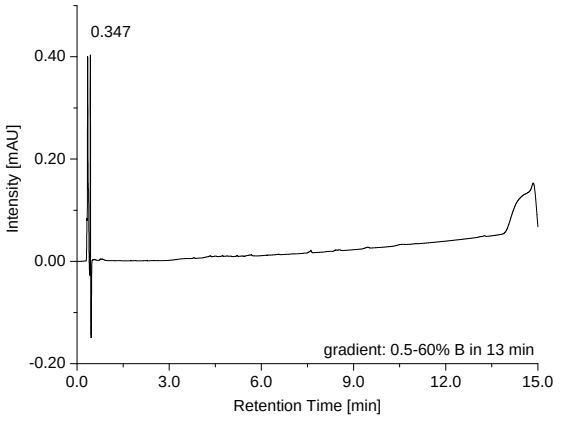

(**B**) ^{Ac}GGpKQG^{CONH_2} **4h**

Figure S16: UPLC-traces (220 nm) of **4g** and **4h**.

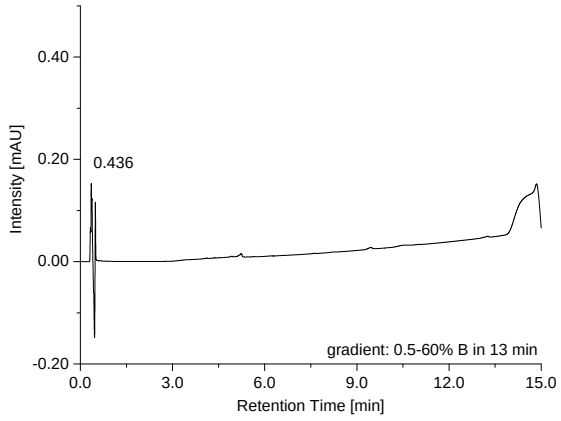

(**A**) ^{Ac}GGpKRG^{CONH_2} **4i**

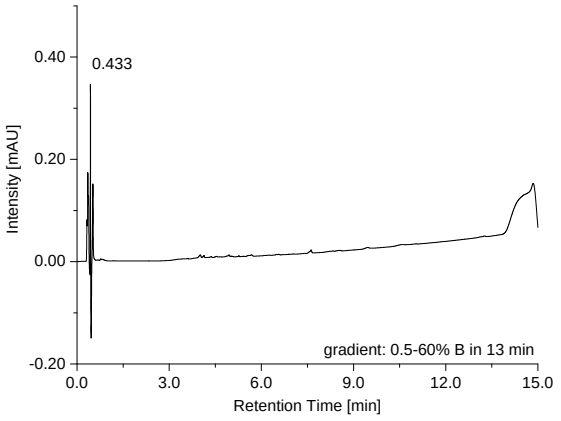

(**B**) ^{Ac}GGpKSG^{CONH_2} **4j**

Figure S17: UPLC-traces (220 nm) of **4i** and **4j**.

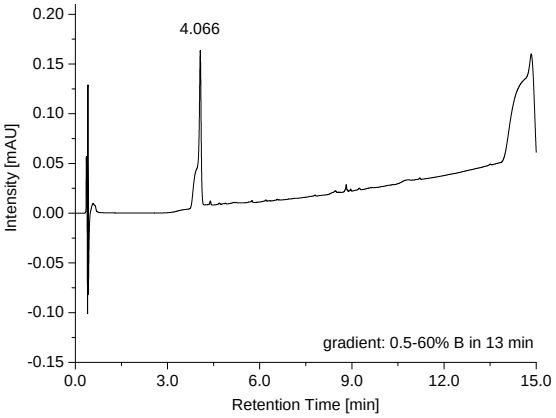

(**A**) ^{Ac}GGK^{N_3}GG^{CONH_2} **5a**

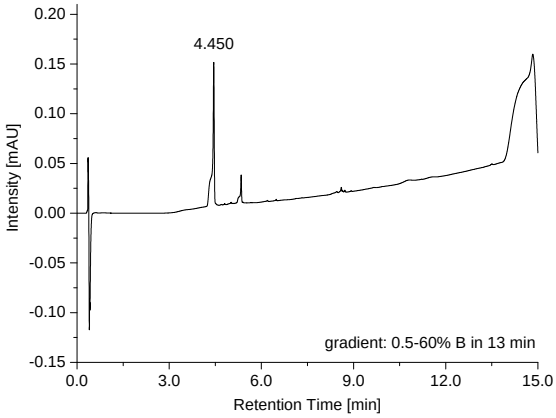

(**B**) ^{Ac}GAK^{N_3}GG^{CONH_2} **5b**

Figure S18: UPLC-traces (220 nm) of **5a** and **5b**.

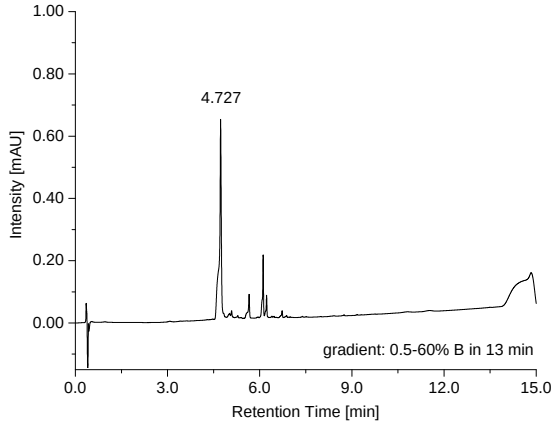

(**A**) ^{Ac}GCK^{N_3}GG^{CONH_2} **5c**

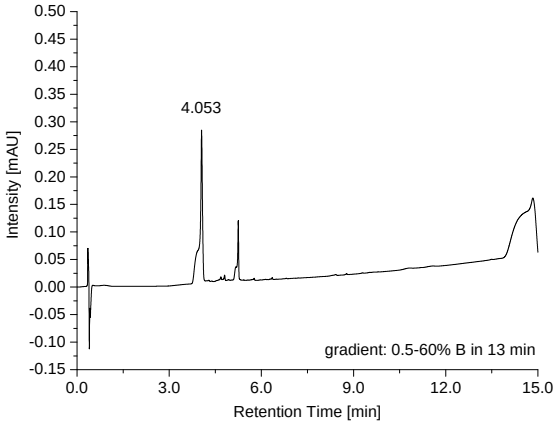

(**B**) ^{Ac}GDK^{N_3}GG^{CONH_2} **5d**

Figure S19: UPLC-traces (220 nm) of **5c** and **5d**.

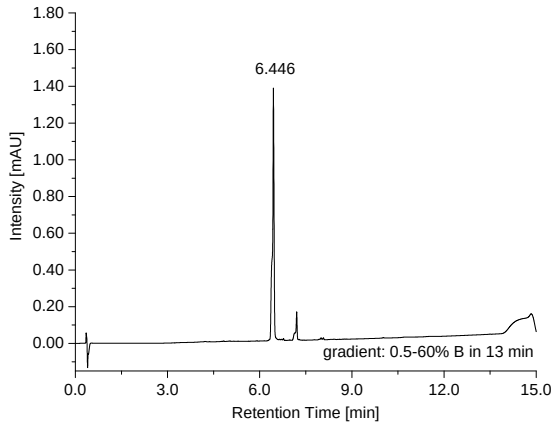

(**A**) ^{Ac}GFK^{N_3}GG^{CONH_2} **5e**

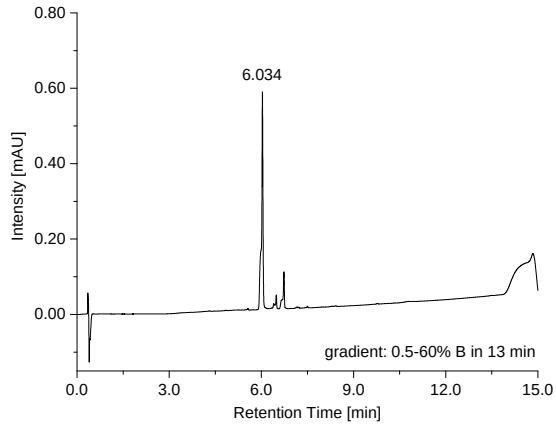

(**B**) ^{Ac}GIK^{N_3}GG^{CONH_2} **5f**

Figure S20: UPLC-traces (220 nm) of **5e** and **5f**.

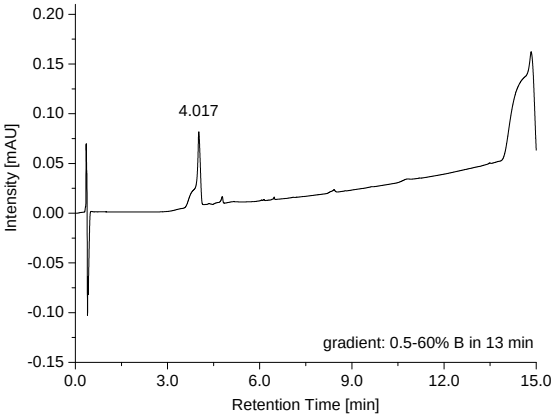

(**A**) ^{Ac}GKK^{N_3}GG^{CONH_2} **5g**

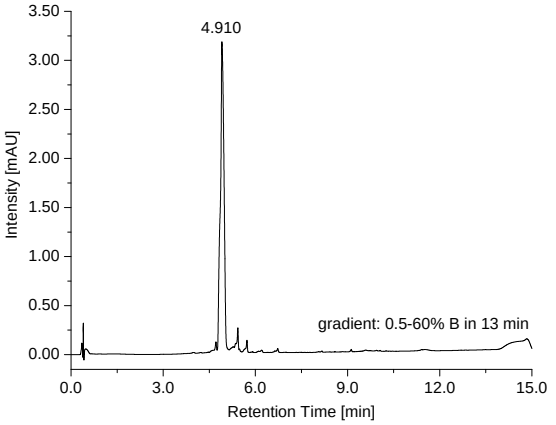

(**B**) ^{Ac}GPK^{N_3}GG^{CONH_2} **5h**

Figure S21: UPLC-traces (220 nm) of **5g** and **5h**.

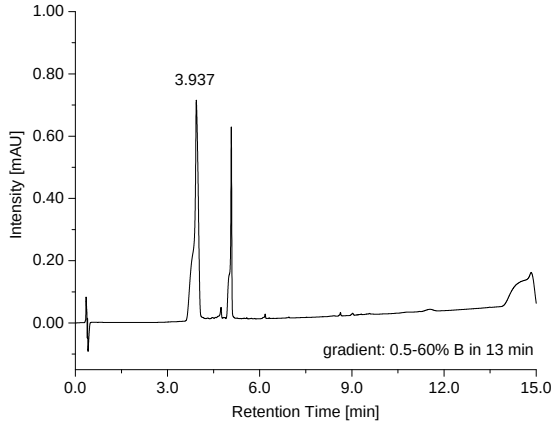

(**A**) ^{Ac}GQK^{N_3}GG^{CONH_2} **5i**

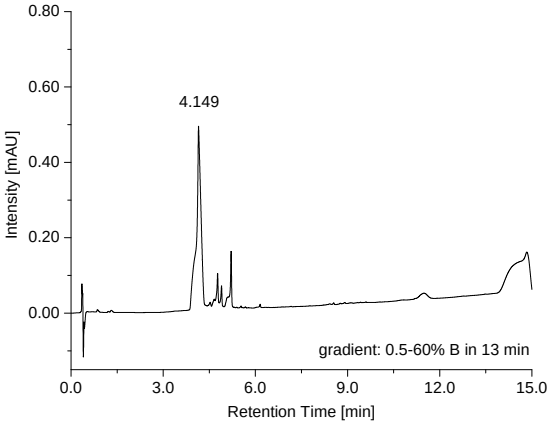

(**B**) ^{Ac}GRK^{N_3}GG^{CONH_2} **5j**

Figure S22: UPLC-traces (220 nm) of **5i** and **5j**.

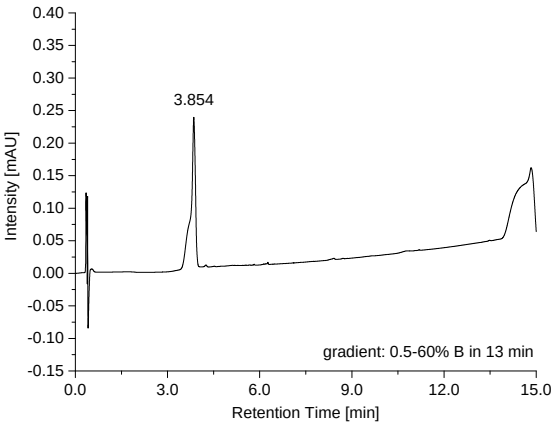

(**A**) ^{Ac}GSK^{N_3}GG^{CONH_2} **5k**

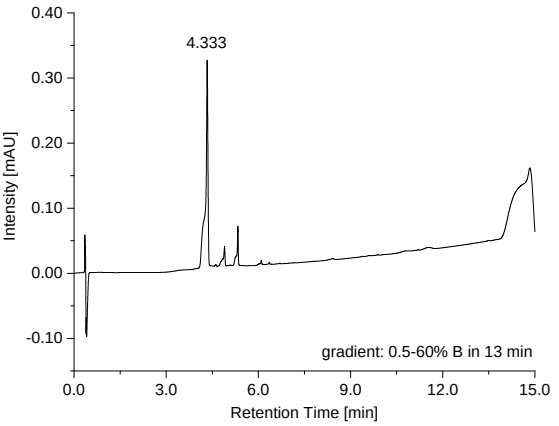

(**B**) ^{Ac}GGK^{N_3}AG^{CONH_2} **5l**

Figure S23: UPLC-traces (220 nm) of **5k** and **5l**.

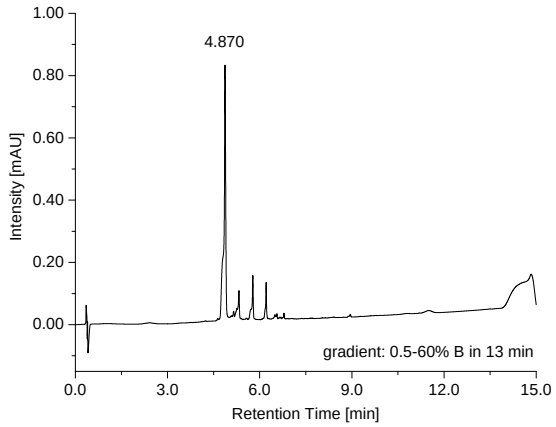

(**A**) ^{Ac}GGK^{N_3}CG^{CONH_2} **5m**

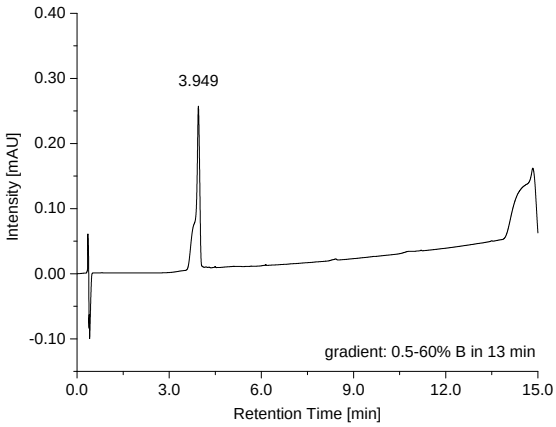

(**B**) ^{Ac}GGK^{N_3}DG^{CONH_2} **5n**

Figure S24: UPLC-traces (220 nm) of **5m** and **5n**.

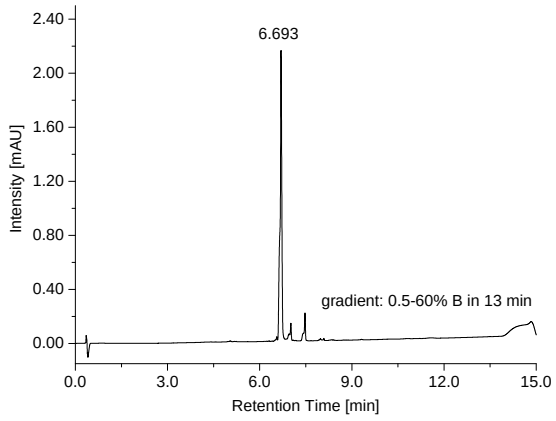

(**A**) ^{Ac}GGK^{N_3}FG^{CONH_2} **5o**

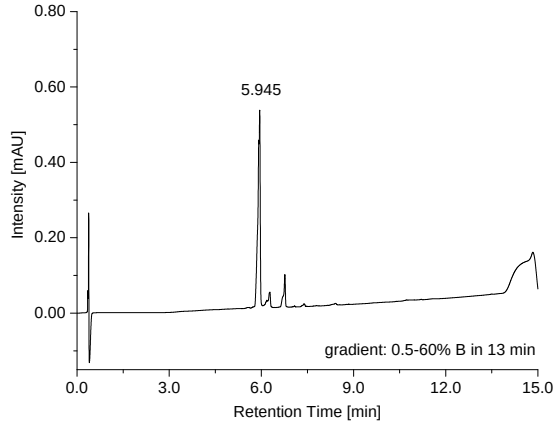

(**B**) ^{Ac}GGK^{N_3}IG^{CONH_2} **5p**

Figure S25: UPLC-traces (220 nm) of **5o** and **5p**.

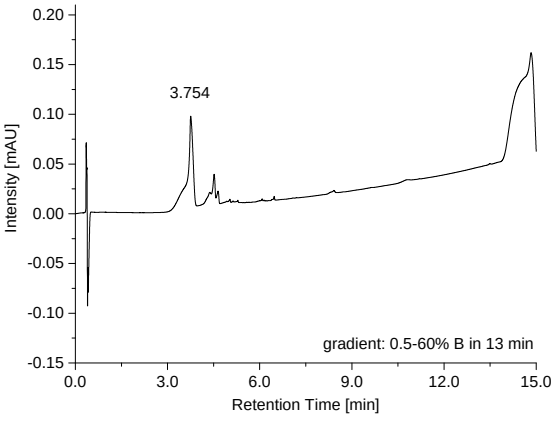

(**A**) ^{Ac}GGK^{N_3}KG^{CONH_2} **5q**

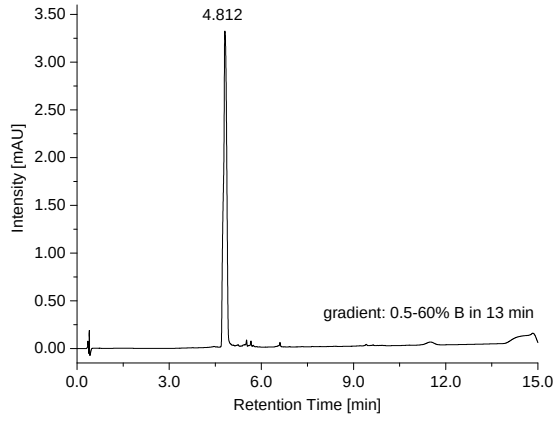

(**B**) ^{Ac}GGK^{N_3}PG^{CONH_2} **5r**

Figure S26: UPLC-traces (220 nm) of **5q** and **5r**.

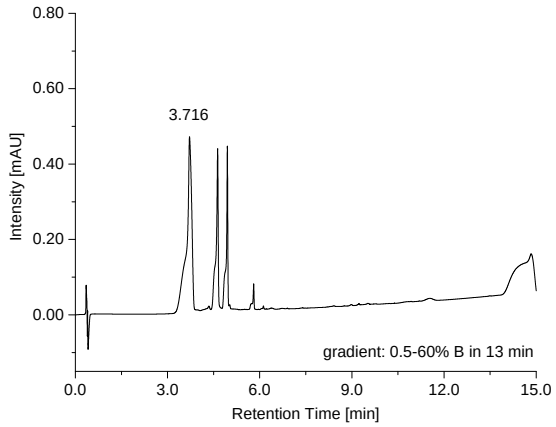

(**A**) ^{Ac}GGK^{N_3}QG^{CONH_2} **5s**

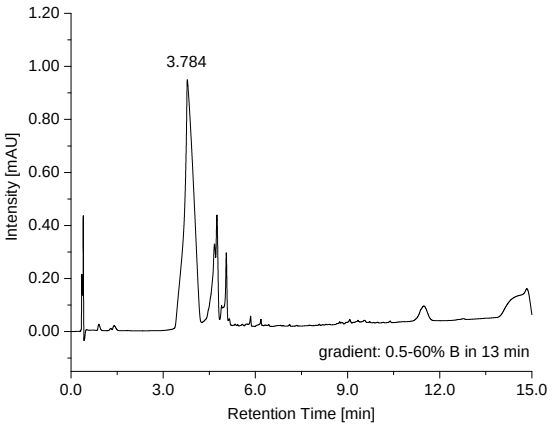

(**B**) ^{Ac}GGK^{N_3}RG^{CONH_2} **5t**

Figure S27: UPLC-traces (220 nm) of **5s** and **5t**.

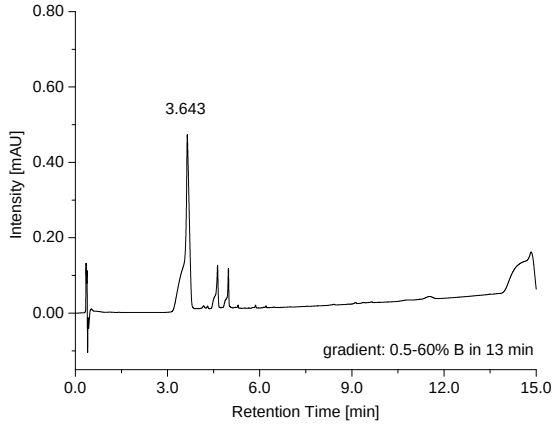

(**A**) ^{Ac}GGK^{N_3}SG^{CONH_2} **5u**

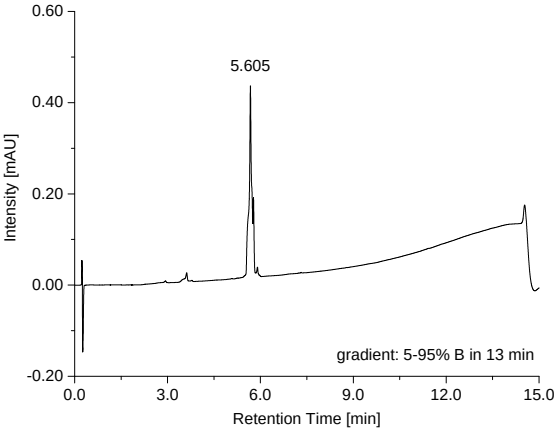

(**B**) NH_2-Lys(NPO(ONPE)$_2$)-OH **6**

Figure S28: UPLC-traces (220 nm) of **5u** and **6**.

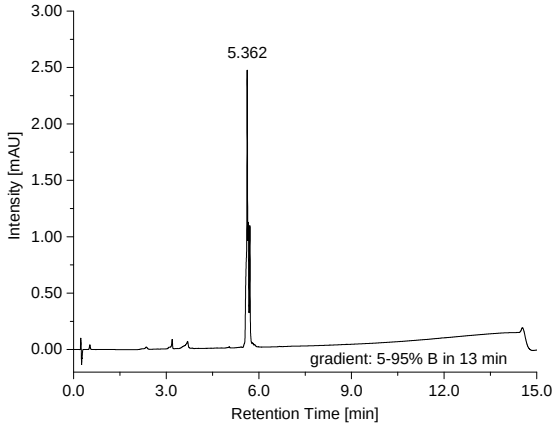

(**A**) ^{Ac}GGcpKGG^{CONH_2} **7a**

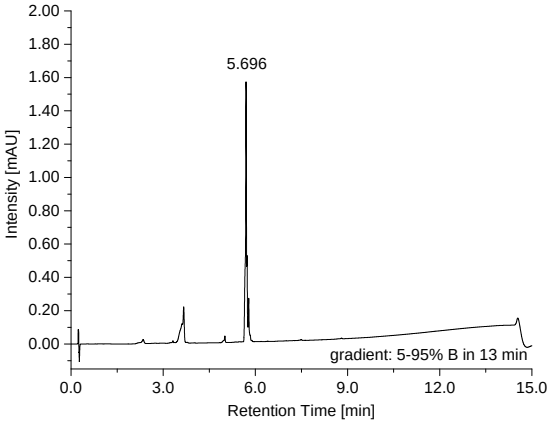

(**B**) ^{Ac}GAcpKGG^{CONH_2} **7b**

Figure S29: UPLC-traces (220 nm) of **7a** and **7b**.

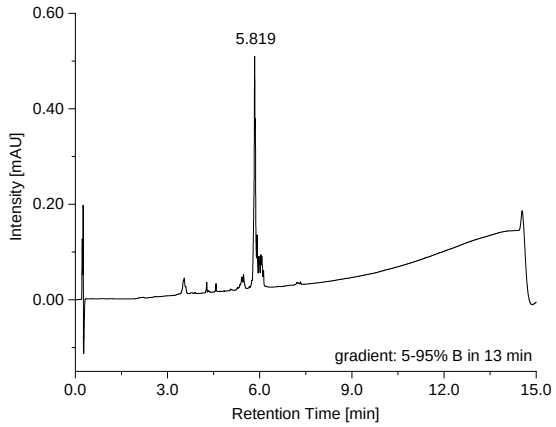

(**A**) ^{Ac}GCcpKGG^{CONH_2} **7c**

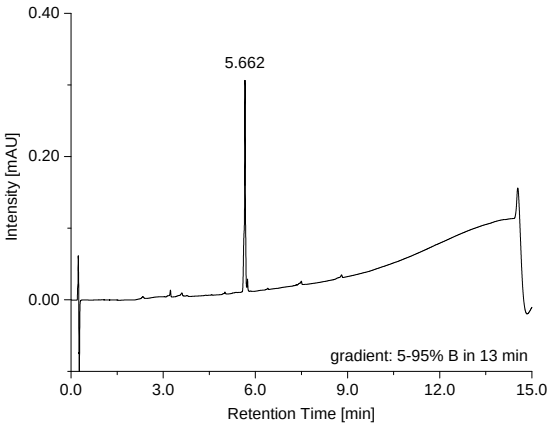

(**B**) ^{Ac}GDcpKGG^{CONH_2} **7d**

Figure S30: UPLC-traces (220 nm) of **7c** and **7d**.

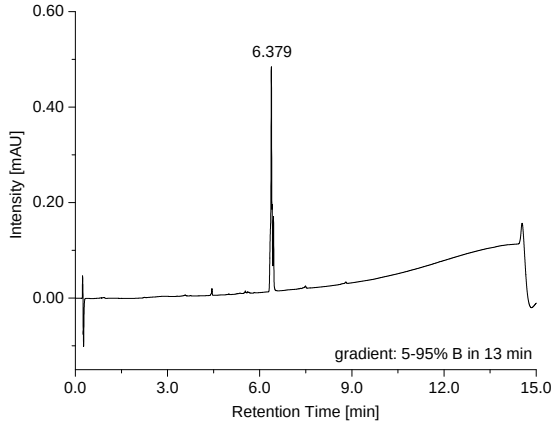

(**A**) ^{Ac}GFcpKGG^{CONH_2} **7e**

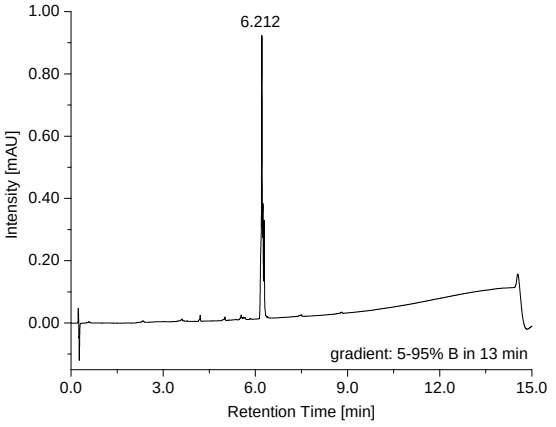

(**B**) ^{Ac}GIcpKGG^{CONH_2} **7f**

Figure S31: UPLC-traces (220 nm) of **7e** and **7f**.

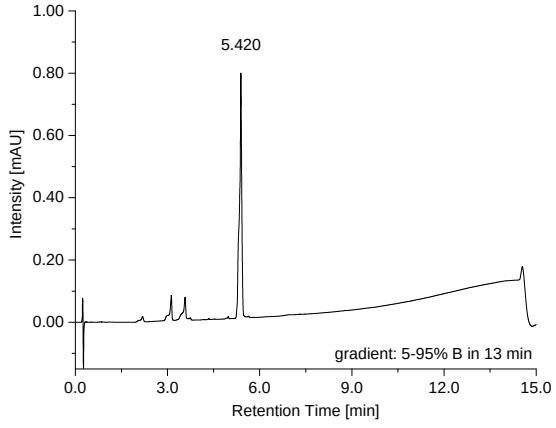

(**A**) ^{Ac}GKcpKGG^{CONH_2} **7g**

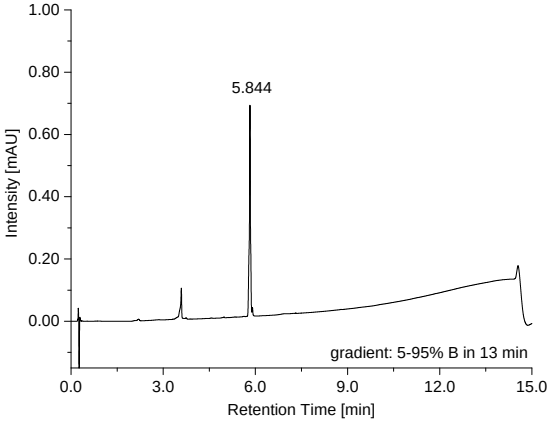

(**B**) ^{Ac}GPcpKGG^{CONH_2} **7h**

Figure S32: UPLC-traces (220 nm) of **7g** and **7h**.

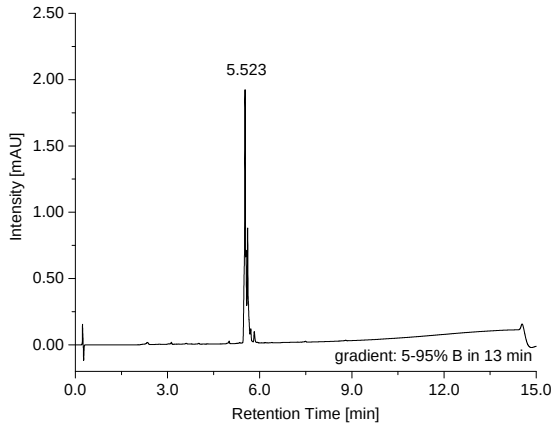

(**A**) ^{Ac}GQcpKGG^{CONH_2} **7i**

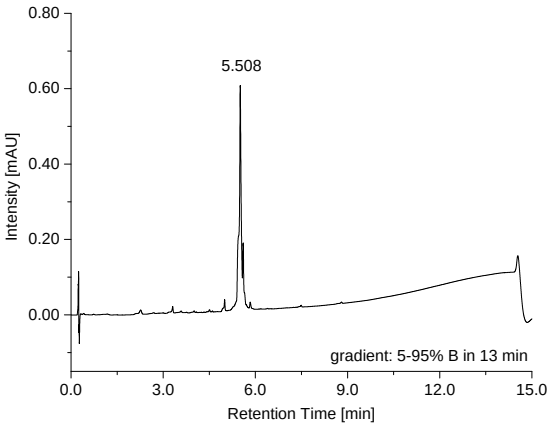

(**B**) ^{Ac}GRcpKGG^{CONH_2} **7j**

Figure S33: UPLC-traces (220 nm) of **7i** and **7j**.

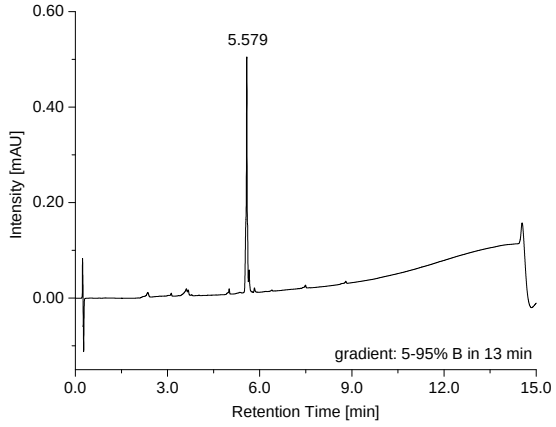

(**A**) ^{Ac}GScpKGG^{CONH_2} **7k**

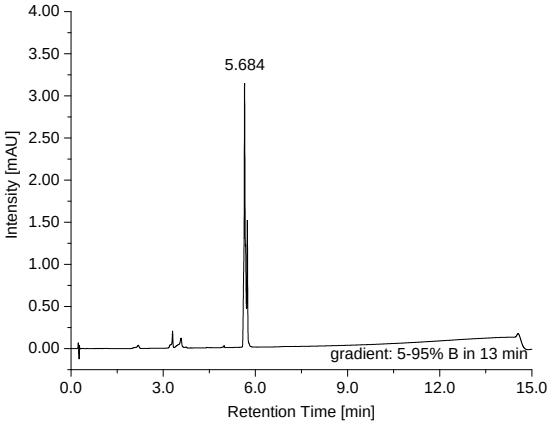

(**B**) ^{Ac}GGcpKAG^{CONH_2} **7l**

Figure S34: UPLC-traces (220 nm) of **7k** and **7l**.

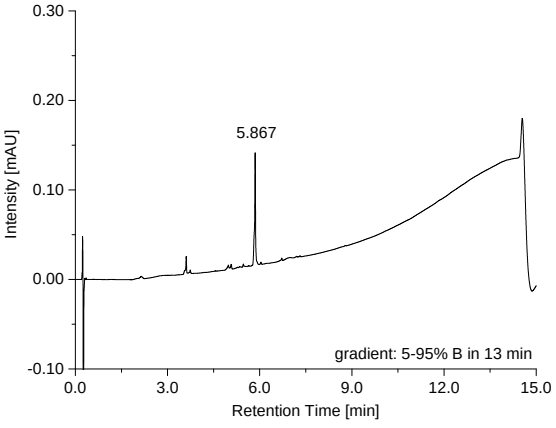

(**A**) ^{Ac}GGcpKCG^{CONH_2} **7m**

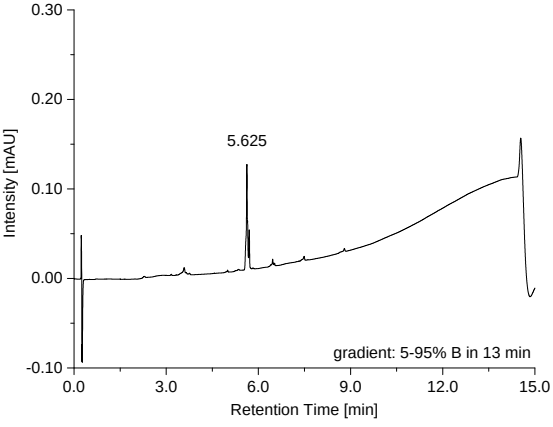

(**B**) ^{Ac}GGcpKDG^{CONH_2} **7n**

Figure S35: UPLC-traces (220 nm) of **7m** and **7n**.

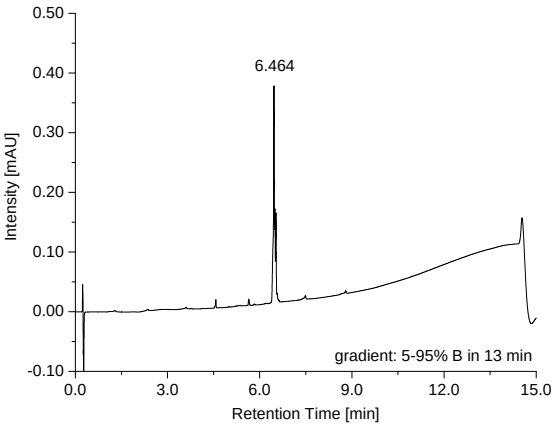

(**A**) ^{Ac}GGcpKFG^{CONH_2} **7o**

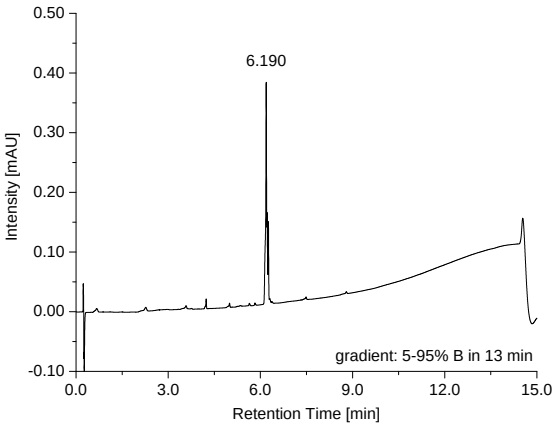

(**B**) ^{Ac}GGcpKIG^{CONH_2} **7p**

Figure S36: UPLC-traces (220 nm) of **7o** and **7p**.

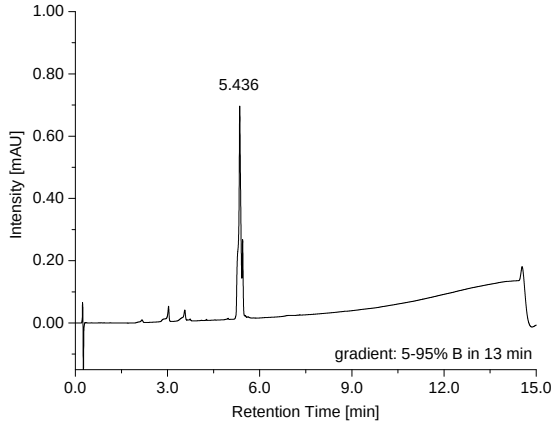

(**A**) ^{Ac}GGcpKKG^{CONH_2} **7q**

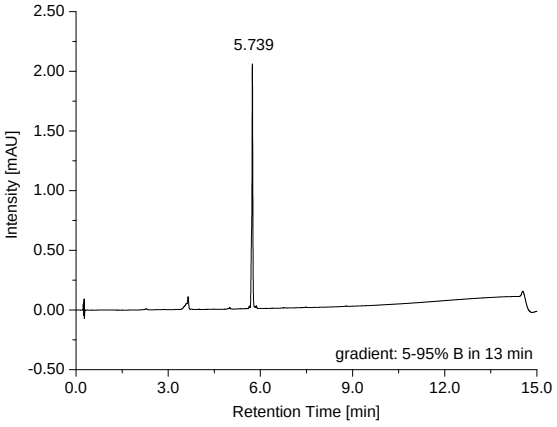

(**B**) ^{Ac}GGcpKPG^{CONH_2} **7r**

Figure S37: UPLC-traces (220 nm) of **7q** and **7r**.

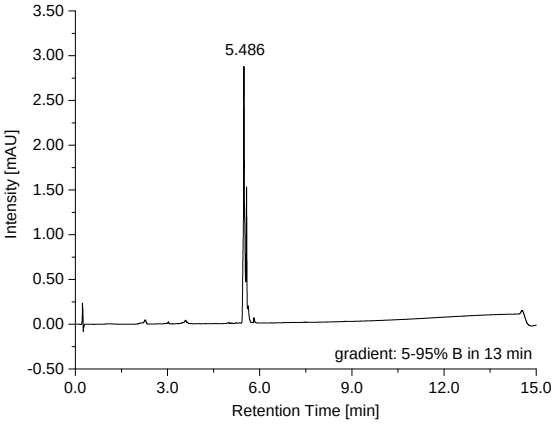

(**A**) ^{Ac}GGcpKQG^{CONH_2} **7s**

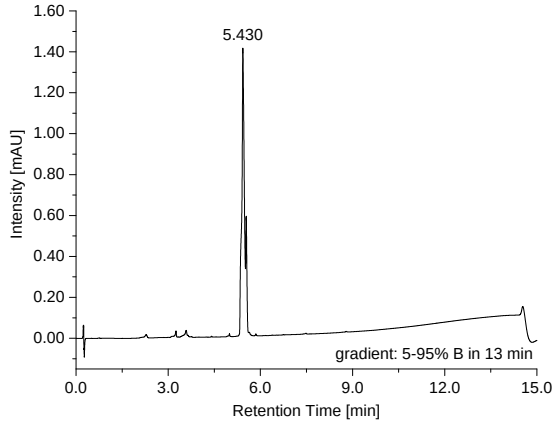

(**B**) ^{Ac}GGcpKRG^{CONH_2} **7t**

Figure S38: UPLC-traces (220 nm) of **7s** and **7t**.

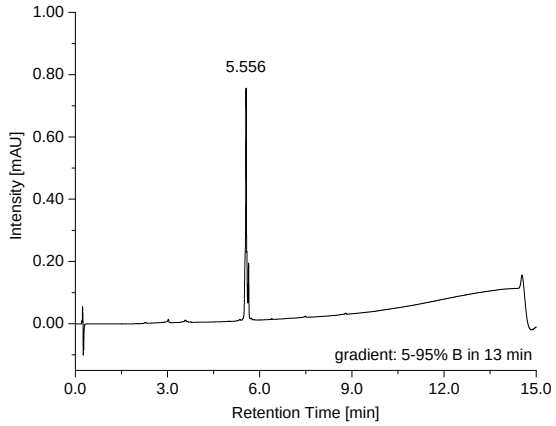

(**A**) ^{Ac}GGcpKSG^{CONH_2} **7u**

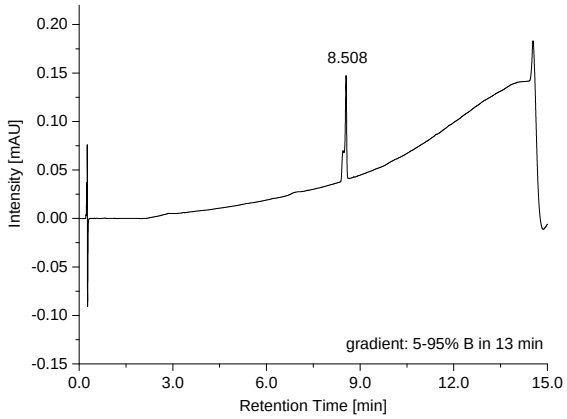

(**B**) Fmoc-Arg(NPO(OTc)$_2$)-OH **11**

Figure S39: UPLC-traces (220 nm) of **7u** and **11**.

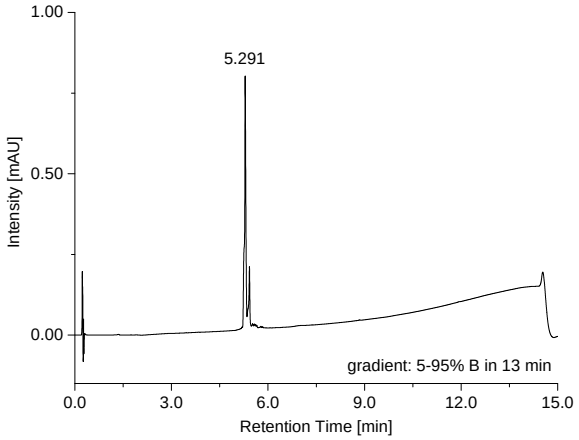

Figure S40: UPLC-trace (220 nm) of ^{Ac}GGcpRGG^{CONH_2} **12**.

6 NMR Spectra of Synthesized Compounds

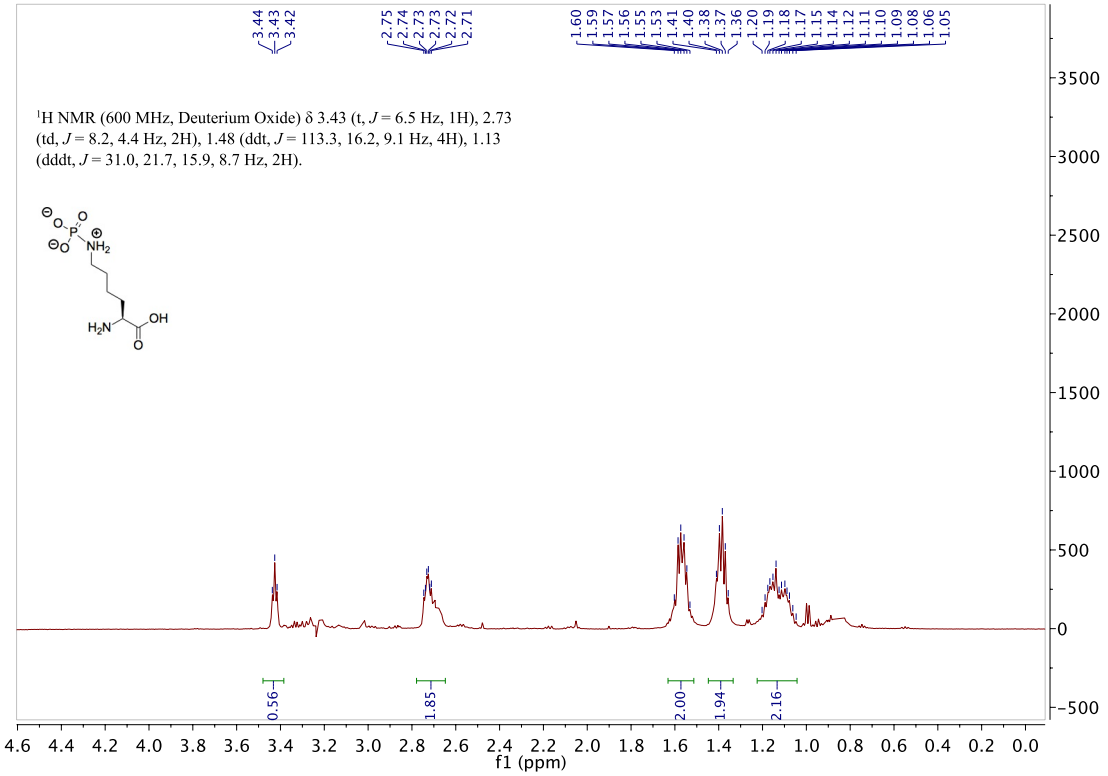

Figure S41: ^{1}H NMR spectrum of compound **1a** (600 MHz, D_2O)

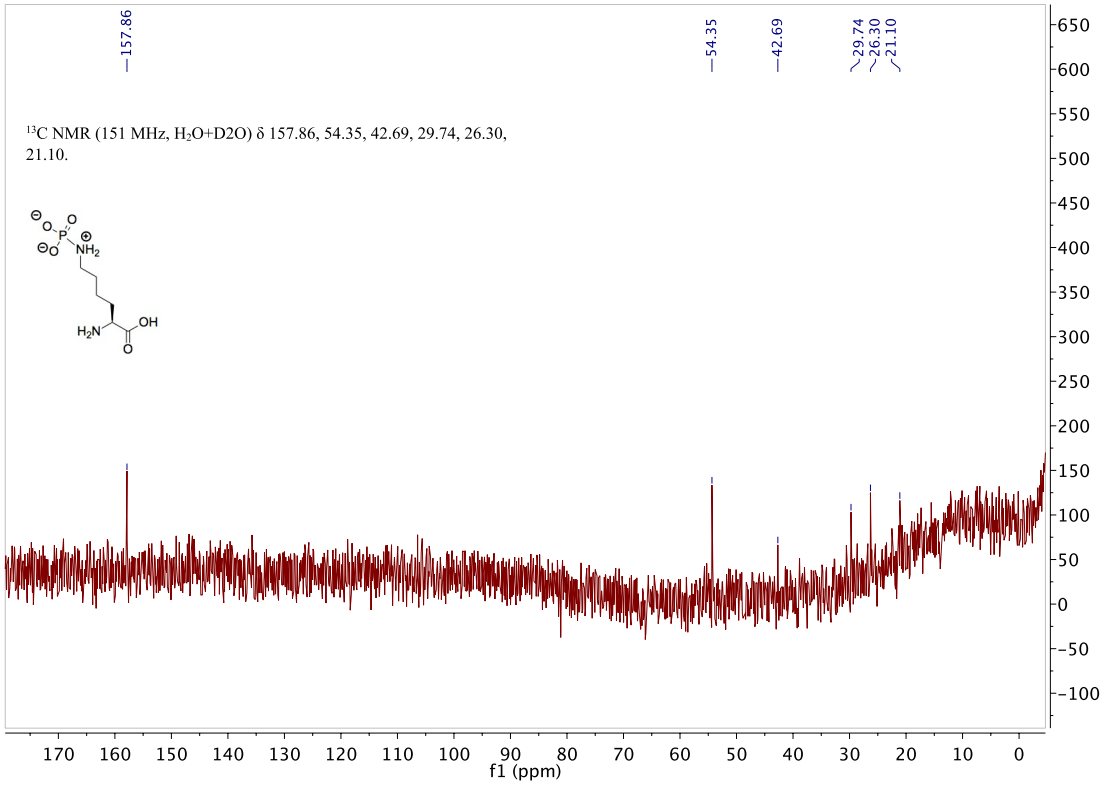

Figure S42: ^{13}C NMR spectrum of compound **1a** (151 MHz, D_2O)

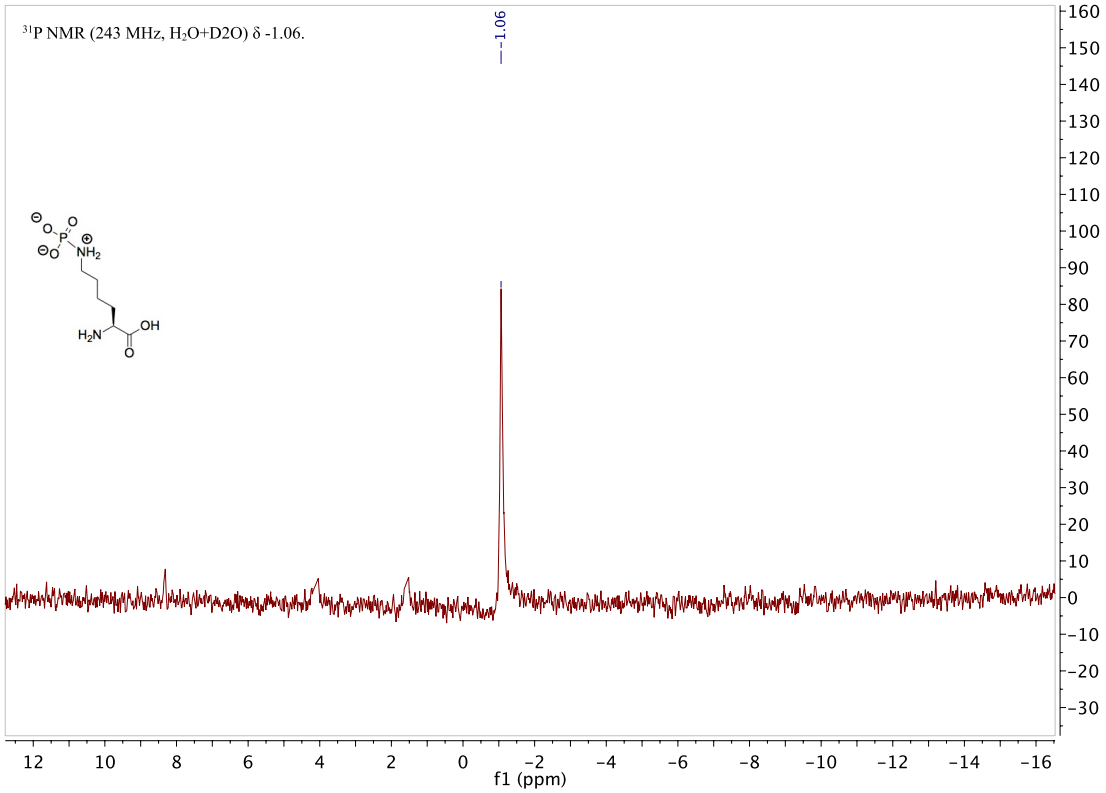

Figure S43: ^{31}P NMR spectrum of compound **1a** (243 MHz, D_2O)

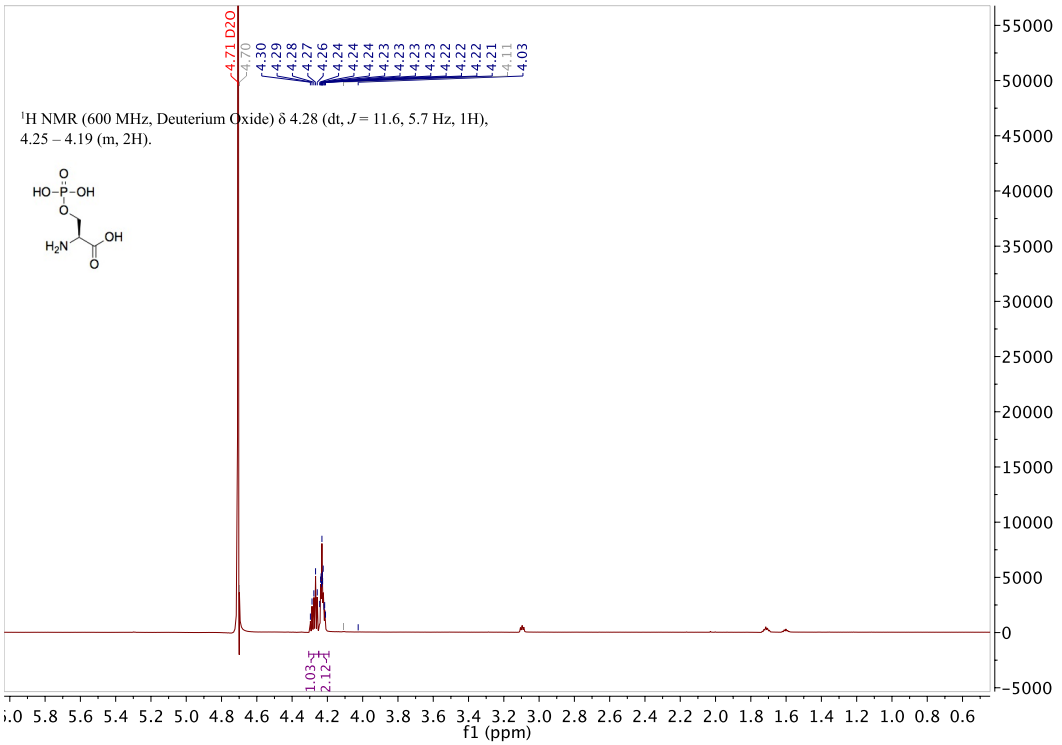

Figure S44: ^{1}H NMR spectrum of compound **1b** (600 MHz, D_2O)

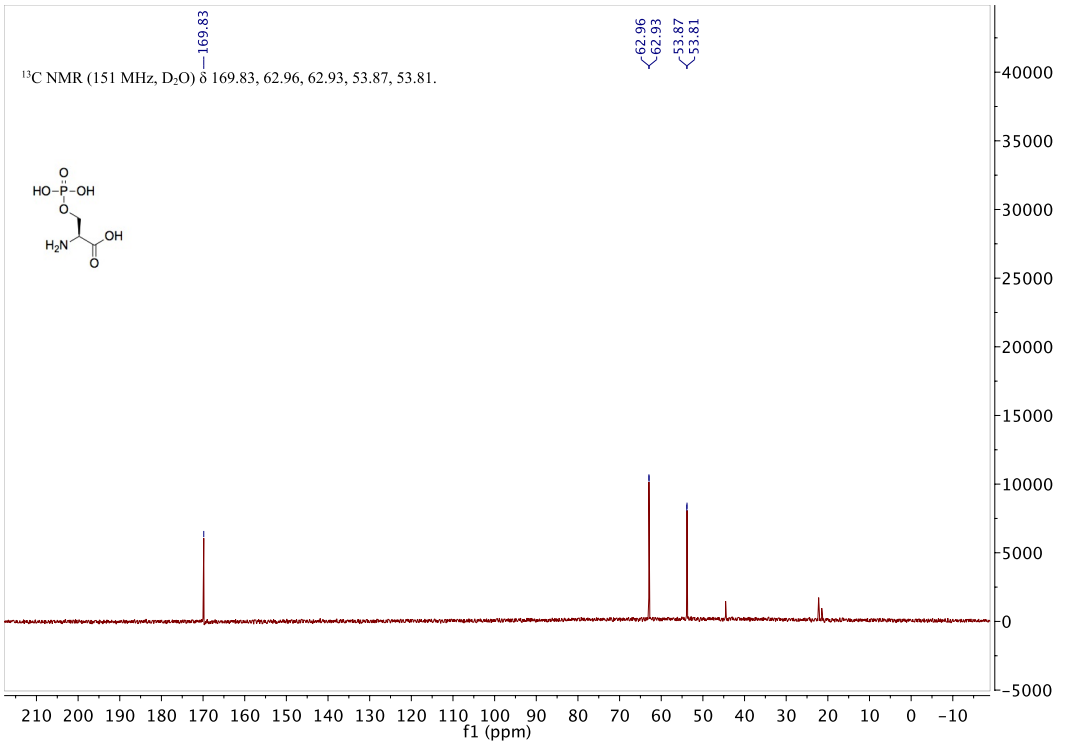

Figure S45: ^{13}C NMR spectrum of compound **1b** (151 MHz, D_2O)

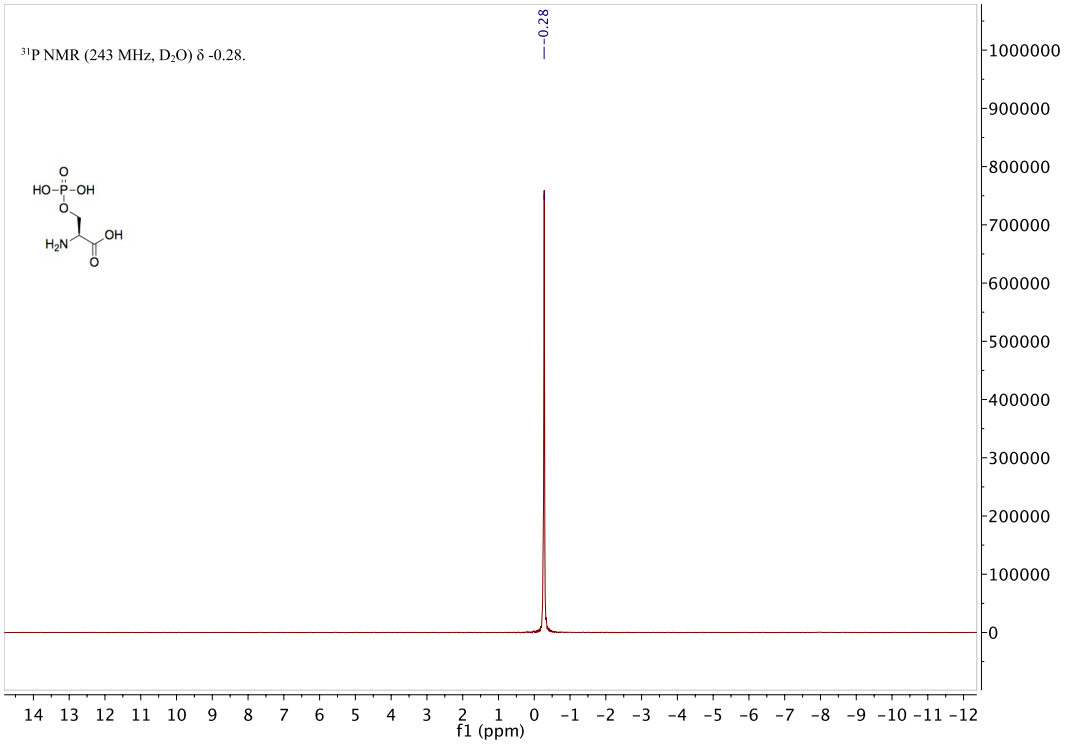

Figure S46: ^{31}P NMR spectrum of compound **1b** (243 MHz, D_2O)

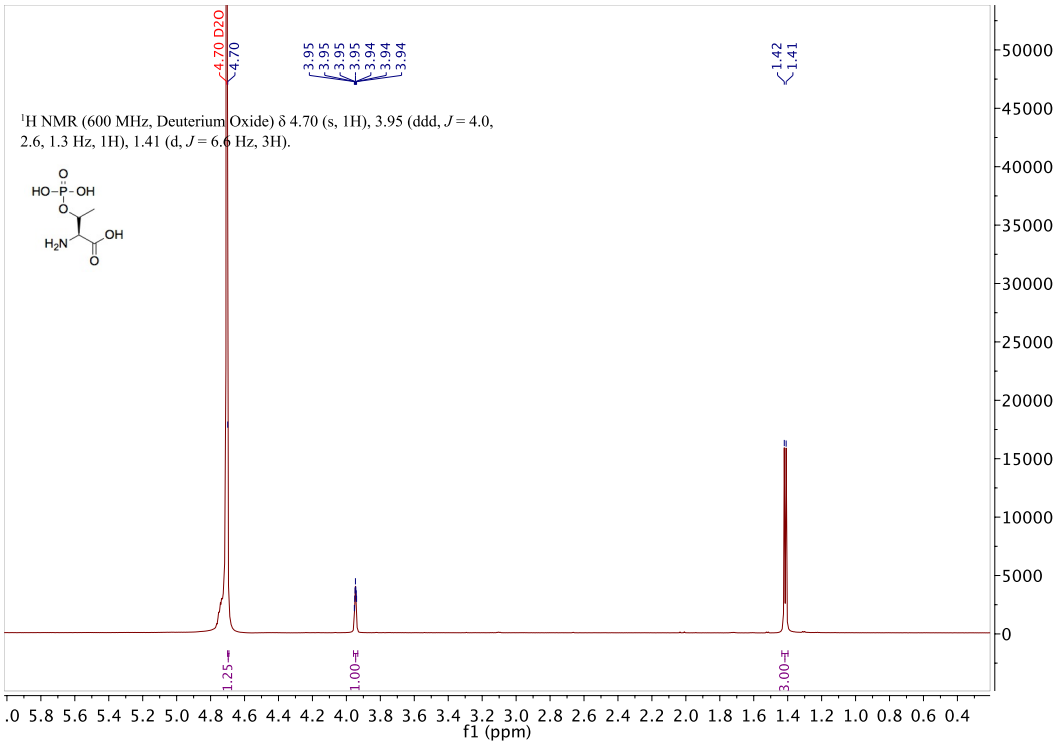

Figure S47: ^{1}H NMR spectrum of compound **1c** (600 MHz, D_2O)

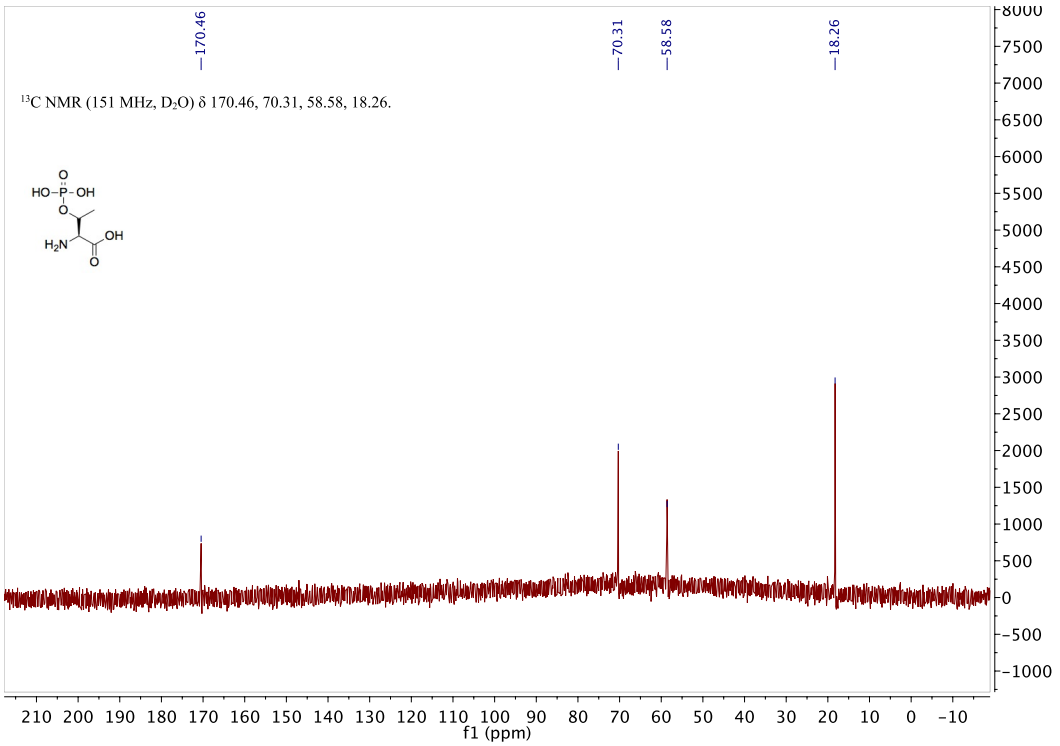

Figure S48: ^{13}C NMR spectrum of compound **1c** (151 MHz, D_2O)

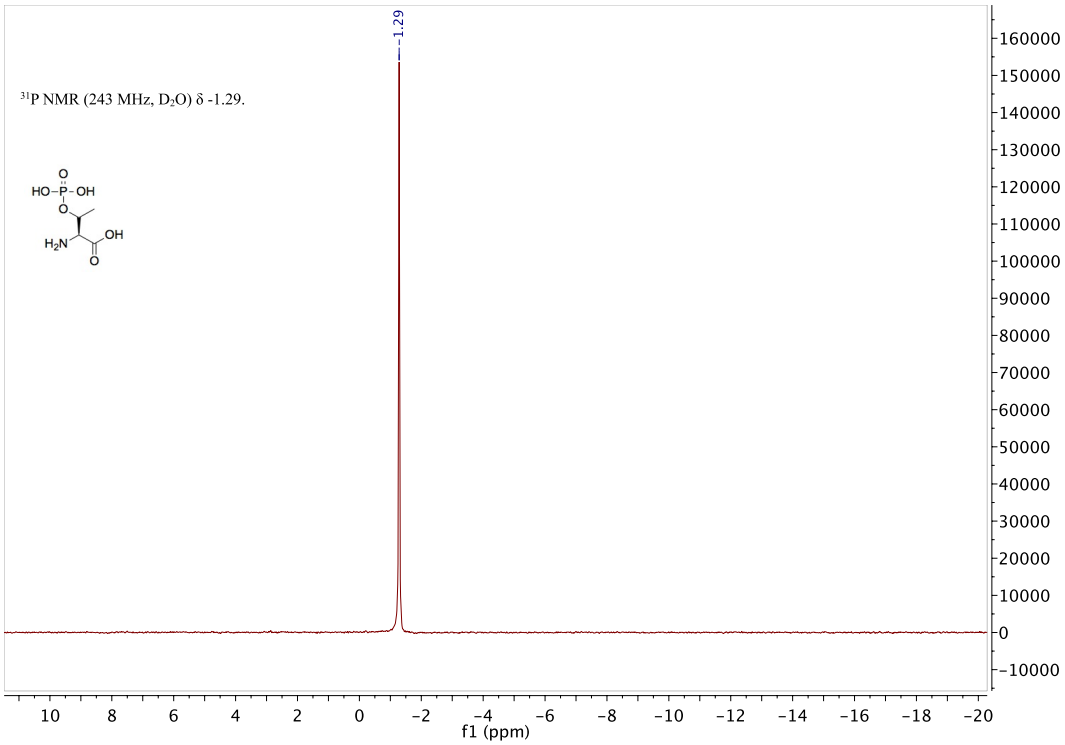

Figure S49: ^{31}P NMR spectrum of compound **1c** (243 MHz, D_2O)

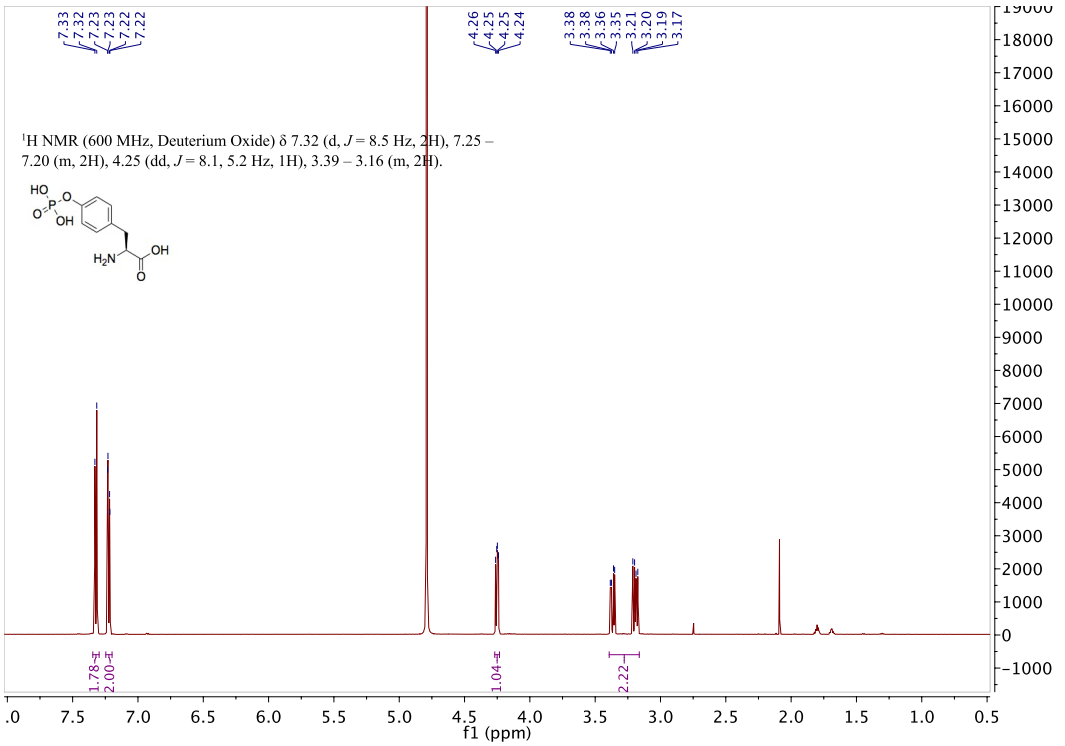

Figure S50: ^{1}H NMR spectrum of compound **1d** (600 MHz, D_2O)

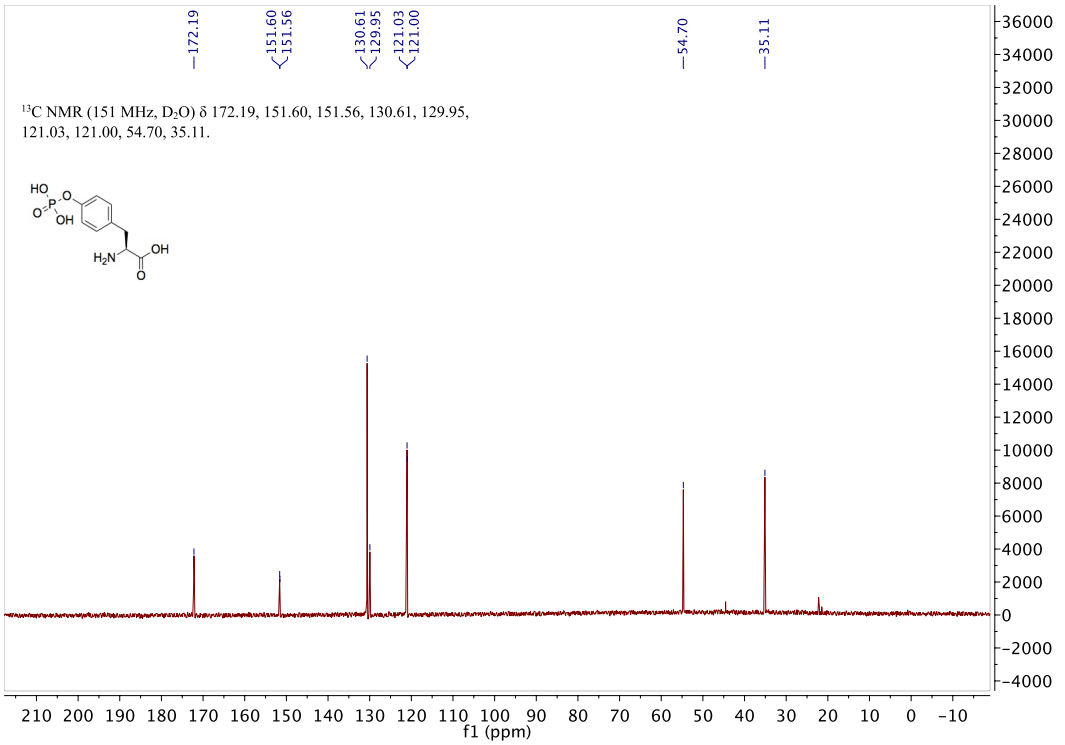

Figure S51: ^{13}C NMR spectrum of compound **1d** (151 MHz, D_2O)

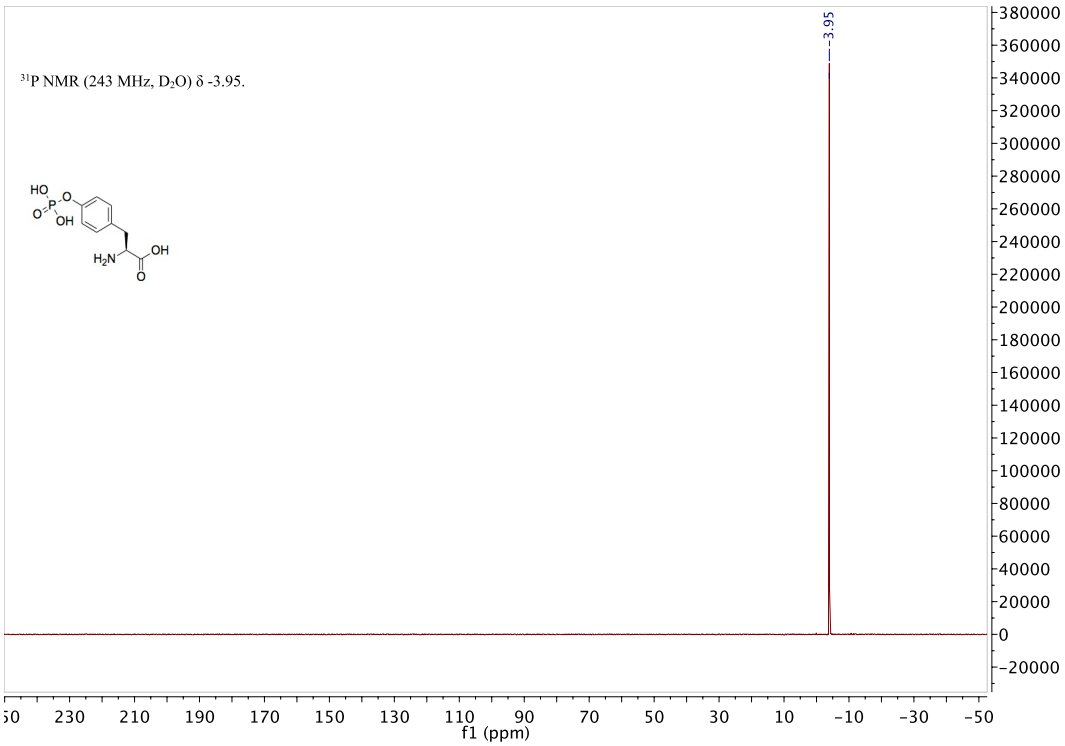

Figure S52: ^{31}P NMR spectrum of compound **1d** (243 MHz, D_2O)

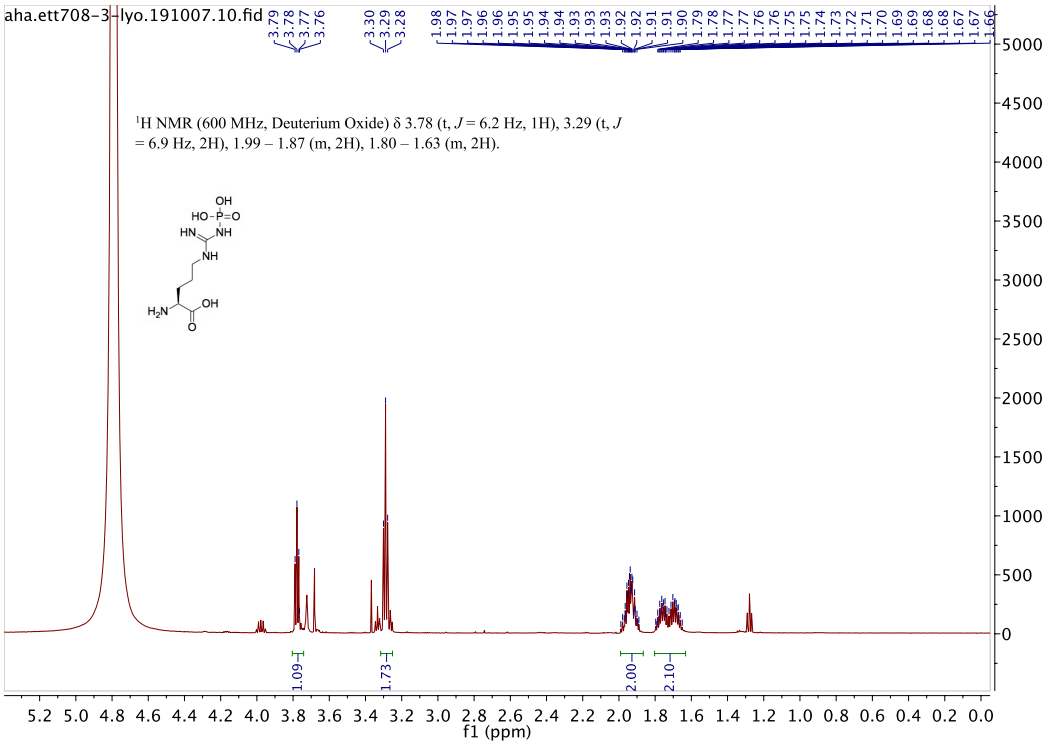

Figure S53: ^{1}H NMR spectrum of compound **1e** (600 MHz, D_2O)

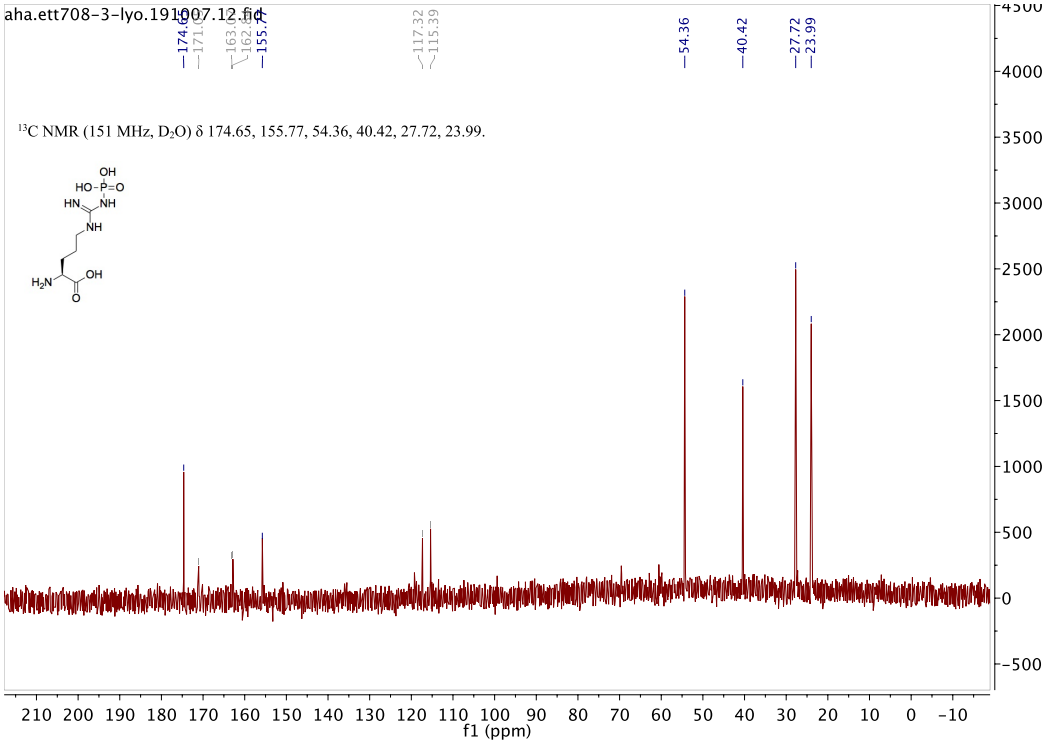

Figure S54: ^{13}C NMR spectrum of compound **1e** (151 MHz, D_2O)

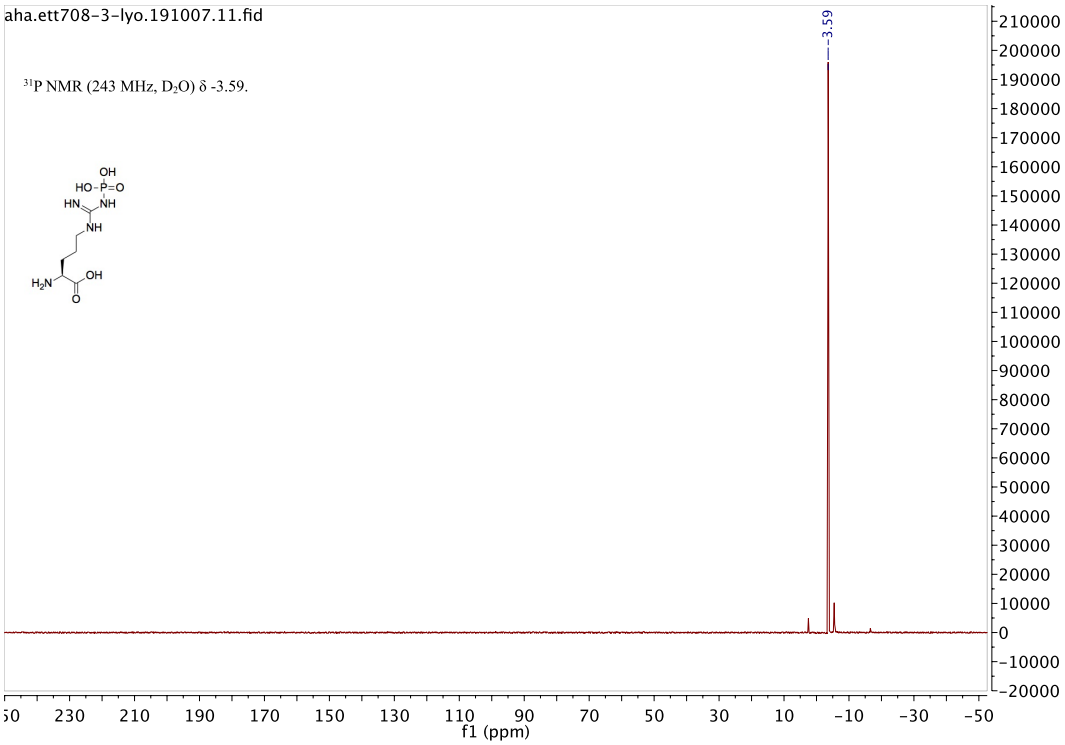

Figure S55: ^{31}P NMR spectrum of compound **1e** (243 MHz, D_2O)

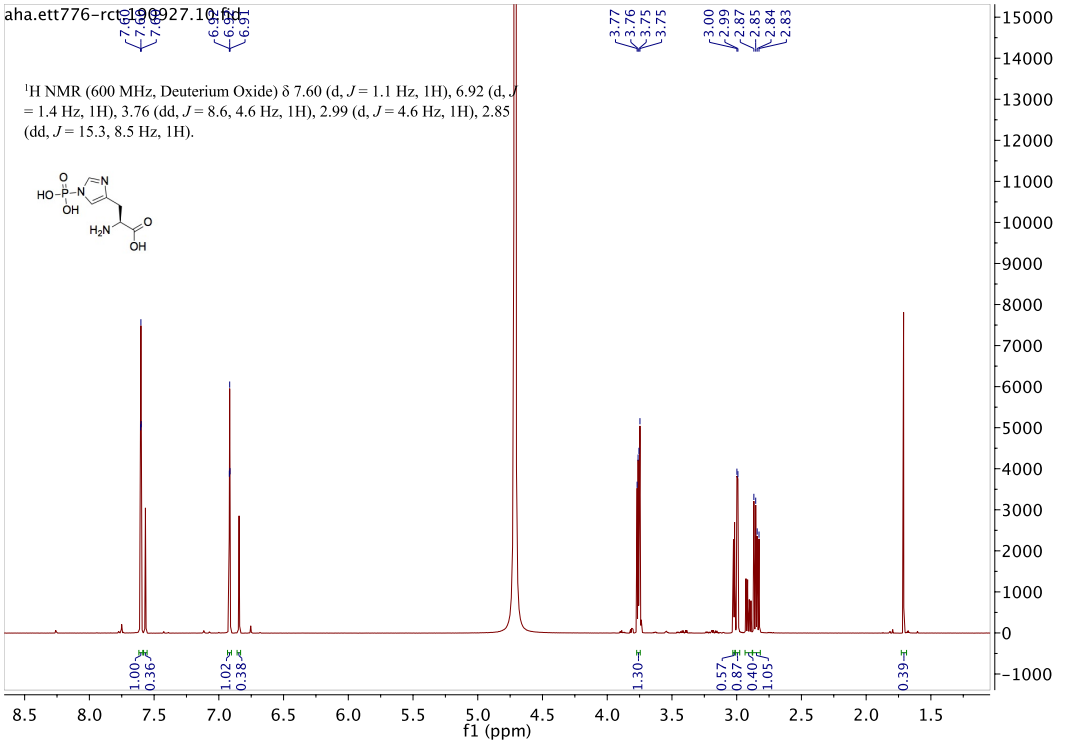

Figure S56: ^{1}H NMR spectrum of compound **1f** (600 MHz, D_2O)

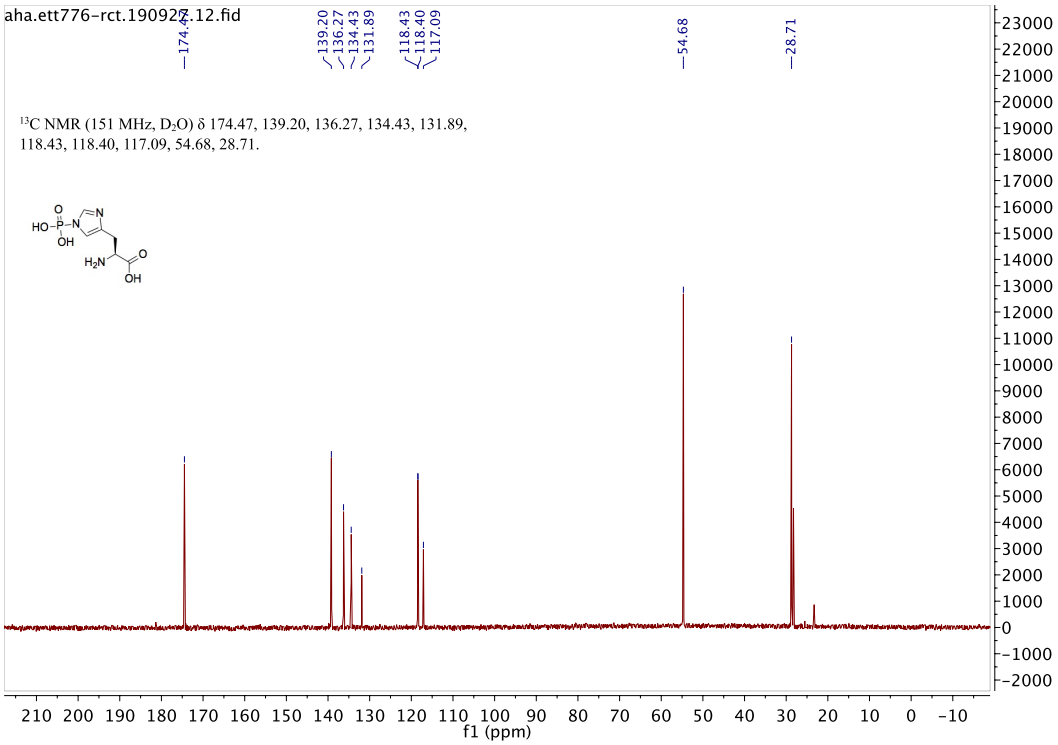

Figure S57: ^{13}C NMR spectrum of compound **1f** (151 MHz, D_2O)

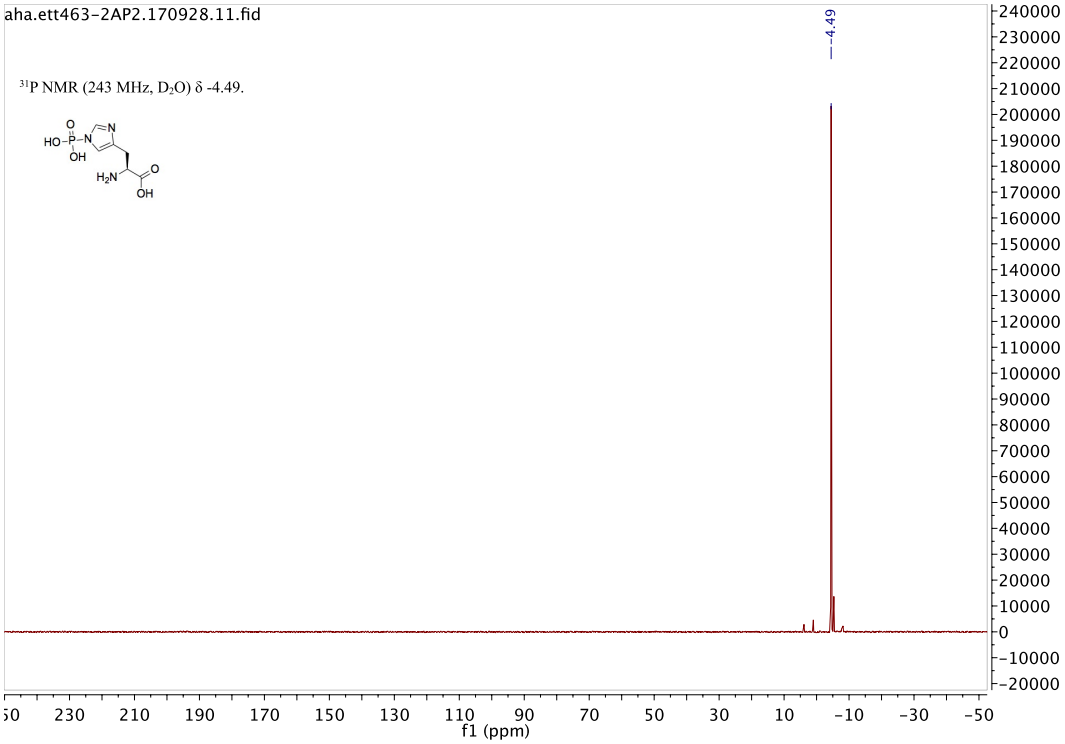

Figure S58: ^{31}P NMR spectrum of compound **1f** (243 MHz, D_2O)

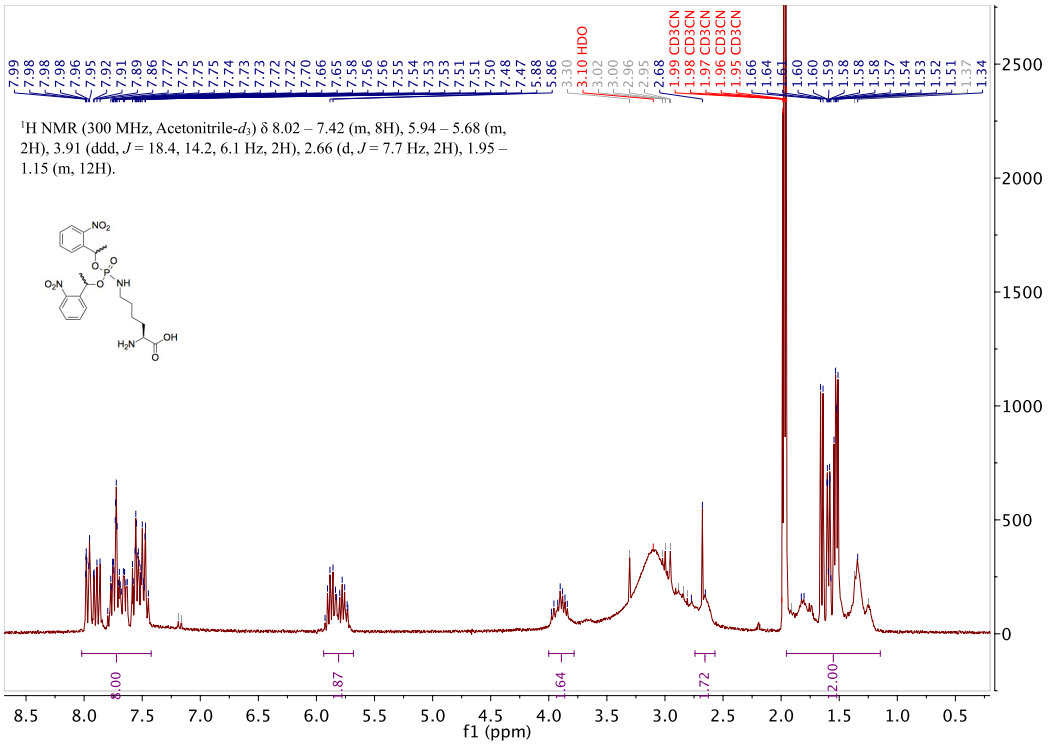

Figure S59: ^{1}H NMR spectrum of compound **6** (300 MHz, CD_3CN)

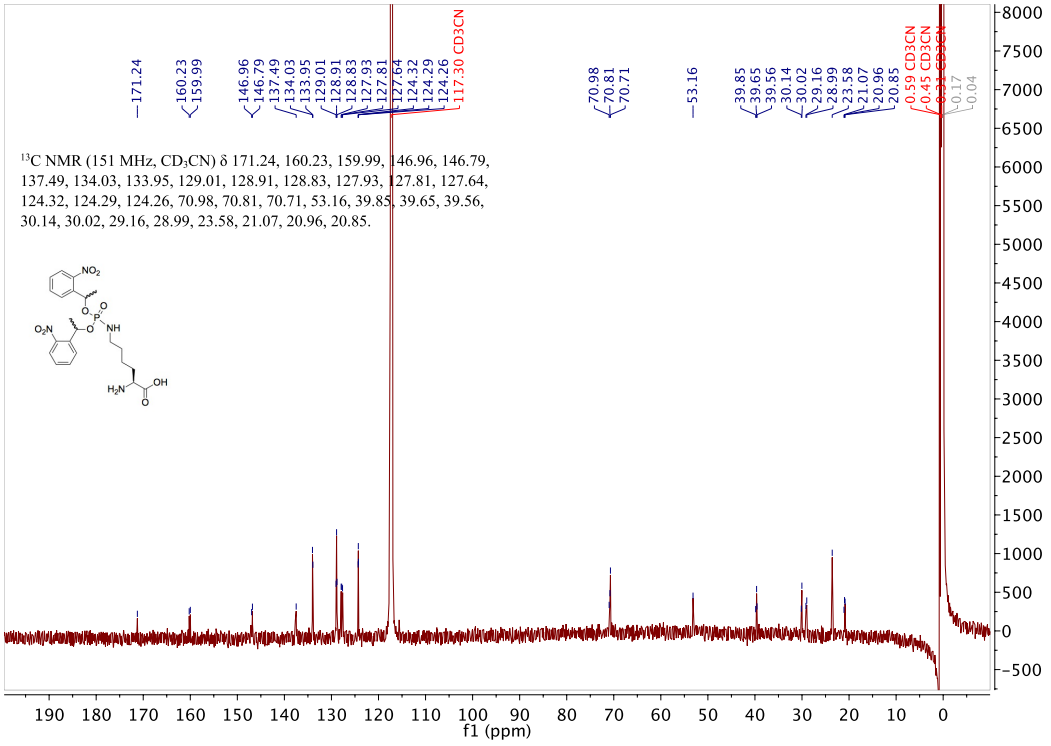

Figure S60: ^{13}C NMR spectrum of compound **6** (151 MHz, CD_3CN)

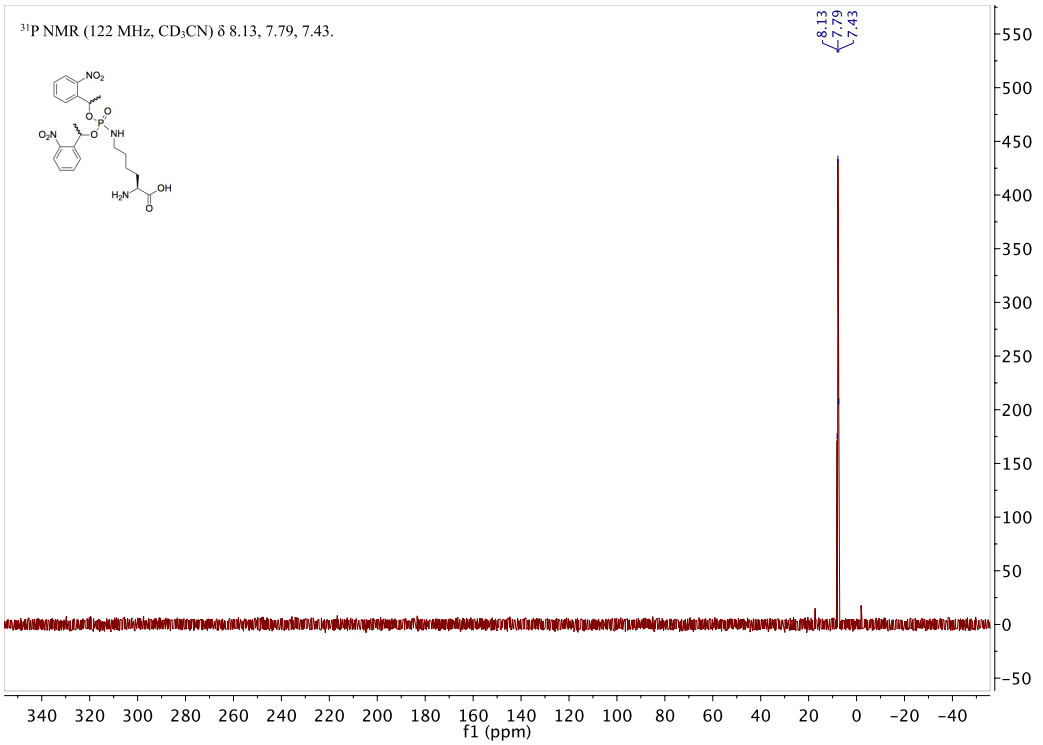

Figure S61: ^{31}P NMR spectrum of compound **6** (122 MHz, CD_3CN)

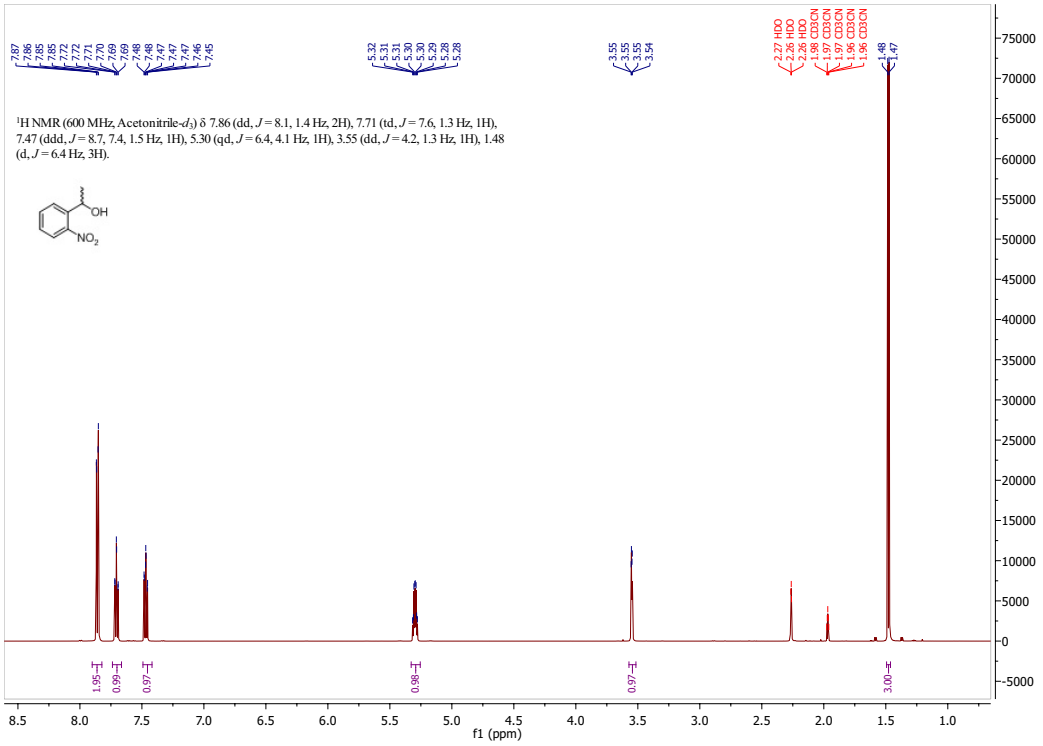

Figure S62: ^{1}H NMR spectrum of compound **8** (600 MHz, CD_3CN)

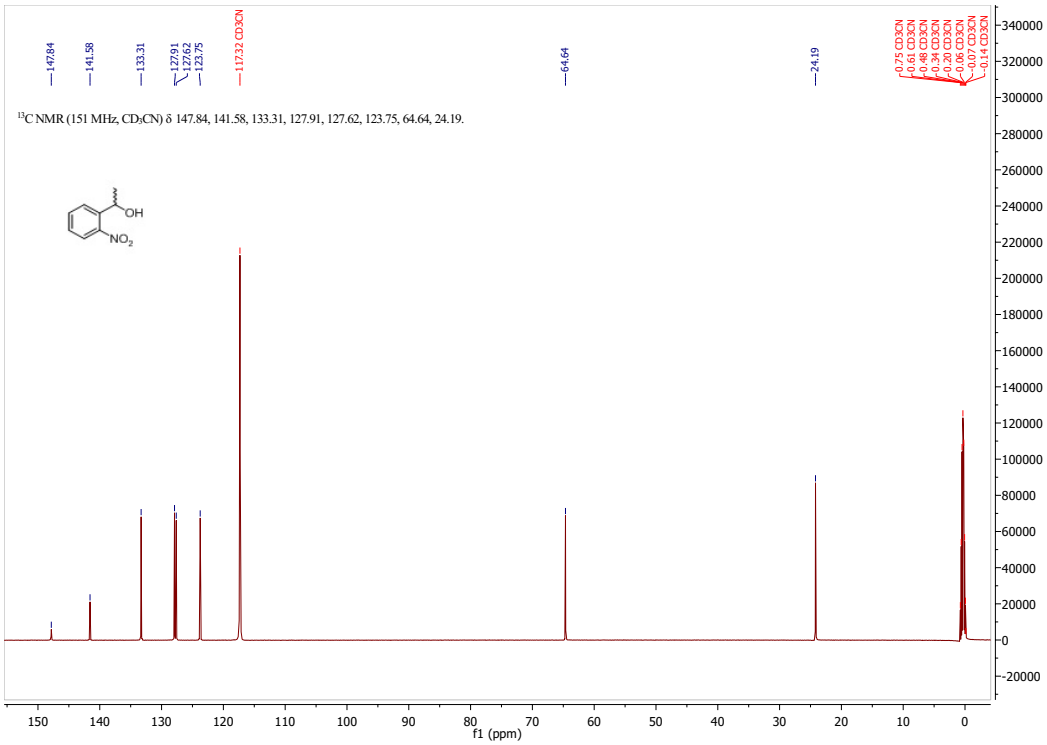

Figure S63: ^{13}C NMR spectrum of compound **6** (151 MHz, CD_3CN)

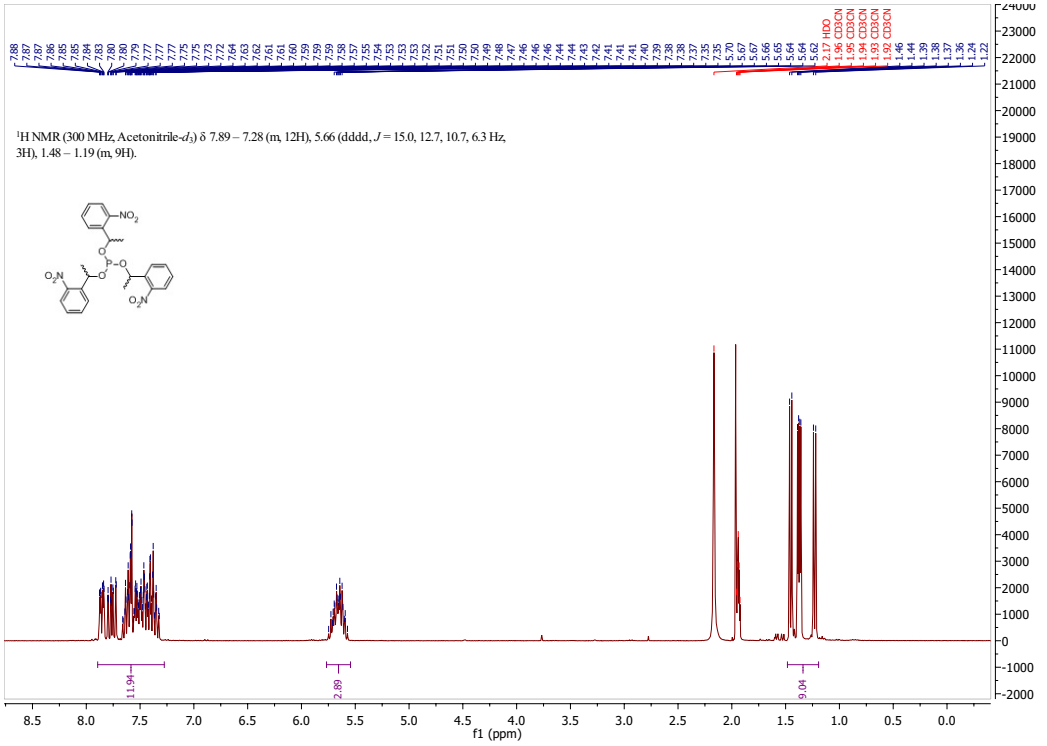

Figure S64: ^{1}H NMR spectrum of compound **9** (300 MHz, CD_3CN)

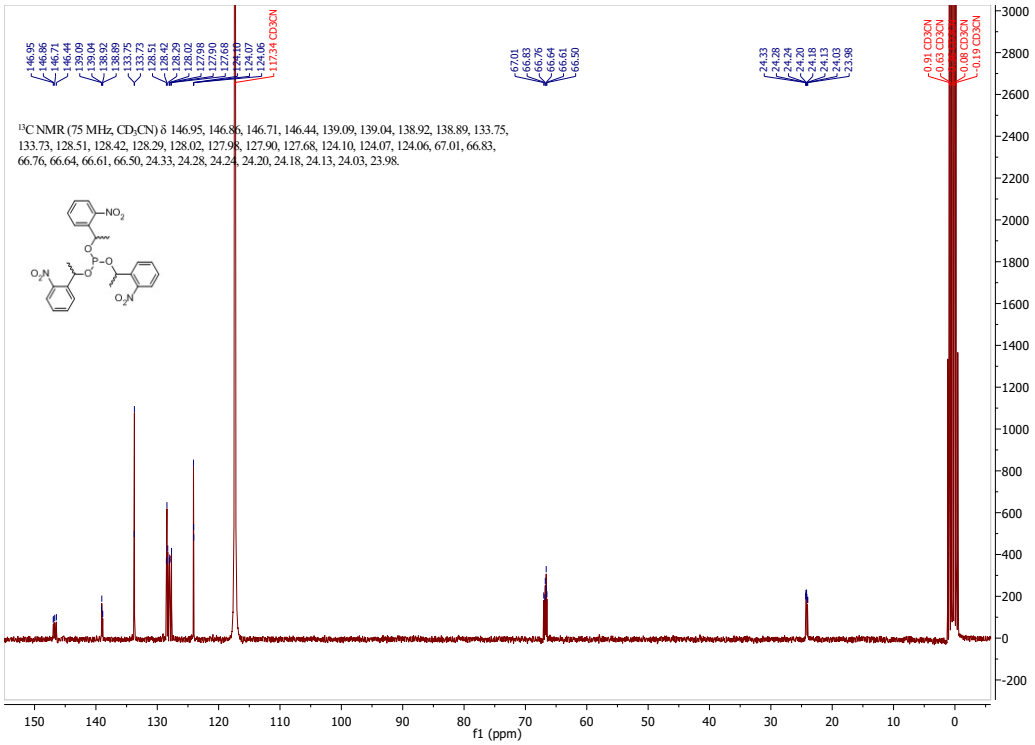

Figure S65: ^{13}C NMR spectrum of compound **9** (75 MHz, CD_3CN)

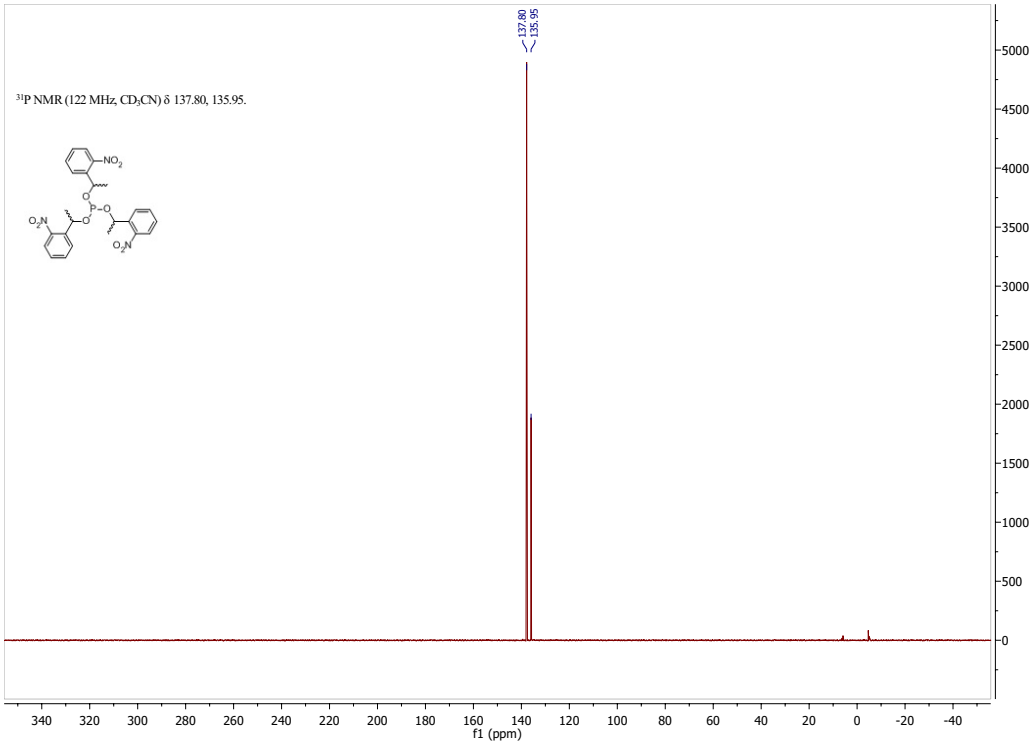

Figure S66: ^{31}P NMR spectrum of compound **9** (122 MHz, CD_3CN)

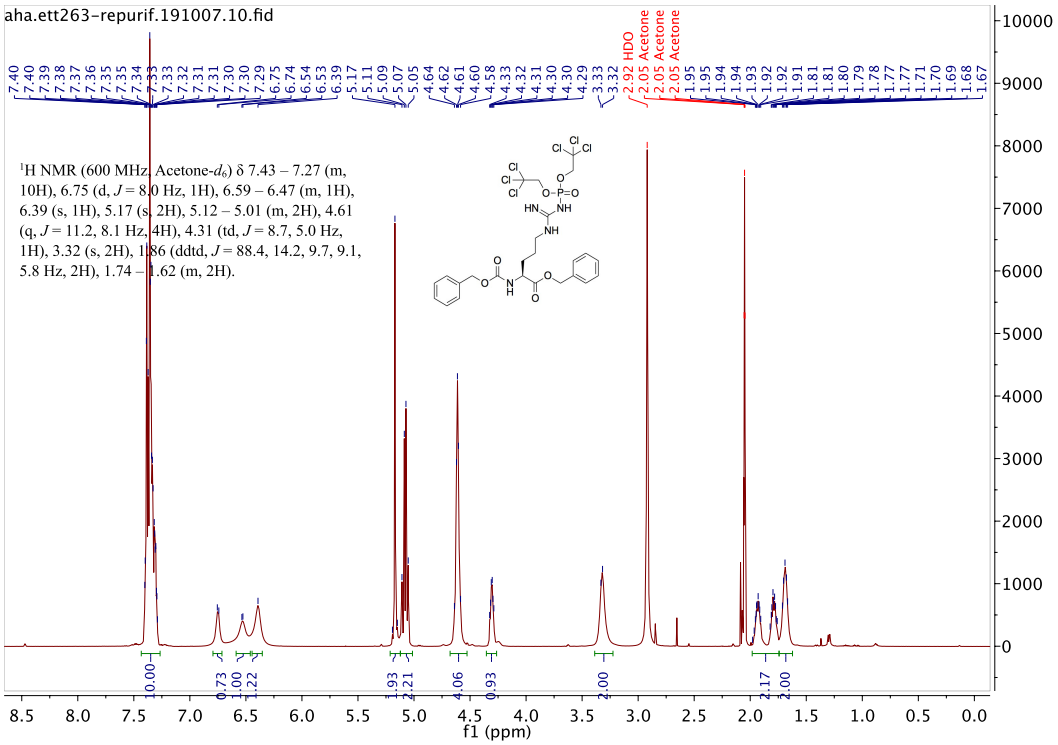

Figure S67: ^{1}H NMR spectrum of compound **10** (600 MHz, acetone-d_6)

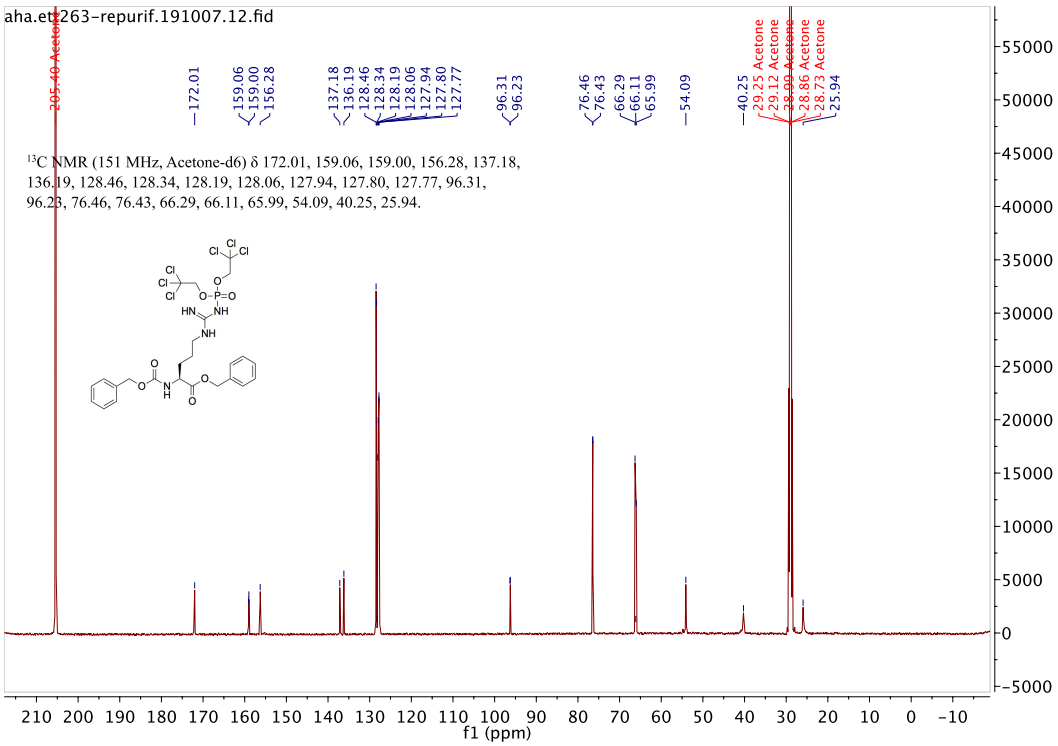

Figure S68: ^{13}C NMR spectrum of compound **10** (151 MHz, acetone-d_6)

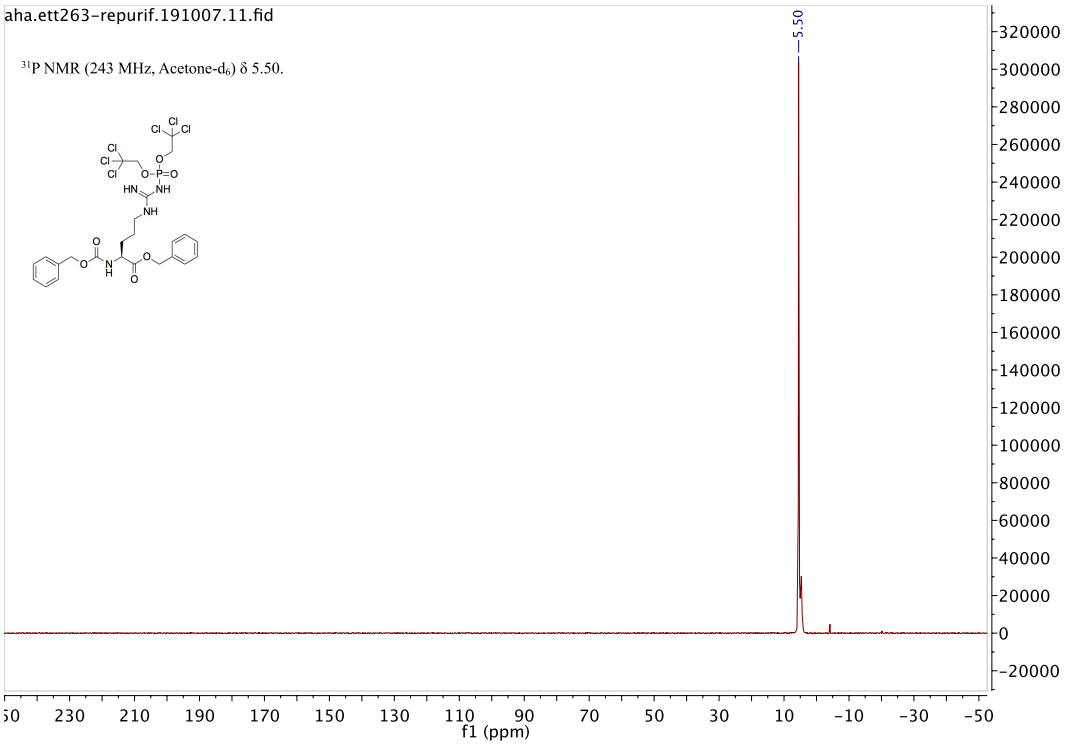

Figure S69: ^{31}P NMR spectrum of compound **10** (243 MHz, acetone-d_6)

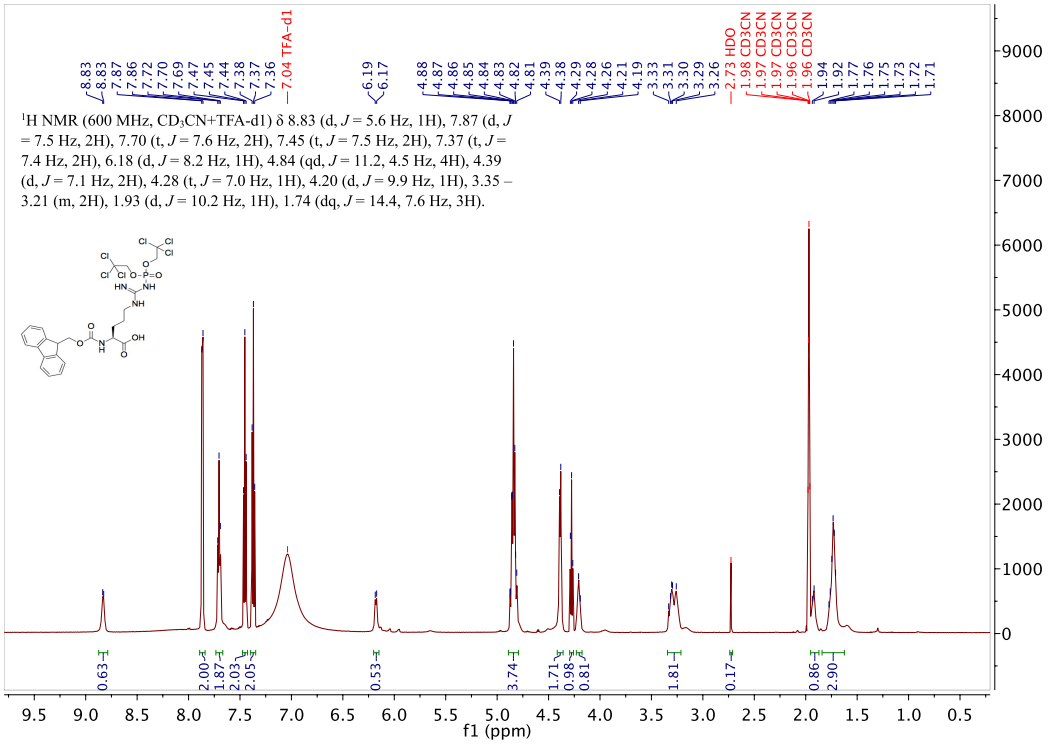

Figure S70: ^{1}H NMR spectrum of compound **11** (600 MHz, CD_3CN+TFA)

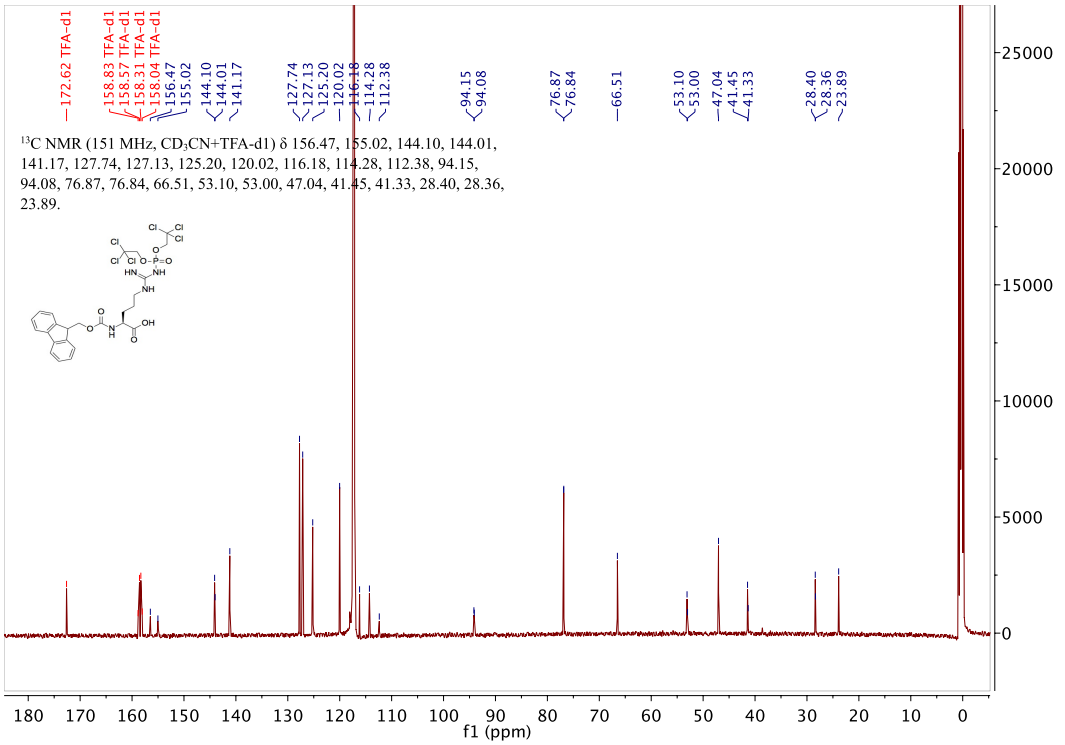

Figure S71: ^{13}C NMR spectrum of compound **11** (151 MHz, CD_3CN+TFA)

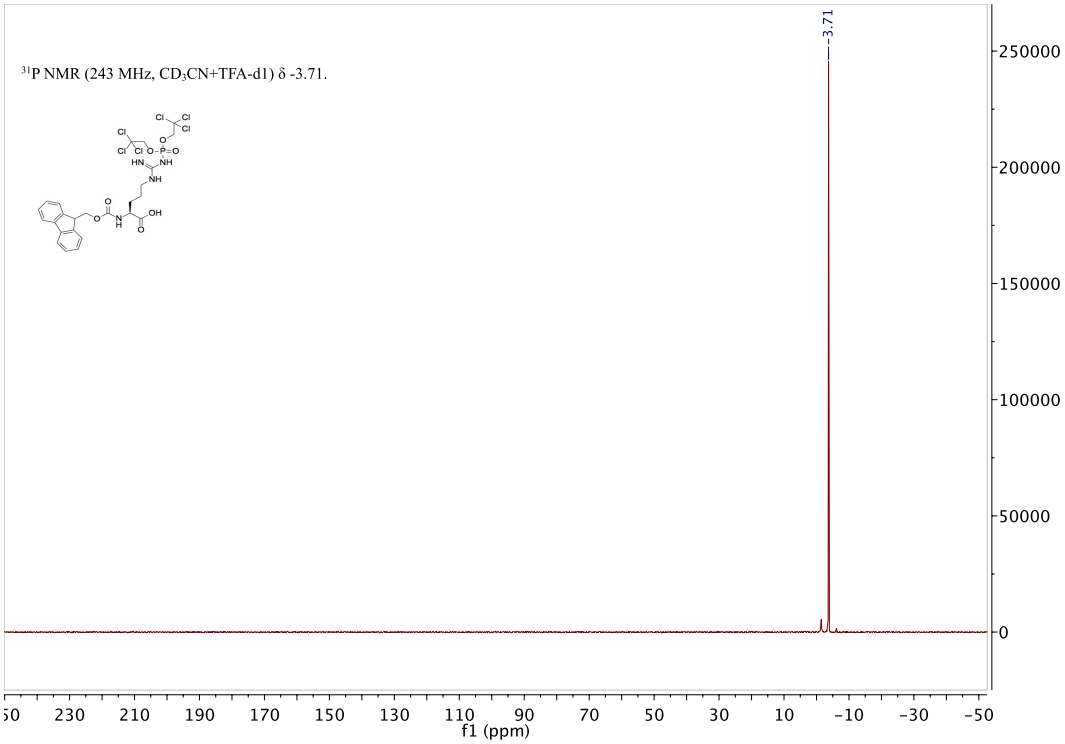

Figure S72: ^{31}P NMR spectrum of compound **11** (243 MHz, CD_3CN+TFA)

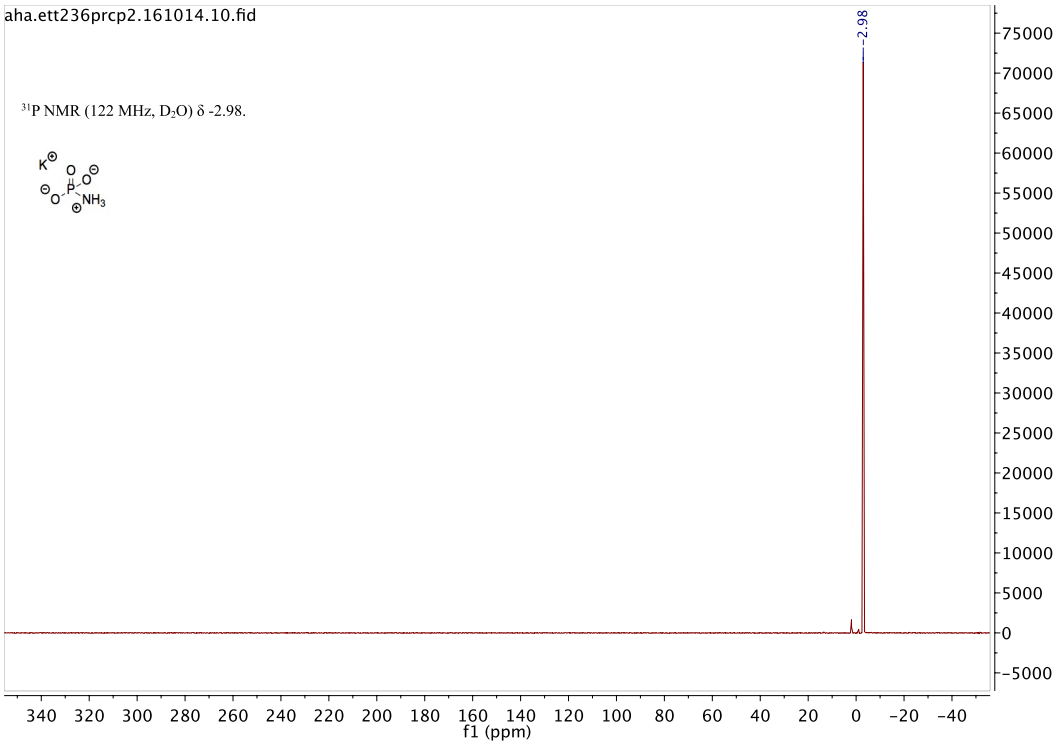

Figure S73: ^{31}P NMR spectrum of compound **13** (122 MHz, D_2O)

References

[1] M. Findeisen, T. Brand, and S. Berger, "A 1h-nmr thermometer suitable for cryoprobes," *Magnetic Resonance in Chemistry*, vol. 45, no. 2, pp. 175–178, 2007.

[2] A. Bax and M. F. Summers, "Proton and carbon-13 assignments from sensitivity-enhanced detection of heteronuclear multiple-bond connectivity by 2d multiple quantum nmr," *Journal of the American Chemical Society*, vol. 108, no. 8, pp. 2093–2094, 1986.

[3] D. O. Cicero, G. Barbato, and R. Bazzo, "Sensitivity enhancement of a two-dimensional experiment for the measurement of heteronuclear long-range coupling constants, by a new scheme of coherence selection by gradients," *Journal of Magnetic Resonance*, vol. 148, no. 1, pp. 209–213, 2001.

[4] M. Piotto, V. Saudek, and V. Sklenář, "Gradient-tailored excitation for single-quantum nmr spectroscopy of aqueous solutions," *Journal of Biomolecular NMR*, vol. 2, no. 6, pp. 661–665, 1992.

[5] M. R. Webb, "A continuous spectrophotometric assay for inorganic phosphate and for measuring phosphate release kinetics in biological systems," *Proceedings of the National Academy of Sciences*, vol. 89, no. 11, pp. 4884–4887, 1992.

[6] J. H. Kaplan, B. Forbush, and J. F. Hoffman, "Rapid photolytic release of adenosine 5'-triphosphate from a protected analog: utilization by the sodium:potassium pump of human red blood cell ghosts," *Biochemistry*, vol. 17, no. 10, pp. 1929–1935, 1978.

[7] F. T. Hofmann, C. Lindemann, H. Salia, P. Adamitzki, J. Karanicolas, and F. P. Seebeck, "A phosphoarginine containing peptide as an artificial sh2 ligand," *Chemical Communications*, vol. 47, no. 37, pp. 10335–10337, 2011.

[8] Y.-F. Wei and H. R. Matthews, *[32] Identification of phosphohistidine in proteins and purification of protein-histidine kinases*, vol. Volume 200, pp. 388–414. Academic Press, 1991.

[9] E. Harder, W. Damm, J. Maple, C. Wu, M. Reboul, J. Y. Xiang, L. Wang, D. Lupyan, M. K. Dahlgren, J. L. Knight, J. W. Kaus, D. S. Cerutti, G. Krilov, W. L. Jorgensen, R. Abel, and R. A. Friesner, "Opls3: A force field providing broad coverage of drug-like small molecules and proteins," *Journal of Chemical Theory and Computation*, vol. 12, no. 1, pp. 281–296, 2016.

[10] W. C. Still, A. Tempczyk, R. C. Hawley, and T. Hendrickson, "Semianalytical treatment of solvation for molecular mechanics and dynamics," *Journal of the American Chemical Society*, vol. 112, no. 16, pp. 6127–6129, 1990.

[11] R. A. Friesner, R. B. Murphy, M. P. Repasky, L. L. Frye, J. R. Greenwood, T. A. Halgren, P. C. Sanschagrin, and D. T. Mainz, "Extra precision glide - docking and scoring incorporating a model of hydrophobic enclosure for protein–ligand complexes," *Journal of Medicinal Chemistry*, vol. 49, no. 21, pp. 6177–6196, 2006.

[12] T. A. Halgren, R. B. Murphy, R. A. Friesner, H. S. Beard, L. L. Frye, W. T. Pollard, and J. L. Banks, "Glide - a new approach for rapid, accurate docking and scoring. 2. enrichment factors in database screening," *Journal of Medicinal Chemistry*, vol. 47, no. 7, pp. 1750–1759, 2004.

[13] R. A. Friesner, J. L. Banks, R. B. Murphy, T. A. Halgren, J. J. Klicic, D. T. Mainz, M. P. Repasky, E. H. Knoll, M. Shelley, J. K. Perry, D. E. Shaw, P. Francis, and P. S. Shenkin, "Glide - a new approach for rapid, accurate docking and scoring. 1. method and assessment of docking accuracy," *Journal of Medicinal Chemistry*, vol. 47, no. 7, pp. 1739–1749, 2004.

[14] N. Homeyer, A. H. C. Horn, H. Lanig, and H. Sticht, "Amber force-field parameters for phosphorylated amino acids in different protonation states: phosphoserine, phosphothreonine, phosphotyrosine, and phosphohistidine," *Journal of Molecular Modeling*, vol. 12, no. 3, pp. 281–289, 2006.

[15] R. Ditchfield, W. J. Hehre, and J. A. Pople, "Self-consistent molecular-orbital methods. ix. an extended gaussian-type basis for molecular-orbital studies of organic molecules," *The Journal of Chemical Physics*, vol. 54, no. 2, pp. 724–728, 1971.

[16] M. J. Frisch, J. A. Pople, and J. S. Binkley, "Self-consistent molecular orbital methods 25. supplementary functions for gaussian basis sets," *The Journal of Chemical Physics*, vol. 80, no. 7, pp. 3265–3269, 1984.

[17] J. Bertran-Vicente, R. A. Serwa, M. Schümann, P. Schmieder, E. Krause, and C. P. R. Hackenberger, "Site-specifically phosphorylated lysine peptides," *Journal of the American Chemical Society*, vol. 136, no. 39, pp. 13622–13628, 2014.

[18] M. Frisch, G. Trucks, H. Schlegel, G. Scuseria, M. Robb, J. Cheeseman, G. Scalmani, V. Barone, V. Petersson, H. Nakatsuji, X. Li, M. Caricato, A. Marenich, J. Bloino, B. Janesko, R. Gomperts, B. Mennucci, H. Hratchian, J. Ortiz, A. Izmaylov, J. Sonnenberg, D. Williams-Young, F. Ding, F. Lipparini, F. Egidi, J. Goings, B. Peng, A. Petrone, T. Henderson, D. Ranasinghe, V. Zakrzewski, J. Gao, N. Rega, G. Zheng, W. Liang, M. Hada, M. Ehara, K. Toyota, R. Fukuda, J. Hasegawa, M. Ishida, T. Nakajima, Y. Honda, O. Kitao, H. Nakai, T. Vreven, K. Throssell, J. J. Montgomery, J. Peralta, F. Ogliaro, M. Bearpark, J. Heyd, E. Brothers, K. Kudin, V. Staroverov, T. Keith, R. Kobayashi, J. Normand, K. Raghavachari, A. Rendell, J. Burant, S. Iyengar, J. Tomasi, M. Cossi, J. Millam, M. Klene, C. Adamo, R. Cammi, J. Ochterski, R. Martin, K. Morokuma, O. Farkas, J. Foresman, and D. Fox, "Gaussian 16," *Gaussian, Inc., Wallingford CT*, 2016.

[19] J. Wang, R. M. Wolf, J. W. Caldwell, P. A. Kollman, and D. A. Case, "Development and testing of a general amber force field," *Journal of Computational Chemistry*, vol. 25, no. 9, pp. 1157–1174, 2004.

[20] J. Wang, W. Wang, P. A. Kollman, and D. A. Case, "Automatic atom type and bond type perception in molecular mechanical calculations," *Journal of Molecular Graphics and Modelling*, vol. 25, no. 2, pp. 247–260, 2006.

[21] A. W. Sousa da Silva and W. F. Vranken, "Acpype - antechamber python parser interface," *BMC Research Notes*, vol. 5, no. 1, p. 367, 2012.

[22] L. Schrodinger, "The pymol molecular graphics system, version 1.3," *The PyMOL Molecular Graphics System, Version 1.3*, 2011.

[23] P. Mark and L. Nilsson, "Structure and dynamics of the tip3p, spc, and spc/e water models at 298 k," *The Journal of Physical Chemistry A*, vol. 105, no. 43, pp. 9954–9960, 2001.

[24] K. Lindorff-Larsen, S. Piana, K. Palmo, P. Maragakis, J. L. Klepeis, R. O. Dror, and D. E. Shaw, "Improved side-chain torsion potentials for the amber ff99sb protein force field," *Proteins*, vol. 78, no. 8, pp. 1950–1958, 2010.

[25] V. Gapsys, S. Michielssens, D. Seeliger, and B. L. de Groot, "pmx: Automated protein structure and topology generation for alchemical perturbations," *Journal of Computational Chemistry*, vol. 36, no. 5, pp. 348–354, 2015.

[26] V. Gapsys, S. Michielssens, J. Peters, B. de Groot, and H. Leonov, *Molecular modeling of proteins*. New York: Humana Press, 2015.

[27] M. Aldeghi, B. L. de Groot, and V. Gapsys, *Accurate Calculation of Free Energy Changes upon Amino Acid Mutation*, pp. 19–47. New York, NY: Springer New York, 2019.

[28] G. Bussi, D. Donadio, and M. Parrinello, "Canonical sampling through velocity rescaling," *The Journal of Chemical Physics*, vol. 126, no. 1, p. 014101, 2007.

[29] M. Parrinello and A. Rahman, "Polymorphic transitions in single crystals: A new molecular dynamics method," *Journal of Applied Physics*, vol. 52, no. 12, pp. 7182–7190, 1981.

[30] T. Darden, D. York, and L. Pedersen, "Particle mesh ewald: An n·slog(n) method for ewald sums in large systems," *The Journal of Chemical Physics*, vol. 98, no. 12, pp. 10089–10092, 1993.

[31] U. Essmann, L. Perera, M. L. Berkowitz, T. Darden, H. Lee, and L. G. Pedersen, "A smooth particle mesh ewald method," *The Journal of Chemical Physics*, vol. 103, no. 19, pp. 8577–8593, 1995.

[32] B. Hess, H. Bekker, H. J. C. Berendsen, and J. G. E. M. Fraaije, "Lincs: A linear constraint solver for molecular simulations," *Journal of Computational Chemistry*, vol. 18, no. 12, pp. 1463–1472, 1997.

[33] B. Hess, C. Kutzner, D. van der Spoel, and E. Lindahl, "Gromacs 4: algorithms for highly efficient, load-balanced, and scalable molecular simulation," *Journal of Chemical Theory and Computation*, vol. 4, no. 3, pp. 435–447, 2008.

[34] M. J. Abraham, T. Murtola, R. Schulz, S. Páll, J. C. Smith, B. Hess, and E. Lindahl, "Gromacs: high performance molecular simulations through multi-level parallelism from laptops to supercomputers," *SoftwareX*, vol. 1-2, pp. 19–25, 2015.

[35] D. Seeliger and B. L. de Groot, "Protein thermostability calculations using alchemical free energy simulations," *Biophysical journal*, vol. 98, no. 10, pp. 2309–2316, 2010.

[36] D. A. Pearlman and P. A. Kollman, "The overlooked bond-stretching contribution in free energy perturbation calculations," *The Journal of Chemical Physics*, vol. 94, no. 6, pp. 4532–4545, 1991.

[37] G. E. Crooks, "Entropy production fluctuation theorem and the nonequilibrium work relation for free energy differences," *Physical Review E*, vol. 60, no. 3, pp. 2721–2726, 1999.